PIECEWISE PREDICTION OF NUCLIDE DENSITIES WITH CONTROL BLADE USE AS A FUNCTION OF BURNUP IN BWR USED NUCLEAR FUEL

A Thesis
Presented to
The Academic Faculty

by

Timothy R. Younkin

In Partial Fulfillment
of the Requirements for the Degree
Master of Science in the
School of Mechanical Engineering

Georgia Institute of Technology
December 2014

PIECEWISE PREDICTION OF NUCLIDE DENSITIES WITH CONTROL BLADE USE AS A FUNCTION OF BURNUP IN BWR USED NUCLEAR FUEL

Approved by:

Dr. C.K. Wang, Advisor
School of Mechanical Engineering
Georgia Institute of Technology

Dr. Bojan Petrovic
School of Mechanical Engineering
Georgia Institute of Technology

Mr. Brian Ade
Oak Ridge National Laboratory

Date Approved: December 3, 2014

To the students of the Georgia Institute of Technology

ACKNOWLEDGEMENTS

I would like to primarily thank my family for their loving support of my academic pursuits. This would not be possible without the sacrifices they have made. I would also like to thank the members of my masters thesis committee for their guidance, accommodation and patience. They contributed significantly to my knowledge in the field and taught me through example how to be professional in research, yet still caring on a personal level. Lastly I would like to thank the United States Nuclear Regulatory Commission, Oak Ridge National Laboratory, and the Georgia Institute of Technology for the incredible opportunities that have been afforded to me.

TABLE OF CONTENTS

LIST OF TABLES

LIST OF FIGURES

LIST OF SYMBOLS AND ABBREVIATIONS

UNF	Used Nuclear Fuel
BUC	Burnup Credit
NRC	United States Nuclear Regulatory Commission
ISFSI	Independent Spent Fuel Storage Installation
DOE	United States Department Of Energy
BWR	Boiling Water Reactor
PDA method	Piecewise Data Approximation Method
SCALE	Standardized Computer Analyses for Licensing Evaluation
TRITON	Transport Rigor Implemented with Time-dependent Operation for Neutronic Depletion
PWR	Pressurized Water Reactor
SCALE	Standardized Computer Analyses for Licensing Evaluation
GBC	Generic Burnup Cask
NEWT	New ESC-based (Extended Step Characteristic) Weighting Transport code
ORIGEN	Oak Ridge Isotope Generation code
PDA	Piecewise Data Approximation

SUMMARY

In order to improve the efficiency of dry used nuclear fuel (UNF) storage, reduced reactivity methods are being developed for various reactor types and operating conditions. Sub-criticality must be maintained in the storage configuration and conservative computer simulations are used as the primary basis for loading the storage casks. Methodologies are now being developed to reduce the amount of modeling and computation in order to make conservative assessments of how densely fuel can be packed. The SCALE/TRITON (Standardized Computer Analyses for Licensing Evaluation / Transport Rigor Implemented with Time-dependent Operation for Neutronic Depletion) code system has been used to simulate boiling water reactor (BWR) operating conditions in order to investigate nuclide densities in UNF and how the use of control rod blades affect nuclide densities found in UNF. Rodded and unrodded operating cases for a fuel assembly have been used as bounding cases and are used as reference solutions in a piecewise data approximation methodology (PDA method). A variety of control blade insertion patterns have been used with the PDA method and simulated in TRITON in order to observe trends in nuclide densities with varying control blade use. The PDA method is compared with TRITON simulated data in order to evaluate the validity and accuracy of the PDA method. The PDA method gives very accurate results for fissile nuclides but is insufficient in treating densities as a function of burnup for fission products and fertile nuclides. Predicting nuclide densities from temporally balanced control blade insertion and withdrawal patterns is also a strength of the PDA method. The PDA method, however, is not capable of properly accounting for neutron spectral shifts and the behavior in nuclide densities brought about by the spectral shift or nuclide density

saturation. Observing the causes for the shortcomings in the PDA method, a more robust methodology can be developed.

CHAPTER 1

INTRODUCTION

This introductory chapter gives some background to the nuclear power industry and the needs within the nuclear power industry that bring about this research. Principles and economics of dry storage of used nuclear fuel (UNF) and the concept of burnup credit (BUC) are introduced. Calculational methods that can serve as a possible step in problem solution are then presented.

1.1 The Role of the U.S. Nuclear Regulatory Commission

The Unites States Nuclear Regulatory Commission (NRC) is responsible for regulation of UNF from commercial nuclear power plants [1]. UNF from the 100 commercial nuclear power plants that are currently licensed to operate in the U.S. is being stored in dry storage systems after a 3-year minimum cooling time in a spent fuel pool [2]. As of July 2013, 54 of the 69 operating general licensed independent spent fuel storage installations (ISFSI) were located at operating reactor sites. The remaining 15 sites are specific licensed ISFSIs at or away from reactor sites [3]. As on-site storage of UNF from commercial power plants becomes more necessary, the efficiency, safety, and effectiveness of storage and transportation of UNF is receiving more attention. In January 2013 the U.S. Department of Energy (DOE) released a "Strategy for the Management and Disposal of Used Nuclear Fuel and High Level Radioactive Waste" that plans a sustainable program to manage UNF and high-level radioactive waste. The framework therein has priorities to implement interim storage, plan an integrated waste management system, and prepare for transportation of UNF and high-level waste [4]. Dry storage containers will be utilized in each of these tasks and utilities will want to make their use in storage and transportation as efficient as possible. Because of extensive future use of

dry container storage and improved efficiency methods, the NRC is evaluating technical needs to broaden the types of applications accepted from commercial plants. One specific type of application the NRC is preparing to accept is an application from commercial power plants petitioning to use dry storage configurations of boiling water reactor (BWR) UNF that use reduced reactivity (burnup credit) methods in the criticality safety calculations. At the present time, the conservative assumption used in criticality calculations for the dry storage configuration for BWR UNF is to use fresh (unirradiated) fuel that does not contain burnable absorbers.

1.2 Dry Storage of UNF

The initial construction of a dry storage facility costs $10 to $20 Million and costs $5 to $7 Million per year for maintenance, security and growth of the facility [5]. Since this is a significant fraction of operating and maintenance costs of a nuclear reactor ($80 Million per year), dry storage of UNF has a significant impact on the economics of commercial nuclear power plant operation, and utilities are looking to minimize this cost. One step towards reducing cost and improving storage efficiency is by allowance for the decrease in fuel reactivity, which results from consumption of fissile material and creation of neutron absorbing actinides and fission products that occur from irradiation of nuclear fuel during the in-reactor fuel assembly lifetime. Using this decrease in fuel reactivity for criticality calculations in UNF storage is termed burnup credit (BUC). This allows for an increased amount of UNF to safely be stored in the same volume dry storage containers. The initial composition of the nuclear fuel and the history of how it has been irradiated and cooled dictate the reactivity of the UNF and therefore the criticality safety of a particular storage configuration. Variables in the history of the in-reactor nuclear fuel such as moderator density, control rod (or blade) use, and use of burnable absorbers need to be investigated in order to assess how they affect the reactivity of UNF and therefore the criticality of the dry storage configuration.

Dry storage containers used for storage and transportation called casks have necessarily been designed to meet criticality safety and structural integrity requirements while also meeting limits on weight, thermal loading, external dose, and containment. A minimum 3-year cooling time in a spent fuel pool is required for UNF before being loaded into a dry storage cask configuration. Criticality is one of six areas considered for regulatory review in dry storage systems by the NRC. The ability of the system to remain subcritical during every phase of storage and transportation is essential. In order for BUC methods to be allowable in regulation of UNF storage the effects of history variables such as moderator density, control blade use, and use of burnable absorbers on UNF reactivity must be well understood and accurately characterized. This research focuses specifically on the history variable of control blade state in boiling water reactors and how the control rod history affects isotopic densities in UNF, which will ultimately affect the criticality of the UNF in dry storage.

Using BUC methods, increased amounts of UNF can safely be stored in the same volume storage casks that are currently being used. However, conservative assumptions must be made in order to preserve criticality safety standards. Therefore it is desirable to conservatively predict nuclide densities within UNF based on reactor operating history. The purpose of this research is to evaluate a methodology that predicts nuclide densities in UNF based on the control rod blade history during fuel irradiation – the piecewise data approximation hereafter referred to as the PDA method. The nuclide densities of actinides and absorbing neutron poisons are not tracked for the present criticality calculations of UNF in a storage configuration and as a result, overly conservative assumptions are made. An accurate methodology can use the fuel irradiation history to predict the nuclide densities in the fuel discharged from the reactor. It can then be demonstrated that the criticality of UNF in a storage configuration is below the criticality threshold required by proper margins for safety and uncertainty. The PDA method will be tested using the Standardized Computer Analyses for Licensing Evaluation (SCALE)

code system and the transport rigor Implemented with time-dependent operation for neutronic depletion (TRITON) control module for reactor analysis to investigate its validity [6]. This report documents the essential physics that need to be considered in such calculations and will evaluate the PDA method for possible future applications for burnup credit.

CHAPTER 2

BACKGROUND

2.1 BWR Fuel Cycle Overview

This section gives an overview of BWR operating principles in order to introduce the physics that needs to be considered in fuel irradiation and depletion calculations. Fuel bundle design for BWRs is characterized and fuel cooling in a spent fuel pool will also be described.

2.1.1 BWR Design and Operation

There are several characteristics that distinguish a BWR from the more common pressurized water reactors (PWR). BWRs were developed later than PWRs for civilian use, reducing cost through design simplification. Many of these design aspects make BWR UNF more difficult to analyze.

General Operation

BWRs are characterized by a single circuit of light water at ~7.6 MPa (75 atm.) that boils in the reactor core at ~285 °C which creates voids (two-phase flow) within the core [7]. The core heats the coolant as it flows upward, boiling and leaving the top of the core to enter moisture separation before the steam goes to drive the main turbine. Boiling water reactor fuel bundles are surrounded by a channel box that directs the coolant up through the fuel assembly and provides a bearing surface for the cruciform shaped control blades, which are inserted from the bottom of the reactor. The power is controlled via reactor-coolant recirculation-flow control and control blade insertion. Control via these methods is dynamic, changing frequently during the reactor operation. A number of modeling complexities have prevented significant progress in research of BUC for BWR

UNF. Those complexities include axial moderator density variation, axial and radial variation in fuel enrichment and burnable absorber content, and extensive control blade usage.

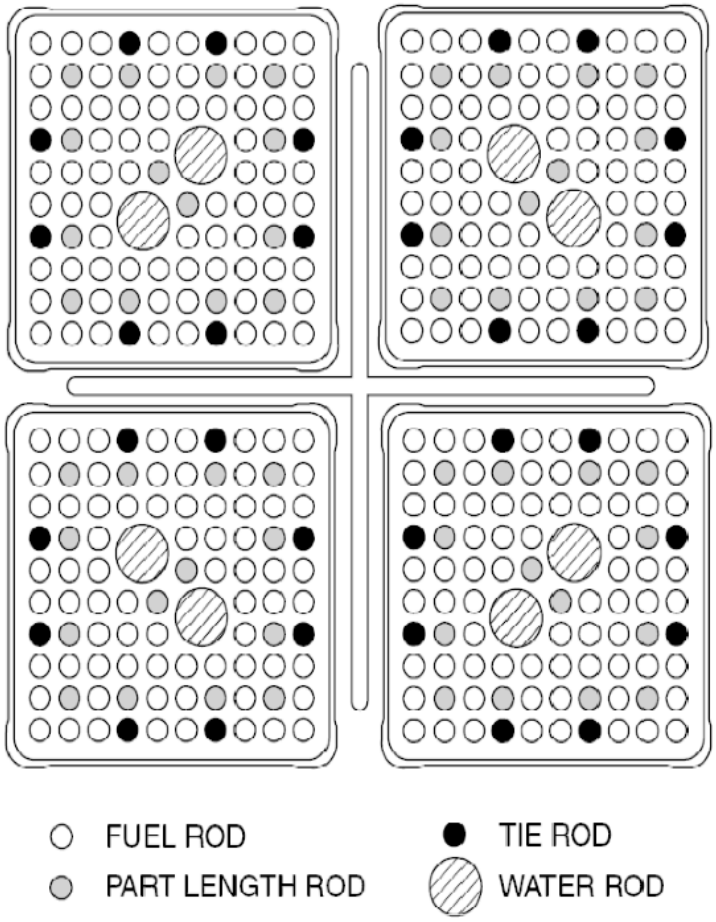

Figure 1. Four GE 10x10 pin fuel assemblies with a control rod blade inserted in the center. General geometry of the fuel pins, water rods, channel box and control rod blade can be observed [8].

Fuel Bundle Design

Another characteristic of BWRs is that many of the fuel pins are control augmented with gadolinium oxide (Gd_2O_3), which depletes with burnup. Since gadolinium is a burnable neutron absorber, it suppresses excess initial reactivity and therefore increases reactor shutdown margin. In modern reactors the Gd poisoned pins contain gadolinia

(Gd_2O_3) in weight concentrations of 3% to 8%. Gadolinium (specifically ^{155}Gd and ^{157}Gd) acts as a neutron poison and also causes spectral shifts, as the absorption cross section is larger for thermal energies as can be seen in the cross-section plot in Fig. 2.

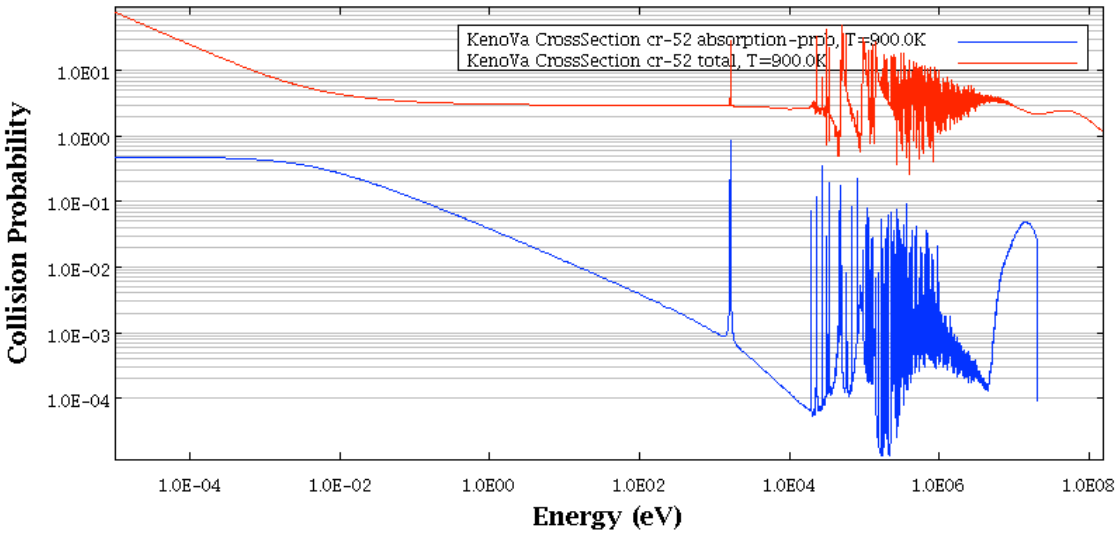

Figure 2. ^{155}Gd total collision probability and absorption probability listed together on a semi-logarithmic scale. ^{155}Gd is much more likely to absorb neutrons at thermal energies than those at intermediate or high energies. This data is taken from the KENO Va continuous energy data files [6].

For the purpose of this research, the GE-14 fuel bundle has been selected as a model for these calculations. The advanced geometry features in the GE-14 allow extension of the results of to other common advanced BWR fuel assemblies. The GE-14 is a 10x10 fuel pin array with 2 water rods, similar to that in Fig. 1. A reactor power of 25 MW_{th} has also been selected for the purpose of this research. In the interest of future research and applications that may be received by the NRC, modeling will be performed to relatively high burnup (~50 GWd/MTU). The data in Figure 3 has been modeled using the SCALE/TRITON techniques described in section 2.6. These results are presented here in order to illustrate the need for the research and results presented in chapters 3 and 4. Figure 3 demonstrates k_{inf} over the burnup (energy extracted) of GE-14 fuel bundles with different fuels in an infinite bundle array (The GE-14 fuel bundle is discussed

Section 2.5). One of the fuel assemblies modeled contains only UO_2 fuel and the other contains UO_2 with gadolinia. As can be seen in the plot, the fuel assembly poisoned with gadolinia has a more moderate k_{inf} value than that of the fuel made up of only UO_2, which depletes linearly with burnup.

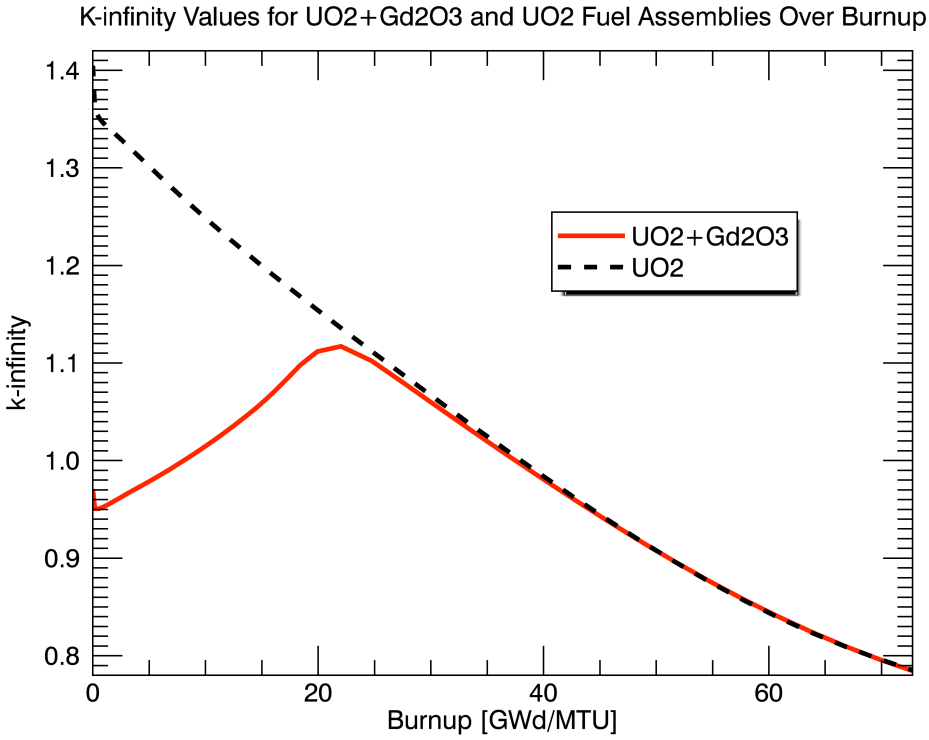

Figure 3. GE-14 fuel assembly (one with Gd augmented fuel, one without) modeled out to a burnup of 75 GWd/MTU. This simulation uses the enrichment values found in Table 8 in Section 2.5.2.

Throughout a BWR core, the exact pin configuration in a fuel assembly (enrichment, number of gadolinium bearing fuel rods, rod length, loading pattern) varies, giving a wide set of circumstances for depletion modeling [9]. Therefore, average-enrichment and pin configuration parameters will be used to examine fuel depletion parameters before moving on to more detailed models and modeling of the many pin arrangements used in the fuel assembly.

2.1.2 Fuel Cooling

In the United States, all operating nuclear reactors place discharged fuel from the reactor into spent fuel pools. These are large reinforced light water pools that are designed to shield radiation from the fuel, and cool the fuel rods. As the spent fuel pools reach their capacity, UNF is removed from the pool and stored into dry containers. The NRC has authorized transfer of UNF from the spent fuel pool to a storage cask as early as three years. Most utilities cool the fuel for at least 5 years, and a time of 10 years is typical in the industry [10].

2.2 Dry Storage Cask Design

This section describes the dry storage cask design and geometry. The relevant regulations for criticality of BWR UNF that are established by the NRC are stated and consequences of these regulations are analyzed.

2.2.1 Dry Storage Cask Design

Dry storage casks store UNF surrounded by inert gas and typically sealed within a steel container. Additional radiation shielding such as concrete is often added to the outside of this container, and these casks can often be used for both transportation and storage. As mentioned previously dry storage cask systems have been designed to meet criticality safety and structural integrity requirements while also meeting limits on weight, thermal loading, external dose, and containment.

Criticality Safety

The NRC has developed a regulatory framework for both storage and transportation of UNF from commercial nuclear power plants, which can be found in Chapter I of Title 10 of the *Code of Federal Regulations* (parts 20,50,51,72,73) [11]. Parts 71 and 72 are of concern to burnup credit and detail circumstances in which sub-criticality must be maintained. Part 72, "Licensing requirements for the independent storage of spent nuclear fuel and high-level radioactive waste, and reactor- related greater than Class C waste" section 72.124, "Criteria for nuclear criticality safety" states:

> (a) *Design for criticality safety*. Spent fuel handling, packaging, transfer, and storage systems must be designed to be maintained subcritical and to ensure that, before a nuclear criticality accident is possible, at least two unlikely, independent, and concurrent or sequential changes have occurred in the conditions essential to nuclear criticality safety. The design of handling, packaging, transfer, and storage systems must include margins of safety for the nuclear criticality parameters that are commensurate with the uncertainties in the data and methods used in calculations and demonstrate safety for the handling, packaging, transfer and storage conditions and in the nature of the immediate environment under accident conditions.

This description from the NRC indicates that sub-criticality must be maintained in the storage configuration including the safety margins and uncertainty in calculations and the data used within.

Generic Cask Design

Because of proprietary limits and for the purpose of comparison, a generic burnup storage cask configuration has been designed and modeled. This cask is designed to hold 10x10 pin BWR fuel assemblies and is capable of storing 68 of them. The generic burnup credit cask (GBC) containing 68 boiling water reactor assemblies is termed GBC-68 [12]. Monte Carlo transport models have been prepared in order to simulate the conditions of the cask and assess criticality of this configuration with the input of UNF composition (nuclide densities). The GBC-68 is depicted in figures 4a and 4b, and physical dimensions and material compositions are given in the source cited by Mueller et. al [12].

License Duration

The current NRC regulation allows for up to 80 years of licensed storage (40 years under the initial license and an additional 40 year license renewal term) and time periods beyond 120 years are being investigated. While extended storage will have a

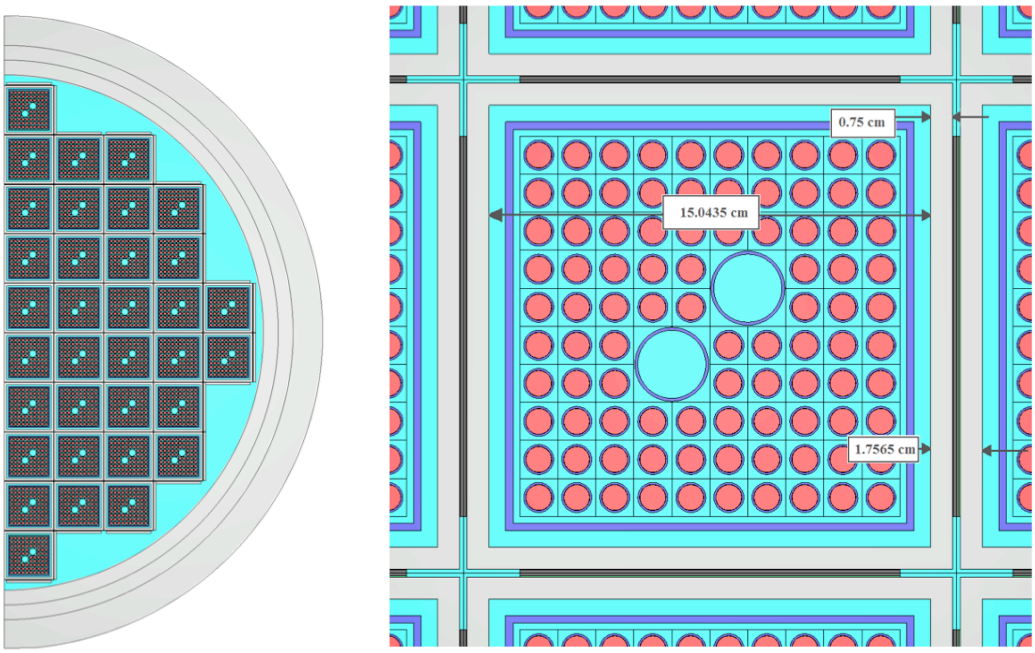

Figure 4a. (left) Radial cross section of (half) the cylindrical GBC-68 is shown to demonstrate the geometry of the storage cask. The diameter of the storage cask is 215 cm. Figure 4b. (right) Cross-sectional view of an assembly cell with some listed dimensions [12].

significant impact on some areas of regulatory review, areas that are fundamental to safety (such as confinement, shielding, and criticality safety) will maintain similar requirements for review. While the standards on criticality safety will not be changing significantly, the current safety margins can be significantly reduced without compromising safety. With proper research and experimental validation, loading of dry storage containers can become more efficient and cost effective.

2.3 Burnup Credit

This section describes the topic of burnup credit in greater detail and the state of the art is outlined. Isotopes of relevance are listed and their paths of transmutation are described. PWR burnup credit guidelines are also listed as a paradigm for ideas moving forward with BWR BUC.

2.3.1 Burnup Credit in PWR

In the past decade, many studies have investigated BUC for the purposes of storing pressurized-water reactor (PWR) fuel in both spent fuel pools and in dry storage casks. In consideration of criticality safety in the storage configuration, an assumption of fresh (unirradiated) fuel (Gd-free fresh fuel for BWRs) was used in criticality calculations for the storage configuration. This was an overly conservative assumption and steps were taken to account for the burnup (energy extracted from the fuel [GWd/MTU]) of the fuel that would reduce the criticality in the calculations for the fuel in the storage or spent fuel pool configuration.

As PWRs make up the majority of commercial power reactors in the United States and operation of PWRs is less dynamic than BWRs, PWRs were the natural choice to first develop burnup credit methodology for the UNF. In 2002 the U.S. NRC recommended burnup credit for the reactivity change due to major actinides only (listed in Table 1). This implementation enabled the elimination of flux traps that allowed higher density packing of the cask, which resulted in approximately a 30% increase in capacity for PWR casks.

In 2012 the NRC also began allowing for minor actinide and fission product burnup credit. This along with the burnup credit of the major actinides is referred to as full burnup credit (listed in Table 2).

Table 1. Major actinides that were considered for use in reduced reactivity calculations to determine criticality of UNF in dry storage configurations beginning in 2002.

Actinide-Only Isotopes (10)				
^{234}U	^{235}U	^{238}U	^{238}Pu	^{239}Pu
^{240}Pu	^{241}Pu	^{242}Pu	^{241}Am	^{16}O

Table 2. Full burnup credit nuclides that are now considered for use in reduced reactivity calculations to determine the criticality of the PWR UNF in a dry storage system.

Major and Minor Actinides and Major Fission Products (29 Isotopes)				
^{234}U	^{235}U	^{236}U	^{238}U	^{237}Np
^{238}Pu	^{239}Pu	^{240}Pu	^{241}Pu	^{242}Pu
^{241}Am	^{243}Am	^{95}Mo	^{99}Tc	^{101}Ru
^{103}Rh	^{109}Ag	^{133}Cs	^{147}Sm	^{149}Sm
^{150}Sm	^{151}Sm	^{152}Sm	^{143}Nd	^{145}Nd
^{151}Eu	^{153}Eu	^{155}Gd	^{16}O	

As was done for PWRs, it is desirable to develop a process for burnup credit for the 35 BWRs licensed to operate in the U.S. to minimize cost and storage resources. At the present time, the conservative assumption for BWR UNF storage configuration criticality calculations is the fresh fuel assumption with no burnable absorber (gadolinium).

2.3.2 Nuclides of Importance

In criticality calculations it is important to consider the buildup and depletion of radioactive nuclides. It is important to accurately represent these pathways in reactor operation, cooling of fuel in the spent fuel pool, as well as the dry cask storage

configuration. Figure 5 indicates the major pathways of transmutation and decay of some actinides that occur in commercial thermal reactor operation. The major and minor actinides that are considered in BUC criticality calculations are listed along with other nuclides that are part of the chain. The major decay mechanism and half-life, transmutation pathway and cross-section (barns), and thermal fission cross sections are listed. This figure is not exhaustive as other transmutation pathways exist and the cross sections displayed are not collapsed for the precise flux spectrum that exists in this research.

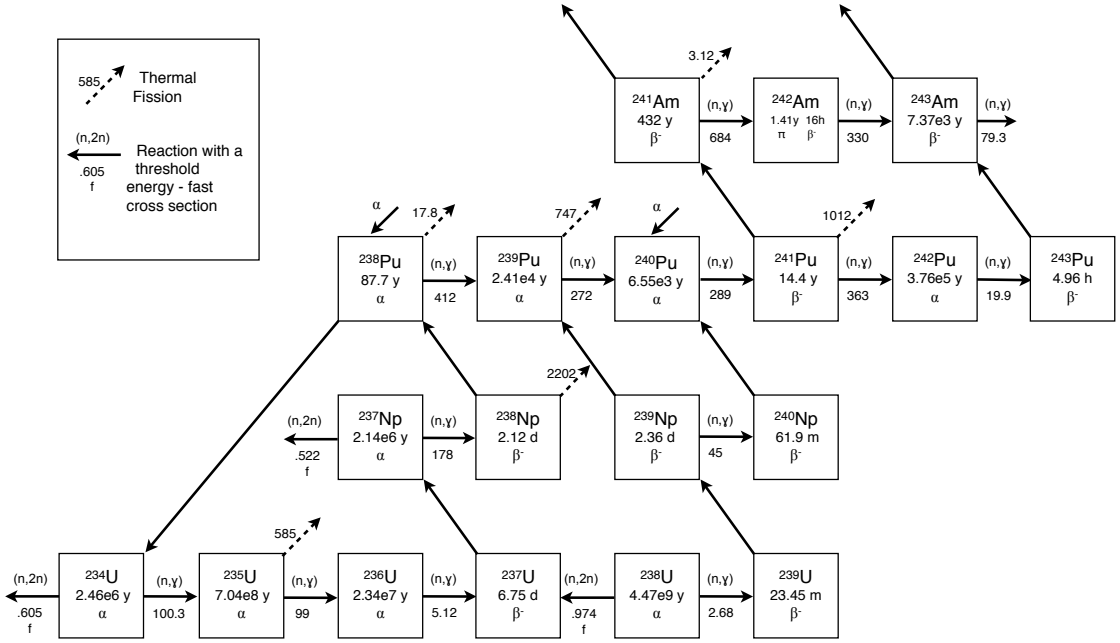

Figure 5. A decay and transmutation chain that includes the major and minor actinides that are in consideration for BUC criticality calculations. Decay data is from Brookhaven National Lab [13] and cross-section data is from JAEA [14]

In nuclear criticality calculations it is also important to consider densities of nuclides that detract from criticality by absorbing neutrons. There exist many fission products with large thermal neutron absorption cross-sections. The following table lists

the fission product cumulative yields for the isotopes of importance for BUC criticality calculations from the most relevant fissile materials in a reactor. Half lives [13] and thermal neutron absorption cross-sections [14] are also stated for these fission products.

Table 3. The nuclides of importance for UNF burnup credit criticality calculations for the dry storage configuration. Sources for cross-sections and fission yields are from [14] and [15] respectively.

Fission Product Neutron Poisons	
^{95}Mo	
	Cumulative fission yield from ^{235}U: 6.54E-2
	Cumulative fission yield from ^{239}Pu: 4.85E-2
	Cumulative fission yield from ^{241}Pu: 3.93E-2
	Thermal Neutron Absorption cross-section: 8 barn
	Half Life: Stable
^{99}Tc	
	Cumulative fission yield from ^{235}U: 6.14E-2
	Cumulative fission yield from ^{239}Pu: 6.23E-2
	Cumulative fission yield from ^{241}Pu: 5.96E-2
	Thermal Neutron Absorption cross-section: 23.6 barn
	Half Life: 2.1E5 y
^{101}Ru	
	Cumulative fission yield from ^{235}U: 5.17E-2
	Cumulative fission yield from ^{239}Pu: 6.04E-2
	Cumulative fission yield from ^{241}Pu: 6.23E-2
	Thermal Neutron Absorption cross-section: 5.23 barn
	Half Life: Stable
^{103}Rh	
	Cumulative fission yield from ^{235}U: 1.55E-9
	Cumulative fission yield from ^{239}Pu: 0
	Cumulative fission yield from ^{241}Pu: 6.71E-2
	Thermal Neutron Absorption cross-section: 133 barn
	Half Life: 56.12 m
^{109}Ag	
	Cumulative fission yield from ^{235}U: 3.22E-4
	Cumulative fission yield from ^{239}Pu: 1.47E-2
	Cumulative fission yield from ^{241}Pu: 0
	Thermal Neutron Absorption cross-section: 90.26 barn
	Half Life: Stable

Table 3 continued.

^{133}Cs	
	Cumulative fission yield from ^{235}U: 6.70E-2
	Cumulative fission yield from ^{239}Pu: 7.01E-2
	Cumulative fission yield from ^{241}Pu: 0
	Thermal Neutron Absorption cross-section: 28.9 barn
	Half Life: Stable
^{143}Nd	
	Cumulative fission yield from ^{235}U: 5.96E-2
	Cumulative fission yield from ^{239}Pu: 4.41E-2
	Cumulative fission yield from ^{241}Pu: 4.58E-2
	Thermal Neutron Absorption cross-section: 325 barn
	Half Life: Stable
^{145}Nd	
	Cumulative fission yield from ^{235}U: 3.93E-2
	Cumulative fission yield from ^{239}Pu: 2.99E-2
	Cumulative fission yield from ^{241}Pu: 3.26E-2
	Thermal Neutron Absorption cross-section: 49.45 barn
	Half Life: Stable
^{147}Sm	
	Cumulative fission yield from ^{235}U: 0
	Cumulative fission yield from ^{239}Pu: 2.00E-2
	Cumulative fission yield from ^{241}Pu: 0
	Absorption cross-section: 57 barn
	Half Life: 1.1E11 y
^{149}Sm	
	Cumulative fission yield from ^{235}U: 1.08E-2
	Cumulative fission yield from ^{239}Pu: 1.22E-2
	Cumulative fission yield from ^{241}Pu: 1.47E-2
	Thermal Neutron Absorption cross-section: 40540 barn
	Half Life: 1E16 y
^{150}Sm	
	Cumulative fission yield from ^{235}U: 3.00E-7
	Cumulative fission yield from ^{239}Pu: 1.15E-5
	Cumulative fission yield from ^{241}Pu: 5.08E-7
	Thermal Neutron Absorption cross-section: 100.9 barn
	Half Life: Stable

Table 3 continued.

^{151}Sm	
	Cumulative fission yield from ^{235}U: 4.19E-3
	Cumulative fission yield from ^{239}Pu: 7.38E-3
	Cumulative fission yield from ^{241}Pu: 9.13E-3
	Thermal Neutron Absorption cross-section: 15160 barn
	Half Life: 90 y
^{152}Sm	
	Cumulative fission yield from ^{235}U: 2.67E-3
	Cumulative fission yield from ^{239}Pu: 5.76E-3
	Cumulative fission yield from ^{241}Pu: 7.18E-3
	Thermal Neutron Absorption cross-section: 205.9 barn
	Half Life: Stable
^{151}Eu	
	Cumulative fission yield from ^{235}U: 4.19E-3
	Cumulative fission yield from ^{239}Pu: 7.38E-3
	Cumulative fission yield from ^{241}Pu: 9.13E-3
	Thermal Neutron Absorption cross-section: 9169 barn
	Half Life: Stable
^{153}Eu	
	Cumulative fission yield from ^{235}U: 1.58E-3
	Cumulative fission yield from ^{239}Pu: 3.61E-3
	Cumulative fission yield from ^{241}Pu: 5.41E-3
	Thermal Neutron Absorption cross-section: 312.7 barn
	Half Life: Stable
^{155}Gd	
	Cumulative fission yield from ^{235}U: 3.21E-4
	Cumulative fission yield from ^{239}Pu: 1.66E-3
	Cumulative fission yield from ^{241}Pu: 2.41E-3
	Thermal Neutron Absorption cross-section: 60740 barn
	Half Life: Stable

2.3.3 Outlook for BWR Burnup Credit

The first task in moving towards burnup credit for BWR UNF is to add the burnable absorber gadolinium into the storage criticality safety calculations. This approach uses the absolute maximum reactivity of the fuel, or "reactivity peak"

conditions in criticality calculations for storage [16]. This ensures that an absolute maximum reactivity of the fuel satisfies the criticality conditions for storage. This approach is valuable in that it requires no verification of burnup in the fuel. However, it completely neglects any additional burnup past the peak reactivity. This can be seen in Fig. 6.

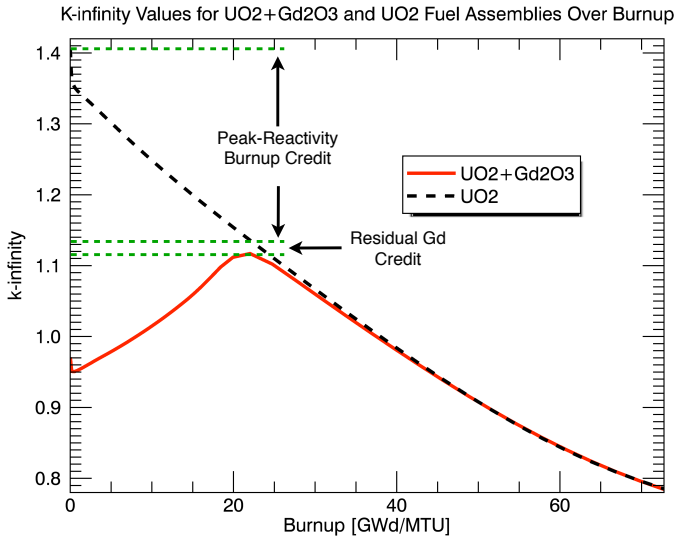

Figure 6. K-infinity values for BWR fuel assemblies with Gd augmented fuel pins, and UO_2 only fuel pins are shown as a function of burnup. These are used to demonstrate the Peak-Reactivity Burnup Credit.

After burnup credit using the peak reactivity methods is established, it is desirable to extend burnup credit beyond the peak reactivity, which occurs at approximately 20 GWd/MTU for the fuel assembly and fuel composition shown in Fig. 6. Using extended burnup credit, the burnup credit can be extended out past the reactivity peak up to the burnup of the fuel discharged from the reactor.

Sensitivity studies have been performed and have identified areas of research that need to be addressed in order to extend burnup credit beyond the peak reactivity method. Those areas include axial burnup distribution data, treatment of axial moderator density distributions, and treatment of control blade usage during depletion calculations [16]. The present thesis research has been performed on the treatment of control blade use during

depletion (in-reactor fuel irradiation) for extended (past the reactivity peak) burnup credit.

2.3.4 PWR Burnup Credit

Full burnup credit for PWR UNF has been established and should be considered as a guideline for developing burnup credit guidance for BWRs. Guidance for a burnup credit approach for criticality safety analysis for PWR UNF is described in the Interim Staff Guidance 8 - Revision 3 (ISG-8R3) [17]. The guidance for burnup credit for PWR used fuel in transportation and storage casks is as follows:

1. There exist limits on fuel parameters for the licensing basis:
    - -Fuel irradiated up to 60 gigawatt-days per metric ton Uranium (GWd/MTU).
    - -Cooled out-of-reactor for a time period between 1 and 40 years.
    - -Up to 5 weight percent enrichment in ^{235}U.
2. History variables of each fuel assembly must be taken into account and treated properly to account for actinide and fission product compositions:
    - -Axial and radial variation of burnup should be modeled effectively.
    - -Potential for increased reactivity from burnable absorbers and control rods should be considered.
    - -Environmental factors such as fuel temperature, moderator temperature and density, soluble boron concentration, specific power, and operating history should be accounted for.
3. Step must be taken to insure that isotopic depletion calculations are valid:
    - -Proper data and solving techniques must be used. Additional guidance for this step can be found in NUREG/CR-7108.
4. Code validation for storage cask model multiplication factor must exist:
    - -k_{eff} values for the storage configuration must be properly demonstrated for using either actinide-only, fission product and minor actinide, or full burnup

credit.

5. Loading curves (diagrams that indicate the minimum burnup required for a safe load of UNF into a storage configuration based on the initial enrichment) should be included in the application for BUC. Measurements should also be made in order to verify that the burnup of an assembly matches the reactor record before loading fuel into a storage or transportation configuration.

2.4 Use of Control Blades

The following section documents BWR control blade use during reactor operation. Research data on an operated reactor and the control blade insertion patterns used during operation are presented. Principles of practical control blade use are drawn from this study. Additionally, a short analysis on reactor physics and general trends of how the use of control blades during operation affects isotopic densities is presented. Time-dependent patterns of control blade insertion that have been modeled and examined are depicted at the end of this section.

2.4.1 Control Rod Blade Structure

Control blades are extensively used during BWR full power operation to control power distribution and reactivity. During BWR operation, a small fraction of the control blades are inserted, however, the depth and configuration at which the control blades are inserted varies.

BWR control rod blades are cruciform in shape and are inserted at the convergence of four channel boxes surrounding the fuel assemblies as shown previously in Fig. 1. Modern BWR control rod blades are composed of Zirconium alloy tubes, which are filled with B_4C powder (Hafnium has also been used as a neutron absorber and stainless steel has been used as a structural material). These cylinders are bundled in additional Zirconium alloy sheath and connected at the center of the cross to a Zirconium alloy center post. The Boron in the control rod acts as a thermal neutron absorber in order to

reduce the amount of fissions taking place in the adjacent fuel bundles. These control rods can be used to regulate power distribution, or to shut down the reactor (full insertion of all control blades). Control blade insertion data in BWRs has been documented in the operating data from the Peach Bottom 2 reactor [18] and also in the Hatch reactor [19].

2.4.2 Peach Bottom 2 Reactor

In 1976-1977 a BWR core design study was performed at the Peach Bottom 2 reactor in Pennsylvania. The study was done to analyze pressure transients and stability in a BWR core, but the report also contains operational data for control blade use and operating data needed to define fuel characteristics. Operating data was recorded for 2 cycles of operation of this reactor to assess core performance. Cycle one spanned 25 months (from April 1974 to March 1976) before the reactor was reloaded for cycle two which spanned 11 months (June 1976 to April 1977).

The reactor was initially loaded with 7x7 pin fuel bundles of different types with ^{235}U enrichments between 1.1% and 2.5%. Many of the assemblies were control augmented with gadolinia (3-4% concentration), while some were not. This information is displayed in Table 4. The reload fuel was 8x8 pin fuel bundles for which detailed information is shown in Table 5.

Table 4. Fuel description of the initial load (Cycle 1) of the Peach Bottom 2 reactor.

	Initial Fuel Description		
Fuel Assembly Type	1	2	3
Number of Fuel Assemblies per Batch	168	263	333
Fuel Rod Array	7x7	7x7	7x7
Fuel Rod Pitch	0.738 inches	0.738 inches	0.738 inches
Bundle Average Enrichment (wt % U-235 in Total U)	1.1	2.5	2.5

Table 4 continued.

Control Augmentation Type	NONE	Fuel Rods Containing Gd_2O_3	Fuel Rods Containing Gd_2O_3
Number of Control Augmented Pins in Fuel Assembly	0	4	5
Length of Control Augmented Pins		144(3), 60(1)	144(3), 108(1) 36(1)
Control Material		3.0 wt % Gd_2O_3	3.0 wt % Gd_2O_3 (3), 4.0 wt % Gd_2O_3 (2)
Weight of U per Fuel Assembly	196.1 kg	187.1 kg	186.9 kg

Table 5. Fuel description of the reload (Cycle 2) of the Peach Bottom 2 reactor.

	Reload Fuel Description		
Fuel Assembly Type	4	5	6
Number of Fuel Assemblies per Batch	68	116	4
Fuel Rod Array	8x8	8x8	8x8
Fuel Rod Pitch	0.640 inches	0.640 inches	0.640 inches
Bundle Average Enrichment (wt % U-235 in Total U)	2.74	2.74	2.6
Control Augmentation Type	Fuel Rods Containing Gd_2O_3	Fuel Rods Containing Gd_2O_3	Fuel Rods Containing Gd_2O_3
Number of Control Augmented Pins in Fuel Assembly	10	5	5
Control Material	3.0 wt % Gd_2O_3	2.0 wt % Gd_2O_3	2.0 wt % Gd_2O_3
Weight of U per Fuel Assembly	366.4 kg	183.3 kg	182.6 kg

The reactor core is made up of 764 fuel assemblies and was designed to operate at 3293 MW_{th}. There are 185 total control elements or control blades (1 for every 4 fuel

assemblies with 24 assemblies with no adjacent control rod on the periphery of the reactor). Control rod structural and geometrical data is presented in Table 6, and the positions for the control blades can be seen in Fig. 7.

Table 6. Structural and material control rod data for the control rods installed in the Peach Bottom 2 reactor.

	Control Rod Data
Shape	Cruciform
Pitch	12.0 inches
Control Material	B_4C granules in Type-304 stainless steel tubes and sheath
Tubes per Rod	84
Tube Dimensions	0.188 in. Outer Diameter 0.025 in. wall thickness
Control Blade Half Span	4.875 inches
Control Blade Full Thickness	0.3120 inches
Control Blade Tip Radius	0.156 inches
Sheath Thickness	0.056 inches
Central Structure Wing Length	0.7815 inches

In the Peach Bottom 2 reactor the enrichment as well as the Gd concentration is much lower than a modern reactor causing the reactivity of the fuel to peak at a lower burnup value than is now typical. According to the operational data, the control blades were inserted the most at a burnup of approximately 7000 MWd/MTU. Using this information, it is predicted that this is approximately the reactivity peak of the reactor fuel.

One way to assess control blade use in the reactor is by the sum of how many “notches” (the Peach Bottom 2 control blades could only be inserted in 3 inch increments called a notch) each control blade element is inserted into the reactor. The greater the

number of notches, the more control via control blades is being used.

The use of control rod blades in BWRs is closely related to the reactivity behavior of the fuel over burnup. Reactor cycle operation begins with very few notches. At this point, the control-augmented fuel pins have a high percent of burnable absorber material, which depresses the overall reactivity of the fuel. As fuel reactivity increases (with depletion of Gd), the number of notches is gradually increased up to the point of maximum fuel reactivity where a maximum number of notches are used as is shown in Fig. 7. During this process of increasing the number of notches, different control blade positions are used in an alternating fashion in order to give all of the fuel bundles similar operating histories (control blade in/out). This is demonstrated in Fig. 8.

Control blade use is most prevalent in the center of the reactor core where neutron leakage is low, decreasing with radial distance from the center of the core. This is done to maintain a somewhat flat power distribution with radial distance from the center of the reactor. The fuel bundles at the periphery of the reactor core rarely experience any control elements inserted.

These assessments have been made based on the first loading of the Peach Bottom 2 reactor. In most cases, reactors are not introducing an entirely fresh batch into the reactor core. The reload and fuel shuffle of a reactor act to reduce peaking of reactivity and increased control blade use. However, the characteristics and trends seen in the Peach Bottom 2 reactor are not completely diminished.

Enrichments and Gd concentrations are much higher in more modern reactor fuel bundles. The trends in behavior of the fuel are similar, but the burnup time scale has been lengthened (i.e. the peak in fuel reactivity occurs at a higher burnup). Also, the strategy of symmetric and uniform control blade use with all fuel assemblies still remains (i.e. It is useful to create similar control blade histories for the fuel bundles so that they can all be characterized similarly). Overall trends of control blade insertion over fuel bundle lifetime also remain the same when considering operation of a modern reactor compare to

the Peach Bottom 2 reactor (i.e. control blade use is proportional to fuel reactivity at any point in the operating cycle).

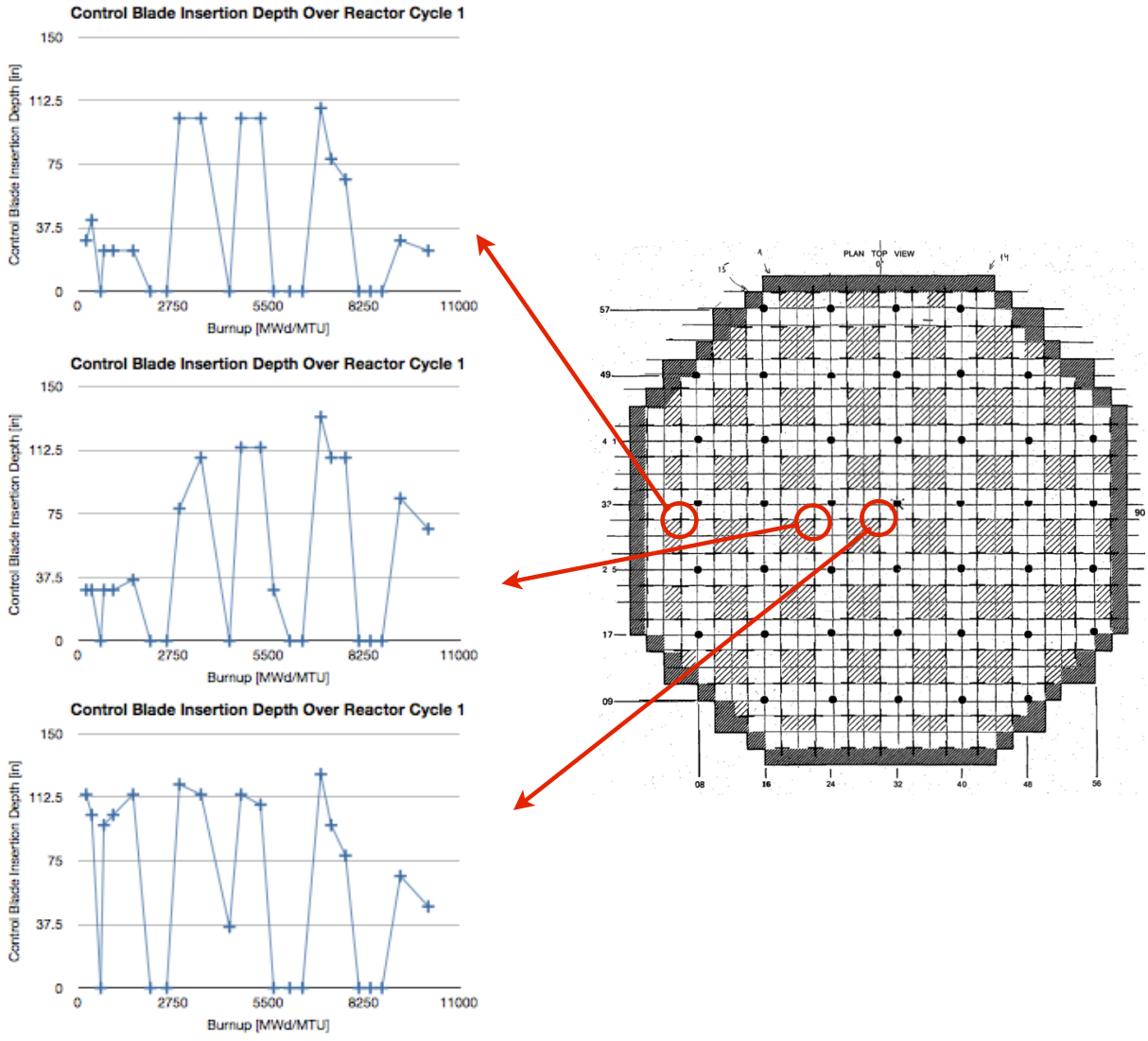

Figure 7. Control blade data based on radial position in the Peach Bottom 2 reactor.

This indicates that for BWRs there exist control blade histories that would be expected during a normal operating cycle of the reactor. However, if a methodology to predict nuclide densities was developed solely on the basis of routine reactor operation

and expected control blade usage patterns, that would limit the applicability of the methodology. The methodology would not be useful in any circumstance where non-routine operation was encountered. Therefore it is desirable to develop a robust methodology that is accurate in accounting for any pattern of control blade use.

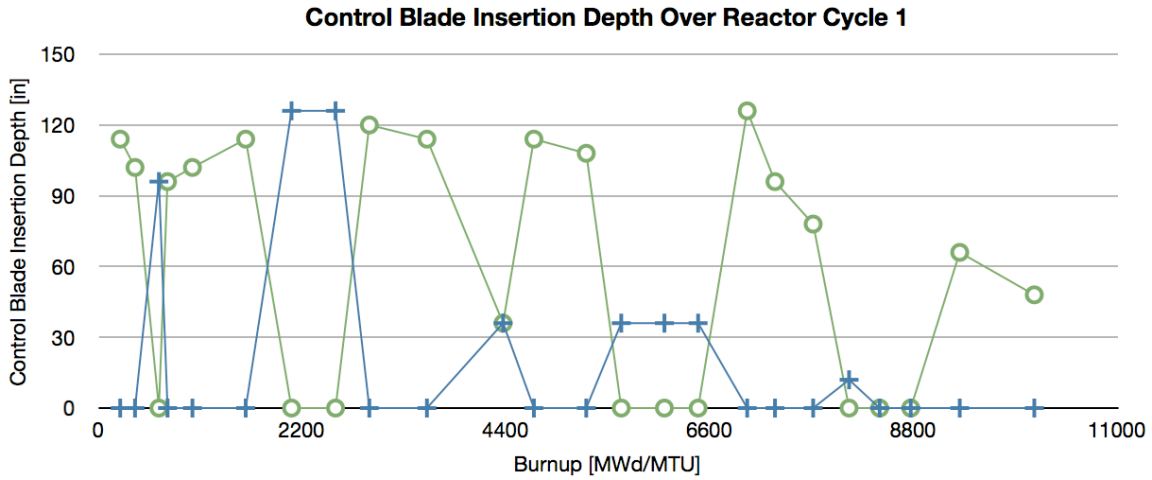

Figure 8. Peach Bottom 2 control blade insertion data for two adjacent control blades over cycle 1 of the reactor. This demonstrates the alternating fashion of control blade insertion for adjacent control locations.

2.4.3 Effects of Control Blade on Fuel Elements

For the purposes of criticality calculations of BWR UNF in the dry storage configuration, it would be unreasonable to model and simulate the wide range of fuel assembly configurations under highly time-dependent conditions for each fuel assembly. Therefore, a methodology (the PDA method) has been tested that will predict isotopic densities in BWR UNF that has a time-dependent history based on bounding cases that are used as a library. In other words, a small number of time-independent cases will be simulated and used to calculate the time-dependent cases using the control blade history. The time-independent and predominately bounding cases that will be used as the library

for the methodology are the rodded (100% time control blade insertion for the in-reactor fuel assembly lifetime) and unrodded (0% time control blade insertion) instances.

2.4.4 Rodded vs. Unrodded

The desired result from the methodology being tested is to use two bounding scenarios to predict the time-dependent scenarios that fall between the two. Two time-independent control blade histories (rodded and urodded) will be used to predict time-dependent cases. In Fig. 9a, the effective multiplication factors for 2D lattices have been modeled and computed for in-reactor fuel assembly lifetime, one for the rodded case and one for the unrodded. Figure 9b shows the difference in k_{eff} between the two cases (rodded k_{eff} subtracted from unrodded k_{eff}), and they vary significantly (0.15 to 0.24).

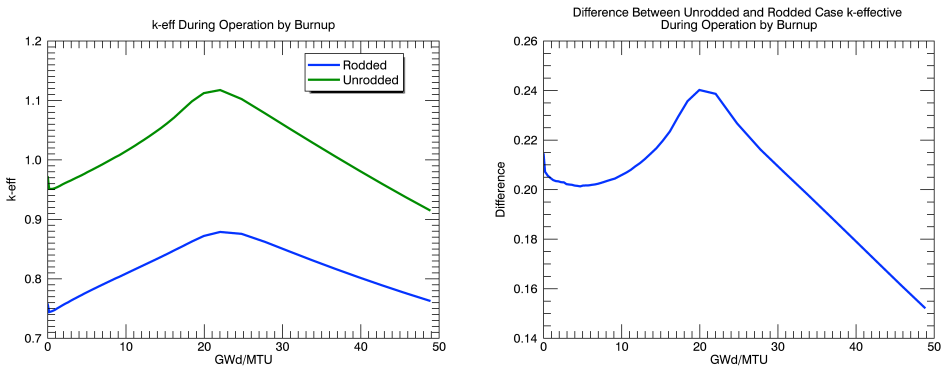

Figure 9a. (left) k_{eff} values for the rodded and unrodded cases over burnup. Figure 9b. (right) Percent difference between the rodded and unrodded k_{eff} values over burnup.

These two cases correspond to the same average burnup of the fuel assemblies, but the insertion of the control blade causes different resulting reactivity of the UNF, which will affect criticality in the dry storage configuration.

Considering nuclides for the cases of rodded and unrodded for the entire lifetime of the fuel (shown to be ~5.5 years or 50.3 GWd/MTU in Figures 10-13) and through 5 years of cooling in the spent fuel pool, the densities of major actinides are shown in Figures 10 and 11. The modeling and plots show higher densities of ^{235}U, Pu isotopes,

and Am isotopes for the rodded case. Trends in fission products can be seen in Figures 12 and 13. In order to assess the effect of control blade use on UNF that is placed in the dry storage configuration, a sequence of modeling approaches can be applied. First the fuel is depleted using the T-DEPL module (described in section 2.6) to simulate reactor operation. Nuclide densities are tracked through this process. Then fuel cooling is simulated using the ORIGEN-ARP module, which simulates the decay of actinides and fission products over the time spent in the spent fuel pool. Finally, the isotopic concentrations are taken and put back into the reactor fuel bundle configuration (no control rod present), and a 2-D NEWT transport calculation is performed. This will yield a k_{inf} value that is proportional to what would be expected from the dry storage configuration. When this is done for the rodded and unrodded cases, a difference in fuel bundle k of 0.07738 (1.05272 for the rodded, 0.9753372 for the unrodded) results.

As will be demonstrated, increased use of control blades results in increased reactivity of UNF. The combination of increased major actinide concentrations and varying buildup/depletion of minor actinides and fission product neutron poisons resulting from control blade use produces higher UNF reactivity. This will be demonstrated to be true for k-infinity values of UNF in the dry storage configuration. The rodded and unrodded cases are upper and lower bounds respectively when it comes to reactivity of UNF. Trends and patterns in nuclide densities will be further analyzed in Chapter 4.

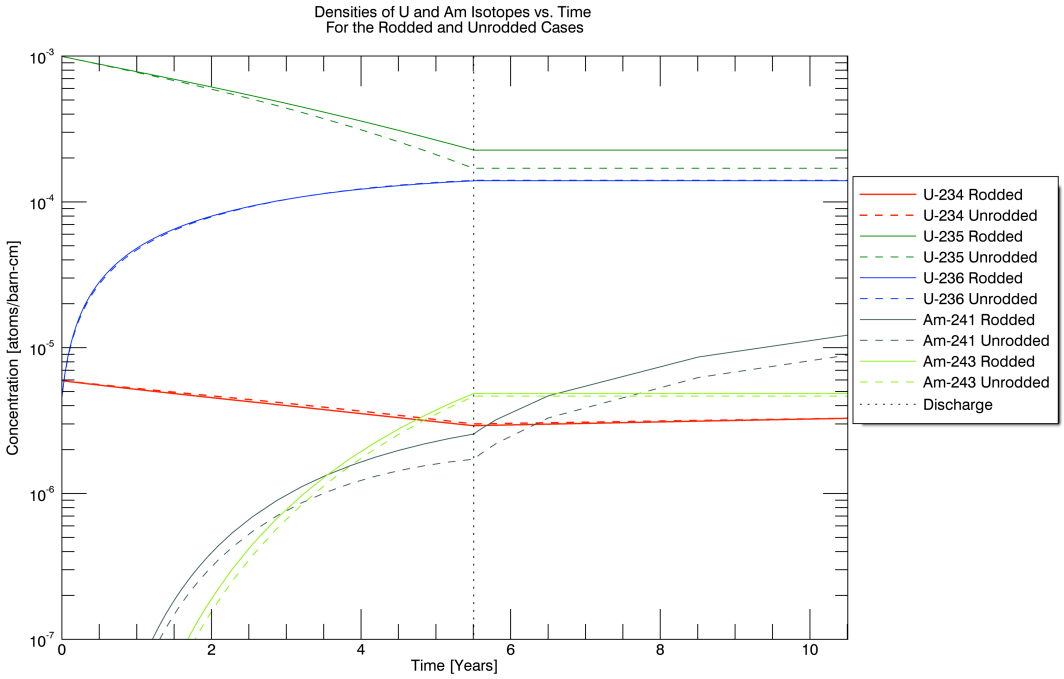

Figure 10. U and Am concentrations in the fuel during the in-reactor fuel assembly lifetime (TRITON data) and 5 years in the spent fuel pool (ORIGEN). Rodded and unrodded cases are plotted.

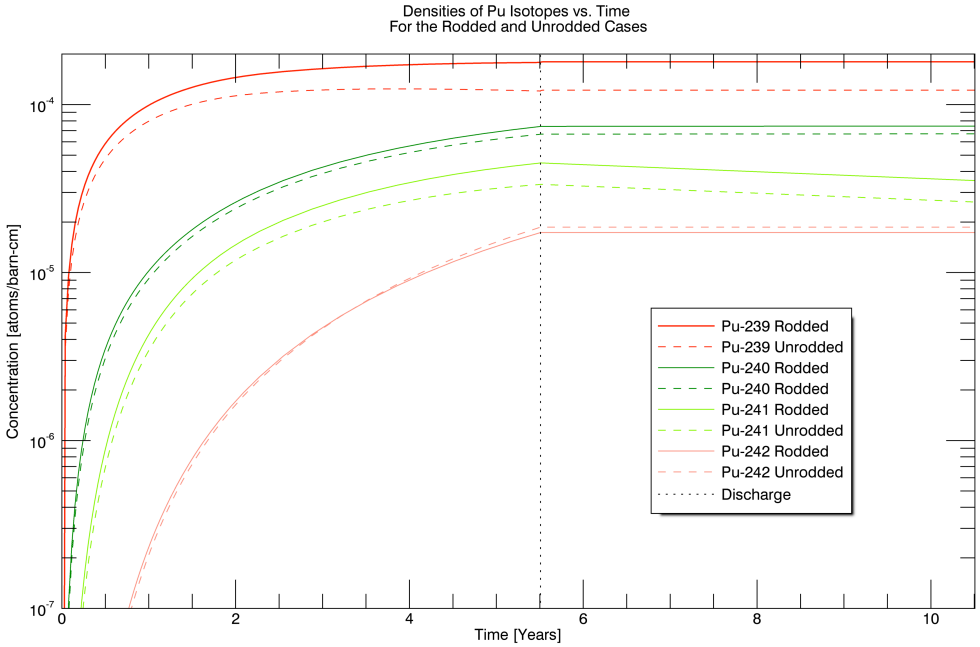

Figure 11. Pu concentration in the fuel during the in-reactor fuel assembly lifetime (TRITON data) and 5 years in the spent fuel pool (ORIGEN). Rodded and unrodded cases are plotted.

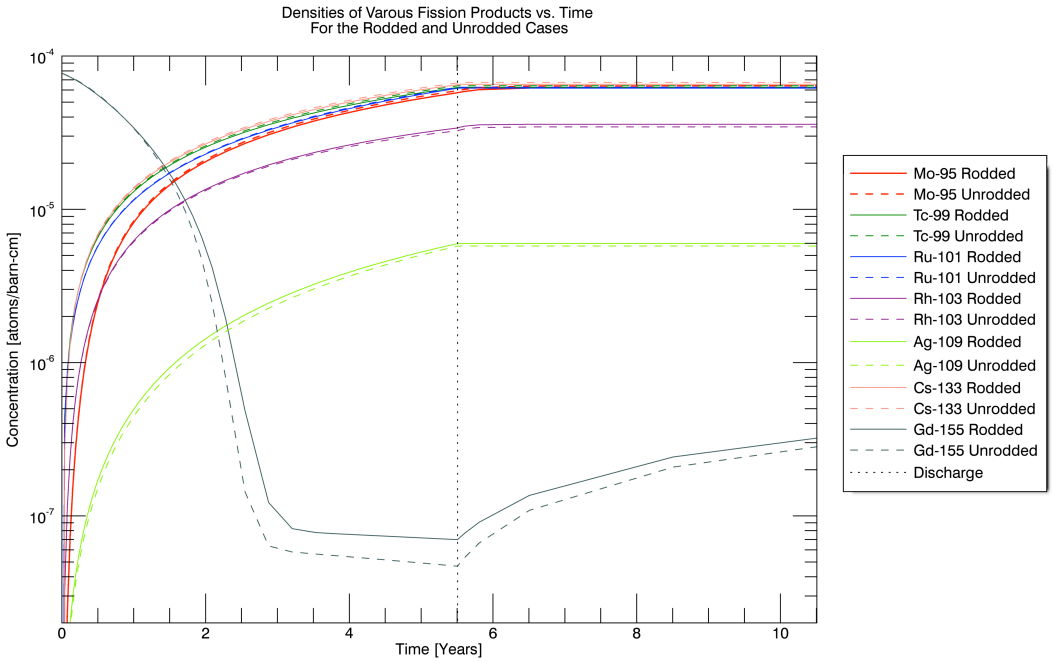

Figure 12. Various fission product concentrations in the fuel during the in-reactor fuel assembly lifetime (TRITON data) and 5 years in the spent fuel pool (ORIGEN). Rodded and unrodded cases are plotted.

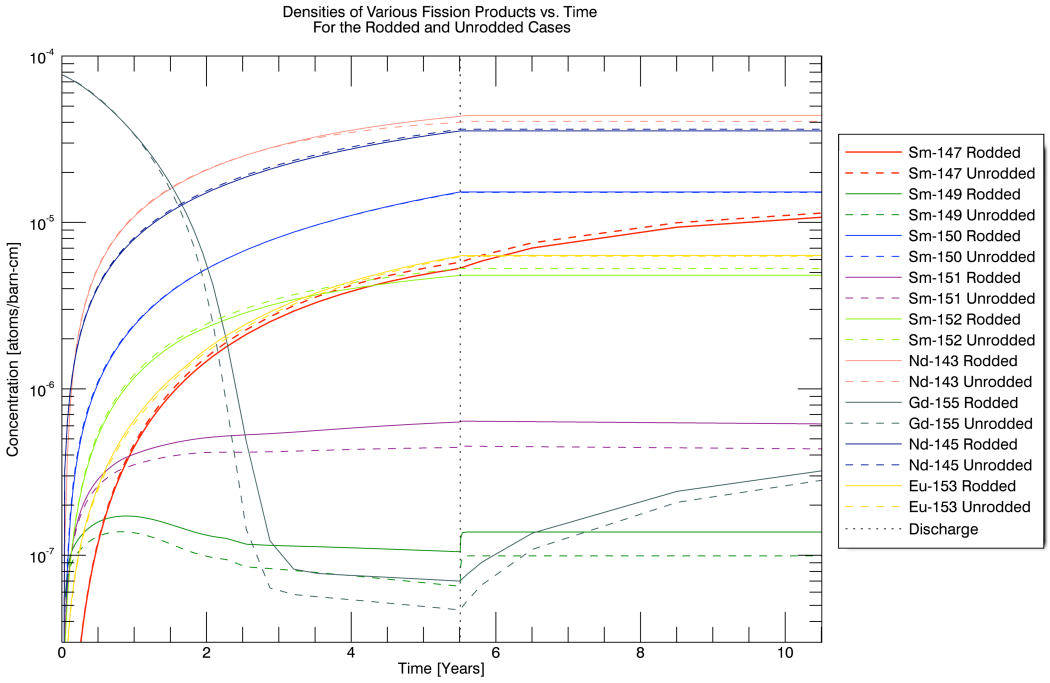

Figure 13. Various fission product concentrations in the fuel during the in-reactor fuel assembly lifetime (TRITON data) and 5 years in the spent fuel pool (ORIGEN). Rodded and unrodded cases are plotted.

For cases in which control rod insertion varies with time, the neutron multiplication factor for storage configurations will lie between the cases of rodded and unrodded. This will also be true for the majority of nuclide densities.

2.4.5 Effect of Control Blade Insertion On Criticality

Rodded versus unrodded cases show there is a significant difference in criticality after fuel irradiation and some storage time. This verifies that in fact control blade histories need to be treated properly in order to calculate the k_{eff} of UNF in the dry storage configuration properly.

2.4.6 Researched Control Blade Insertion Patterns

As stated previously, it is desirable to be able to predict the effects of all control blade patterns on nuclide densities, not just practical and predictable patterns that may come from routine operation. In turn, the methodology will be more broadly applicable to

BWR UNF characterization. Therefore, for the purpose of this research a variety of control blade histories have been generated as test scenarios. Figure 14 depicts the control blade histories for the time-independent cases (unrodded and rodded) that will be used to predict the nuclide densities in the time-dependent cases shown in Figure 15.

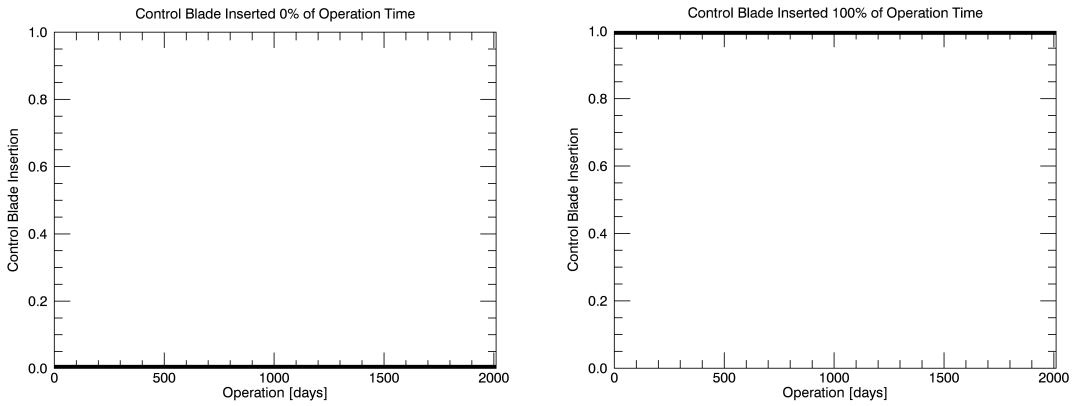

Figure 14a. (left) The control blade history variable for a 2-dimensional model is represented here by a 0 (control blade not inserted) or a 1 (control blade fully inserted). This is a time-independent case for no control blade inserted. Figure 14b. (right) This figure represents the time-independent case where the lattice is modeled with a control blade fully inserted over burnup.

Three classes of time-dependent histories have been developed for testing. Those include histories that have 25%, 50%, and 75% time control blade insertion. This means that over the period, which the fuel assembly is being irradiated in the reactor, the control rod is inserted at that fuel assembly for 25%, 50%, or 75% of the fuel irradiation, irrespective of the pattern in which this is done. This is done to investigate the dependence of time (percent) insertion of control blade on isotopic densities. For each of these three classes, there are four sequences, which have been designed for each class. Differing time sequences are used to investigate the result of continuous control blade insertion with that of sporadic insertion with the same time percent insertion. Additionally, each of these sequences has been temporally reversed to give a total of 8 patterns for each time percent class. This has been done to investigate the symmetry of the control blade insertion pattern on isotopics in the used fuel.

For each class (25%, 50%, or 75% time insertion) there are 4 sequences (referred to as 25-1, 25-2, 25-3, 25-4, 50-1, 50-2, 50-3, 50-4, 75-1, 75-2, 75-3, and 75-4) and each sequence is also temporally reversed to give a total of 8 patterns for each class. These are referred to as 25-1A, 25-1B, 25-2A, 25-2B, etc. These cases are depicted below in Fig. 15 and numerically described in Table 7.

Figure 15. Below are the control blade insertion patterns that will be simulated and tested with the developed methodology to investigate nuclide densities in UNF

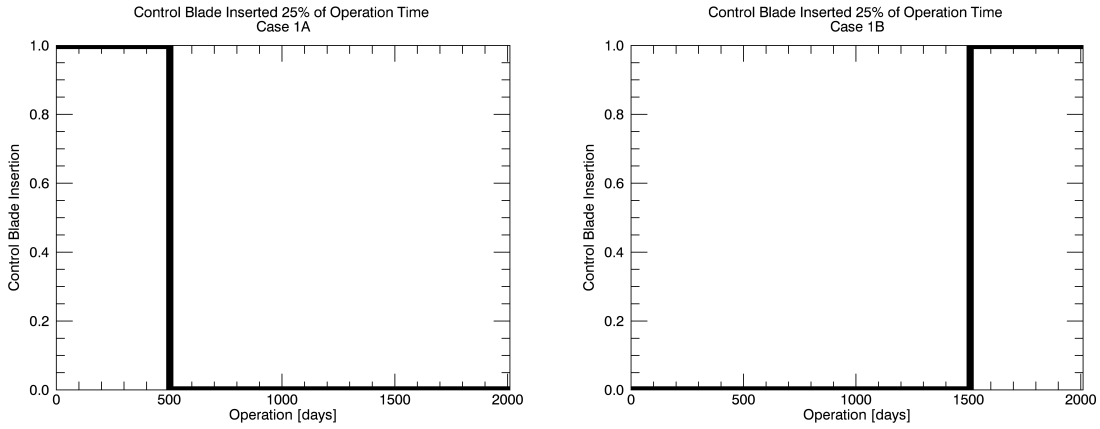

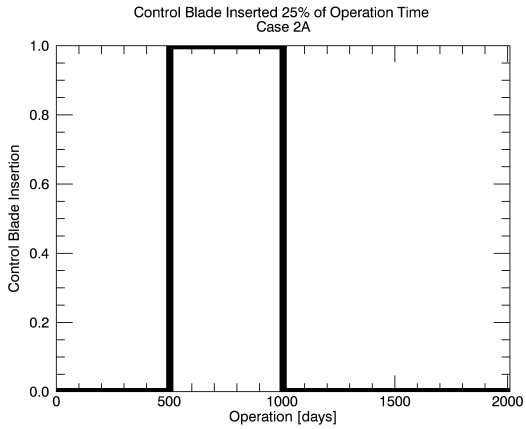
Control Blade Inserted 25% of Operation Time
Case 2A
Control Blade Insertion
Operation [days]
0.0
0.2
0.4
0.6
0.8
1.0
0
500
1000
1500
2000

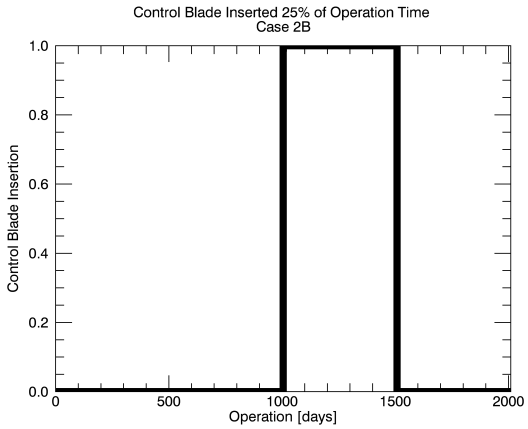
Control Blade Inserted 25% of Operation Time
Case 2B
Control Blade Insertion
Operation [days]
0.0
0.2
0.4
0.6
0.8
1.0
0
500
1000
1500
2000

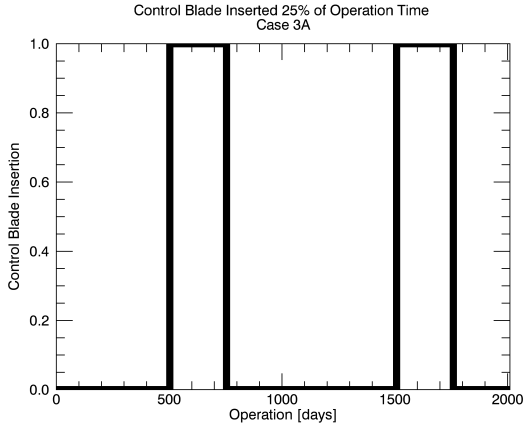
Control Blade Inserted 25% of Operation Time
Case 3A
Control Blade Insertion
Operation [days]
0.0
0.2
0.4
0.6
0.8
1.0
0
500
1000
1500
2000

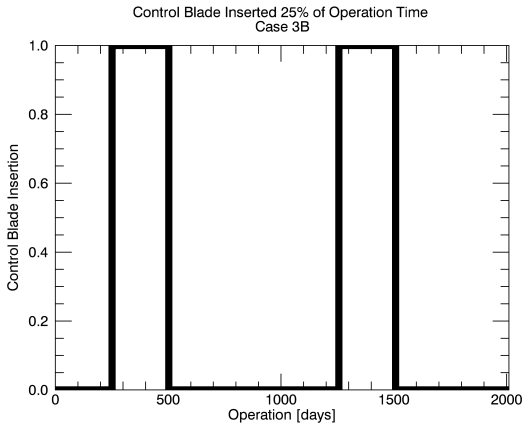
Control Blade Inserted 25% of Operation Time
Case 3B
Control Blade Insertion
Operation [days]
0.0
0.2
0.4
0.6
0.8
1.0
0
500
1000
1500
2000

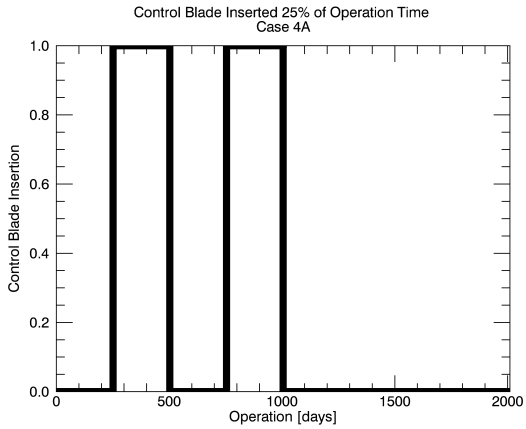
Control Blade Inserted 25% of Operation Time
Case 4A
Control Blade Insertion
Operation [days]
0.0
0.2
0.4
0.6
0.8
1.0
0
500
1000
1500
2000

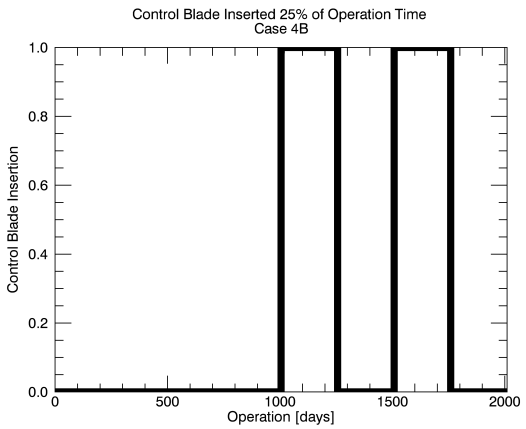
Control Blade Inserted 25% of Operation Time
Case 4B
Control Blade Insertion
Operation [days]
0.0
0.2
0.4
0.6
0.8
1.0
0
500
1000
1500
2000

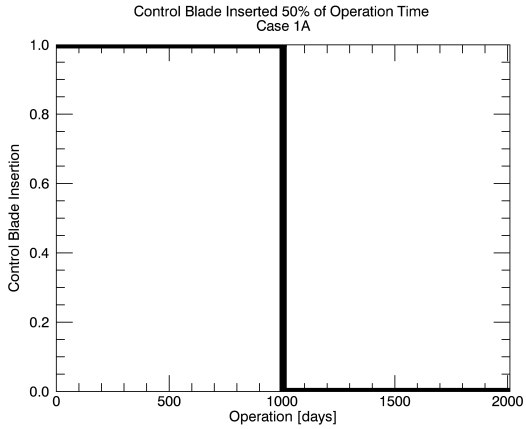
Control Blade Inserted 50% of Operation Time
Case 1A
Control Blade Insertion
Operation [days]
0.0
0.2
0.4
0.6
0.8
1.0
0
500
1000
1500
2000

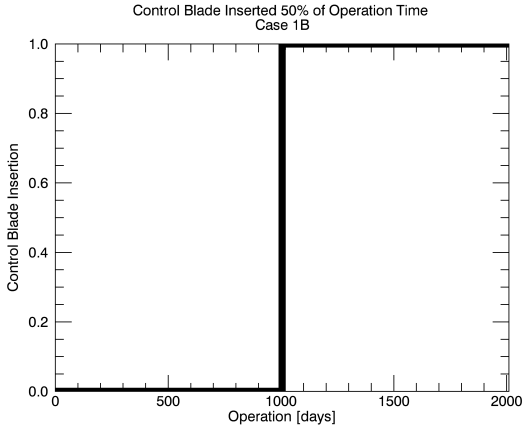
Control Blade Inserted 50% of Operation Time
Case 1B
Control Blade Insertion
Operation [days]
0.0
0.2
0.4
0.6
0.8
1.0
0
500
1000
1500
2000

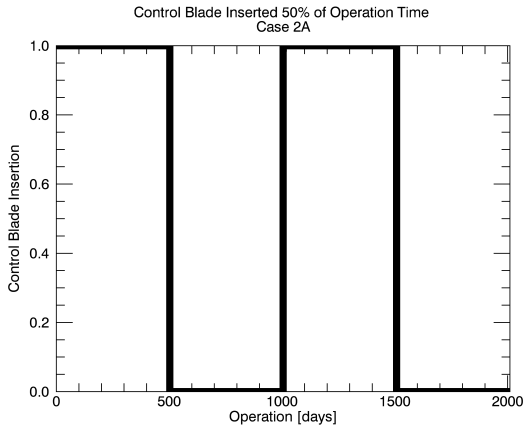
Control Blade Inserted 50% of Operation Time
Case 2A
Control Blade Insertion
Operation [days]
0.0
0.2
0.4
0.6
0.8
1.0
0
500
1000
1500
2000

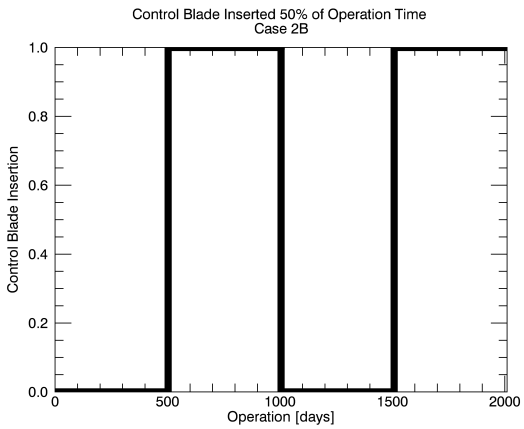
Control Blade Inserted 50% of Operation Time
Case 2B
Control Blade Insertion
Operation [days]
0.0
0.2
0.4
0.6
0.8
1.0
0
500
1000
1500
2000

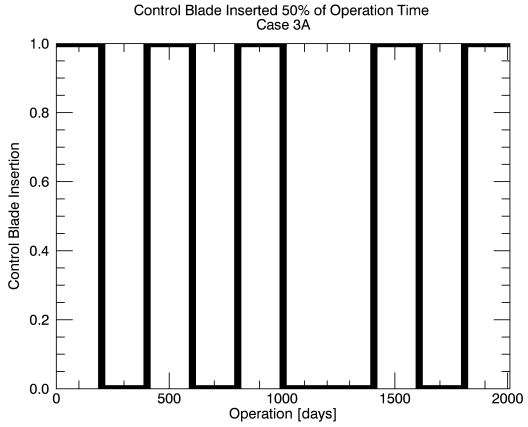
Control Blade Inserted 50% of Operation Time
Case 3A
Control Blade Insertion
Operation [days]
0.0
0.2
0.4
0.6
0.8
1.0
0
500
1000
1500
2000

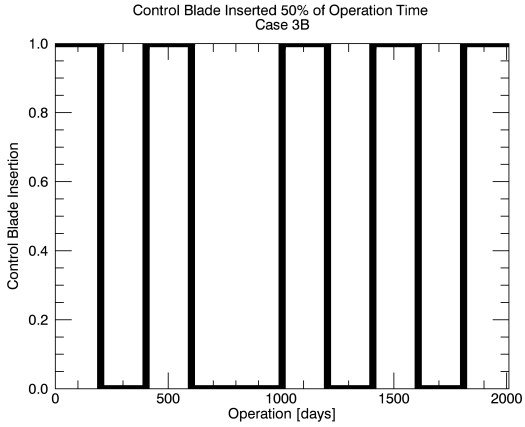
Control Blade Inserted 50% of Operation Time
Case 3B
Control Blade Insertion
Operation [days]
0.0
0.2
0.4
0.6
0.8
1.0
0
500
1000
1500
2000

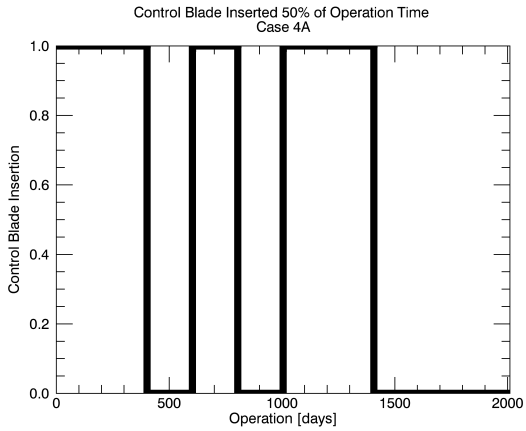
Control Blade Inserted 50% of Operation Time
Case 4A
Control Blade Insertion
Operation [days]
0.0
0.2
0.4
0.6
0.8
1.0
0
500
1000
1500
2000

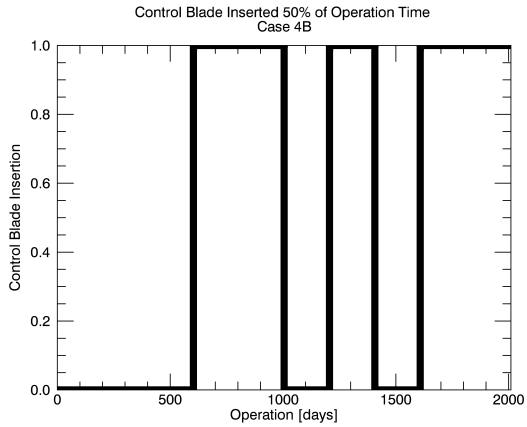
Control Blade Inserted 50% of Operation Time
Case 4B
Control Blade Insertion
Operation [days]
0.0
0.2
0.4
0.6
0.8
1.0
0
500
1000
1500
2000

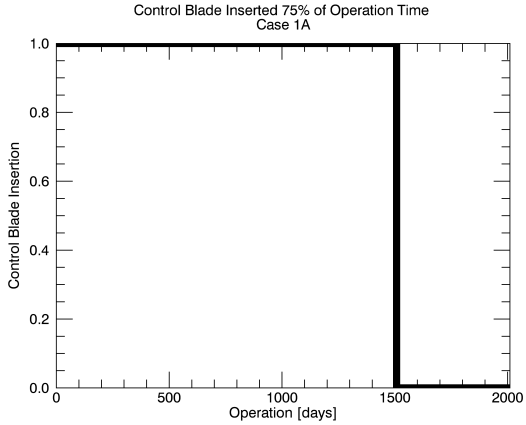
Control Blade Inserted 75% of Operation Time
Case 1A
Control Blade Insertion
Operation [days]
0.0
0.2
0.4
0.6
0.8
1.0
0
500
1000
1500
2000

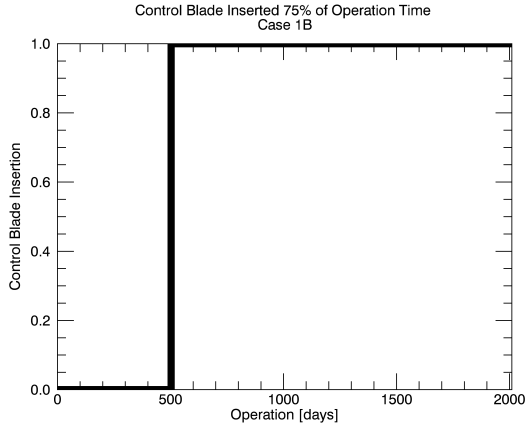
Control Blade Inserted 75% of Operation Time
Case 1B
Control Blade Insertion
Operation [days]
0.0
0.2
0.4
0.6
0.8
1.0
0
500
1000
1500
2000

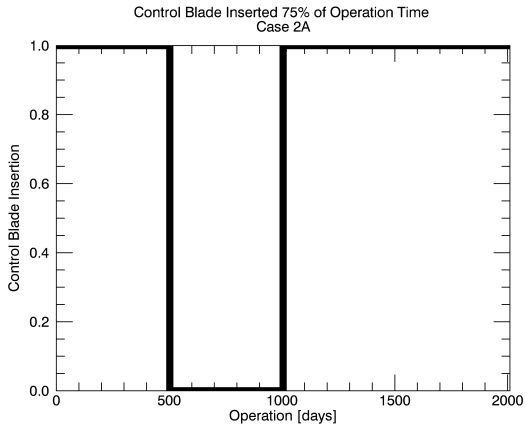
Control Blade Inserted 75% of Operation Time
Case 2A
Control Blade Insertion
Operation [days]
0.0
0.2
0.4
0.6
0.8
1.0
0
500
1000
1500
2000

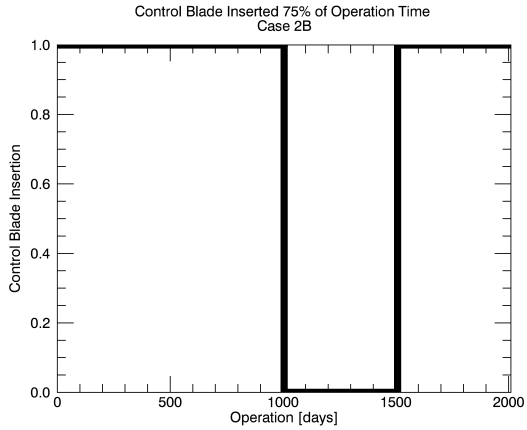
Control Blade Inserted 75% of Operation Time
Case 2B
Control Blade Insertion
Operation [days]
0.0
0.2
0.4
0.6
0.8
1.0
0
500
1000
1500
2000

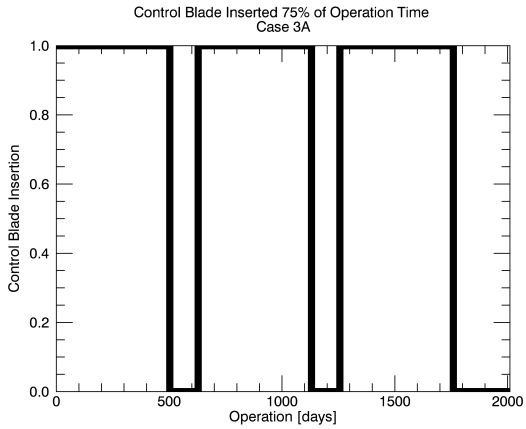
Control Blade Inserted 75% of Operation Time
Case 3A
Control Blade Insertion
Operation [days]
0.0
0.2
0.4
0.6
0.8
1.0
0
500
1000
1500
2000

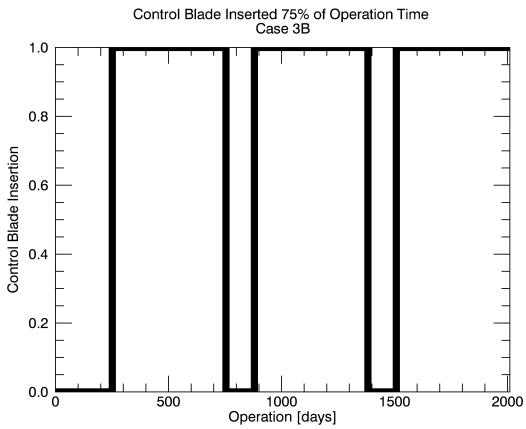
Control Blade Inserted 75% of Operation Time
Case 3B
Control Blade Insertion
Operation [days]
0.0
0.2
0.4
0.6
0.8
1.0
0
500
1000
1500
2000

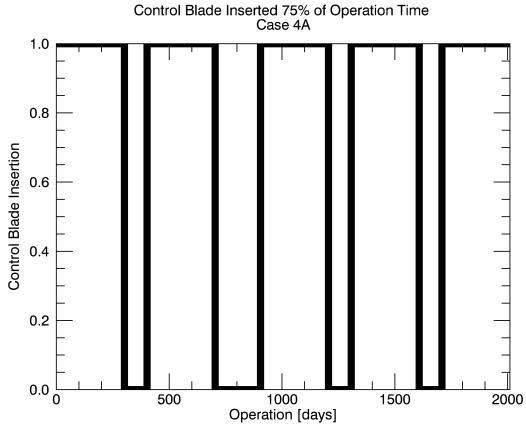
Control Blade Inserted 75% of Operation Time
Case 4A
Control Blade Insertion
Operation [days]
0.0
0.2
0.4
0.6
0.8
1.0
0
500
1000
1500
2000

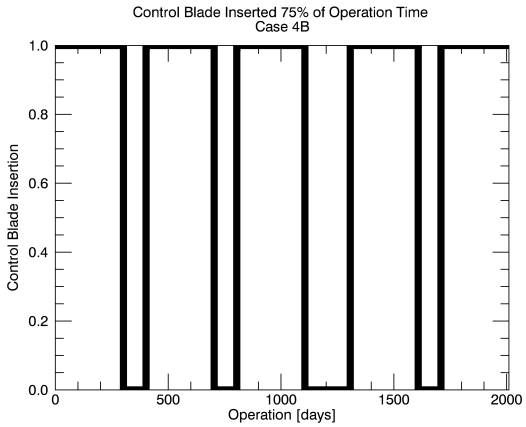
Control Blade Inserted 75% of Operation Time
Case 4B
Control Blade Insertion
Operation [days]
0.0
0.2
0.4
0.6
0.8
1.0
0
500
1000
1500
2000

Table 7. The control blade insertion patterns are described in the table below. For each pattern, the sequence is given in order with control blade insertion time and then the control blade state given in parentheses.

Control Blade Pattern	Percent Time Control Blade Insertion Over Fuel Irradiation (Control Rod State)								
25-1A	25 (1)	75 (0)							
25-1B	75 (0)	25 (1)							
25-2A	25 (0)	25 (1)	50 (0)						
25-2B	50 (0)	25 (1)	25 (0)						
25-3A	25 (0)	12.5 (1)	37.5 (0)	12.5 (1)	12.5 (0)				
25-3B	12.5 (0)	12.5 (1)	37.5 (0)	12.5 (1)	25 (0)				
25-4A	12.5 (0)	12.5 (1)	12.5 (0)	12.5 (1)	50 (0)				
25-4B	50 (0)	12.5 (1)	12.5 (0)	12.5 (1)	12.5 (0)				
50-1A	50 (1)	50 (0)							
50-1B	50 (0)	50 (1)							
50-2A	25 (1)	25 (0)	25 (1)	25 (0)					
50-2B	25 (0)	25 (1)	25 (0)	25 (1)					
50-3A	10 (1)	10 (0)	10 (1)	10 (0)	10 (1)	20 (0)	10 (1)	10 (0)	10 (1)
50-3B	10 (1)	10 (0)	10 (1)	20 (0)	10 (1)	10 (0)	10 (1)	10 (0)	10 (1)
50-4A	20 (1)	10 (0)	10 (1)	10 (0)	20 (1)	30 (0)			
50-4B	30 (0)	20 (1)	10 (0)	10 (1)	10 (0)	20 (1)			
75-1A	75 (1)	25 (0)							
75-1B	25 (0)	75 (1)							
75-2A	25 (1)	25 (0)	50 (1)						
75-2B	50 (1)	25 (0)	25 (1)						
75-3A	25 (1)	6.25 (0)	25 (1)	6.25 (0)	25 (1)	12.5 (0)			
75-3B	12.5 (0)	25 (1)	6.25 (0)	25 (1)	6.25 (0)	25 (1)			
75-4A	15 (1)	5 (0)	15 (1)	10 (0)	15 (1)	5 (0)	15 (1)	5 (0)	15 (1)
75-4B	15 (1)	5 (0)	15 (1)	5 (0)	15 (1)	10 (0)	15 (1)	5 (0)	15 (1)

2.5 GE-14 Model

In this section, some characteristics of the GE-14 fuel bundle geometry will be discussed. Structure of the fuel assembly, fuel characteristics used in the model, and boundary conditions are given.

2.5.1 Geometry and Structure

In order to model the GE-14 fuel assembly, a 2-dimensional model has been developed in order to examine depletion characteristics and isotopic densities over the burnup of the fuel. One fuel assembly and one quarter of a control blade have been selected as a symmetrical fragment from the core of the reactor. This lattice can be seen geometrically in Figure 16. The symmetry will allow reflective boundary conditions to be approximated at the boundary of this lattice. Both the structural materials and control blade can be viewed in Figure 16.

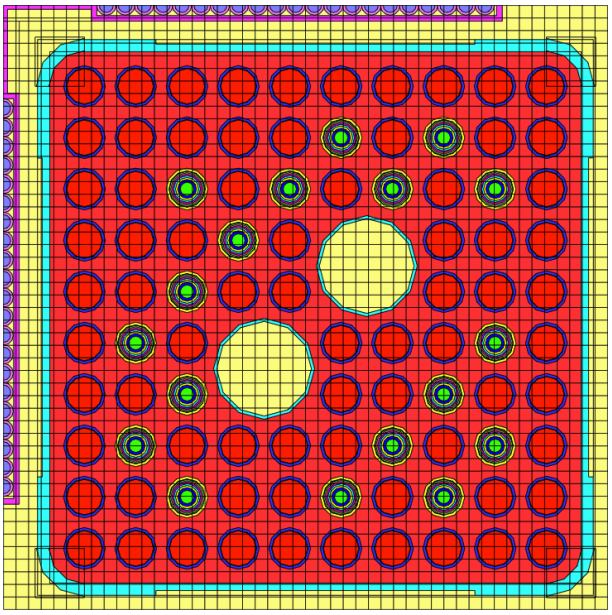

Figure 16. A 2-dimensional lattice is shown for the geometry of the GE-14 fuel bundle. The multi-colored fuel pins are fuel pins augmented with Gadolinium.

2.5.2 Fuel Characteristics

In order to maximize fuel performance in a BWR many different fuel pin arrangements are used in the fuel bundles that are then properly spatially distributed in the reactor core. An operating reactor will have fuel assemblies that contain varying enrichments, arrangements, partial length rods, varying control augmentation (Gd enrichment), and missing rods [9]. For the model in this research, average enrichment values of a full (no missing rods) fuel bundle have been chosen. This includes 18 fuel pins with Gd (74 UO_2 only pins). Average values have been selected in order to have an accurate representation of a realistic fuel bundle, and to be able to focus on the effects of control blade use on the nuclide densities of the fuel bundle over burnup of the fuel. The average enrichments that are used in all of the following modeling and simulations are listed in Table 8.

Table 8. Average enrichments for the two types of fuel pins used in the model. A constant value for void fraction is also used in this model.

GE-14 Full Fuel Assembly with Average Enrichments	
Fuel Pin Enrichment Weight Percent U^{235} (UO_2 Pins)	4.23378
Fuel Pin Enrichment Weight Percent U^{235} (UO_2 +Gd_2O_3 Pins)	4.6
Fuel Pin Enrichment Weight Percent Gd_2O_3 (UO_2 +Gd_2O_3 Pins)	0.0772
Void Fraction In Channel Box	40%

The moderator temperature and coolant void fraction varies axially along the fuel assemblies in BWRs. This will be taken into account upon further research, however, for

the research that is solely investigating effects of control blade usage on UNF, this variation will be omitted. Therefore, a constant value has been chosen for all calculations in this research.

2.5.3 Boundary Conditions

As mentioned previously, this lattice is a symmetric fragment of the center of a hypothetically infinite reactor. This gives validity to the reflective boundary conditions in the model. In a real world analysis this condition is affected by a varying power for any given fuel bundle and the bundles surrounding it. In this model, the lattice is depleted at an average assembly power of 25 MW/MTU. However, as the fuel is shuffled and depleted the specific power value for a fuel bundle can vary significantly. This power value and position in the reactor can have a significant impact on the actual boundary conditions for a lattice and can perturb the result for the UNF in a dry storage configuration.

2.6 SCALE Modeling

In this section, a description of the SCALE modules used for the 2-dimensional lattice physics and fuel depletion is presented. The approach of using a 2-dimensional model as an approach to burnup credit calculations will also be visited. Specific methods used in the research will be mentioned (Gad pin rings, MCDancoff, addnux).

2.6.1 SCALE 6.1

All calculations for this research were performed in the SCALE 6.1 code system (version 6.1.2) using the 238-neutron energy group ENDF/B-VII-based nuclear data library [20]. SCALE has been used to model and simulate the reactor geometry and operating conditions.

Modules such as T-NEWT and T-DEPL have been used because of their speed and ease of use. It is desirable to develop an accurate methodology for calculating isotopic densities using these methods that will then be checked for accuracy by more precise methods and experimental validation. In that way, the prediction of isotopics can be expedited through the more simple yet accurate calculations.

2.6.2 Statement of the Problem

At this point it is appropriate to properly state the problem to be solved. In order to solve for the time dependence of nuclide concentrations, all sources of formation and disappearance of a nuclide must be taken into account. In a reactor there are two processes that contribute: those include radioactive disintegration and neutron transmutation. The mathematical expression of this problem is formally known as the Bateman equation and can be written:

$$\frac{dN_i}{dt} = \sum_{j=1}^{m} l_{ij}\lambda_j N_j + \bar{\Phi}\sum_{k=1}^{m} f_{ik}\sigma_k N_k - (\lambda_i + \bar{\Phi}\sigma_i)N_i, \quad (i = 1,...,m) \ , \qquad (17)$$

(2.2.1)

where

N_i = atom density of nuclide i,
λ_i = radioactive disintegration constant of nuclide i,
σ_i = spectrum-averaged neutron absorption cross section of nuclide i,
$\bar{\Phi}$ = space- and energy-averaged neutron flux,
l_{ij} = branching fractions of radioactive disintegrations from other nuclides j,
f_{ik} = branching fractions for neutron absorption by other nuclides k that lead to the formation of species i.

Much of what is necessary to solve this equation comes from proper data such as branching fractions, proper energy and space-averaged neutron cross-sections that are prepared by the SCALE/TRITON modules, and space and energy-averaged flux that is prepared by NEWT. After all of this is provided, ORIGEN is able to solve the above stated equation for many nuclides very rapidly. The compositions in the model are updated based on the changes in density and the process starts over again, progressing forward in time until the maximum burnup is reached.

2.6.3 TRITON

TRITON (Transport Rigor Implemented with Time-dependent Operation for Neutronic depletion) [21] is characterized by SCALE developers as a multipurpose control module used to perform transport, depletion and sensitivity and uncertainty analysis. For the purposes of depletion calculations, TRITON is used to automate the process of creating problem-dependent cross-sections followed by multigroup transport calculations and used in tandem with the ORIGEN depletion module to calculate isotopic concentrations. TRITON automates execution of SCALE modules and manages data

transfer and input/output processes for easy and efficient communication between analysis sequences.

2.6.4 NEWT

NEWT (New ESC-based (Extended Step Characteristic) Weighting Transport code) is a multigroup discrete-ordinates radiation transport computer code with capabilities to handle complex geometry features that are characterized in an input file. NEWT can be incorporated into the SCALE TRITON sequence where TRITON will provide NEWT with the properly prepared cross sections based on the execution of the following modules. For the calculations done in this research, an S_n quadrature of order 6 was used.

CRAWDAD

The Code to Read And Write Data for Discretized solution (CRAWDAD) reads nuclear data from the general pointwise library files (nuclear data libraries) and puts it into the format needed for the discretized energy solution in CENTRM. Effectively, this module creates a continuous energy library for use by CENTRM and PMC.

BONAMI

BONAMI performs resonance self-shielding calculations for nuclides that have Bondarenko data associated with their cross sections. This module is always used in conjunction with NITAWL

WORKER

WORKER is a SCALE system module for creating and modifying working format libraries. It creates an AMPX working format library from a master format library.

CENTRM

CENTRM is a one-dimensional neutron transport code for computing pointwise energy spectra. Using the pointwise continuous cross-section library and a cell description, CENTRM creates a pointwise continuous flux spectrum. For the calculations done in this research, CENTRM used 1^{st} order P_L scattering.

PMC

PMC is a program to produce multigroup cross sections using pointwise energy spectra from CENTRM. Using the pointwise continuous flux spectrum created in CENTRM, PMC collapses pointwise continuous cross sections to a set of multigroup cross sections

2.6.5 T-DEPL

T-DEPL is a 2D TRITON depletion sequence that uses NEWT for the transport calculations. It also provides the capability to generate lattice-physics data for nodal core calculations. The depletion calculation can be broken into 3 major steps:

1. The post-processing of the flux – the transport solution is used to prepare region-averaged multigroup cross sections and flux values for each depletion material based on user input power or flux.

2. The COUPLE calculation – uses the region-averaged multigroup cross sections and fluxes to generate a one-group cross-section library for each depletion material.

3. The ORIGEN calculation – depletes each material using the power or flux from the post-processing and the one-group cross sections from the COUPLE calculation.

COUPLE

COUPLE is a nuclear decay and cross section data processing code for creating ORIGEN-S libraries. COUPLE computes weighted, problem-dependent ORIGEN-S neutron cross sections from a multigroup, AMPX working format library. COUPLE uses the multi-energy-group neutron cross sections to compute the properly weighted problem-dependent cross sections that will be used in the ORIGEN-S depletion calculations. It also produces the binary nuclear data libraries required by ORIGEN-S.

ORIGEN

(Oak Ridge Isotope Generation code) ORIGEN-S [22] is a code for computing changes in isotopic concentrations during neutron irradiation and radioactive decay. This code was developed to calculate nuclide compositions and radioactivity of fission products, activation products, and products of heavy metal transmutation. The time steps that were used in the depletion calculations are listed in Table 9.

Table 9. Burnup depletion steps used in the rodded and unrodded TRITON T-depl calculations. Steps this size or smaller were used in the time-dependent control blade insertion cases.

Steps [Days]	Steps [MWd/MTU]	Total [Days]	Total [GWd/MTU]
0.01	0.25	0.01	0.00
14.09	352.25	14.10	0.35
13.92	347.93	28.02	0.70
13.79	344.77	41.81	1.05
13.70	342.62	55.51	1.39
13.65	341.34	69.17	1.73
13.63	340.85	82.80	2.07
13.64	341.08	96.44	2.41
13.68	341.99	110.12	2.75
13.74	343.54	123.86	3.10
13.83	345.70	137.69	3.44
13.94	348.48	151.63	3.79
14.07	351.86	165.71	4.14
14.23	355.86	179.94	4.50
14.42	360.49	194.36	4.86
14.63	365.78	208.99	5.22
14.87	371.77	223.86	5.60
15.14	378.48	239.00	5.98
15.44	385.99	254.44	6.36
15.77	394.36	270.22	6.76
16.15	403.68	286.36	7.16
16.56	414.03	302.92	7.57
17.02	425.55	319.95	8.00
17.54	438.38	337.48	8.44
18.11	452.70	355.59	8.89
18.75	468.75	374.34	9.36
19.47	486.79	393.81	9.85
20.29	507.19	414.10	10.35
21.22	530.38	435.31	10.88
22.28	556.96	457.59	11.44
23.51	587.70	481.10	12.03
24.95	623.64	506.05	12.65
26.65	666.25	532.70	13.32
28.70	717.62	561.40	14.04

Table 9 continued.

31.24	780.89	592.64	14.82
34.44	861.01	627.08	15.68
38.65	966.30	665.73	16.64
44.48	1111.98	710.21	17.76
53.18	1329.54	763.39	19.08
67.88	1697.06	831.27	20.78
99.13	2478.22	930.40	23.26
120.00	3000.00	1050.40	26.26
120.00	3000.00	1170.40	29.26
120.00	3000.00	1290.40	32.26
120.00	3000.00	1410.40	35.26
120.00	3000.00	1530.40	38.26
120.00	3000.00	1650.40	41.26
120.00	3000.00	1770.40	44.26
120.00	3000.00	1890.40	47.26
120.00	3000.00	2010.40	50.26

2.6.6 Special Considerations

In modeling the 2-D BWR lattice, two special considerations were taken into account in order to make the calculations more realistic. The first was to modify the infinite pin cell calculation with a Monte Carlo correction factor using MCDANCOFF-calculated Dancoff factors. The second was to create a greater number of spatial regions in the gadolinium bearing rods in order to properly treat the flux depression and non-uniform depletion across the radius of the rod.

CHAPTER 3

METHODOLOGY

In this chapter, the piecewise data approximation method (PDA method) is described and illustrated. The role that the TRITON modeling plays in the PDA method is demonstrated in detail. How the PDA method is used to predict nuclide densities in UNF is also described and illustrated. A mathematical formulation is stated and hypotheses are made.

3.1 Previous Approach

At the present time, in order to accurately track nuclide densities in BWR fuel, detailed branch calculations must be performed to model operating conditions. Full simulation from beginning to end of in-reactor fuel lifetime has to be simulated with proper history variables (control blade state, void fraction) taken into account. This must be done for very many lattice conditions (void fractions, control rod state) and fuel assemblies (different enrichments and configurations) in order to provide data for UNF storage configuration criticality calculations. In many cases, cross-sections are tabulated for a variety of operating conditions and burnup values, and then nuclide concentrations are tracked in few-group nodal simulators that use diffusion theory. In order to reduce the amount of modeling, computation, and time necessary to represent isotopic densities in UNF for burnup credit, methodologies for predicting nuclide densities in BWR UNF based on a limited number of operating conditions (and computations) are being investigated. For the present case (the PDA method), a tabulated library of nuclide density values is compiled and then used to calculate nuclide density values as a function of burnup based control blade usage.

There exists a methodology for predicting few group homogenized cross sections of

a fuel assembly as a function of burnup based on history variables of the operating reactor for full core nodal simulators. This has been done in nodal core simulators such as SIMULATE and is used in burnup calculations in CASMO (MICROBURN-B2) [23]. It is done in the GENPMAXS cross-section processing module for the nodal simulator PARCS [24]. In this approach, the macroscopic cross section is equal to a reference solution with the addition of a cross section term that is dependent on the history variables. In the case for GenPMAXS a mathematical formulation for the interpolated cross sections can be represented by Equation 2.

$$\Sigma(\bar{H},B)=\Sigma(\bar{H}^{r},B)+\sum_{j=2}^{nh}\Delta h_j\left.\frac{\partial\Sigma}{\partial h_j}\right|_{(\bar{H}_j^{m},B)} \tag{2}$$

In this representation, H represents the array of history variable (control blade state, coolant density, etc.) and B represents burnup. The first term on the right hand side of the equation is a reference cross section Σ where all history variables are set to the default values H^r (control blade not inserted, etc.). The second term is a sum of the change in cross section based on the dependence of the cross section on that history variable h_j, and the step change in that variable that is made, Δh_j. This approach is simplified considerably for the case where only one history variable is considered, and for a 2-dimensional model the step change in state of the control rod variable can only be one or zero.

3.2 Present Methodology

The present methodology, "the piecewise data approximation" (referred to hereafter as "the PDA method"), is based on extending the previous approach of Eq. (2) to one that can be used for an arbitrary number of burnup steps and gives the nuclide-density dependence on burnup. The PDA method is used to predict nuclide densities in BWR UNF past the reactivity peak. The PDA method uses the isotopic density data obtained from TRITON for the rodded and unrodded cases as reference solutions to piece together

time-dependent behavior of nuclide densities over in-reactor fuel assembly lifetime with varying control blade insertion. The mathematical representation of this approach is shown in Eq. (3) below.

$$N\left(CB,B_j\right) = N_0 + \sum_{i=1}^{j} \Delta B_i \left.\frac{\partial N_R(CB,B)}{\partial B}\right|_{B=B_i} \tag{3}$$

In this representation, the density of a particular nuclide as a function of control blade history variable (CB = 1 for inserted or 0 for withdrawn) and burnup B is given by the density at the beginning of the in-reactor fuel lifetime with the addition of changes in density based on the burnup dependence of the reference solutions and the burnup step size. The first term on the right hand side is the density of the nuclide in the fuel upon insertion of the fuel assembly into the reactor. The second term on the right hand side is a sum over j burnup steps where ΔB_i is the size of the burnup step in consideration (GWd/MTU), and $N_R(CB,B)$ represents the reference solution being used at the burnup time step in consideration. If CB=1 at B_i then N_R is the rodded solution, if CB=0 at B_i then N_R is the unrodded solution. In this way a density function for any arbitrary control blade history and a burnup up to the value of the reference solutions can be constructed.

The essence of the above approach is to form a piecewise function using the slopes of the reference solutions. At points in burnup value where there is a change in control blade state there will be a change in reference solution being used in the sum. At these points, the tail of the present reference solution as a function of burnup is concatenated onto the previous solution. This is demonstrated in Fig. 17 below.

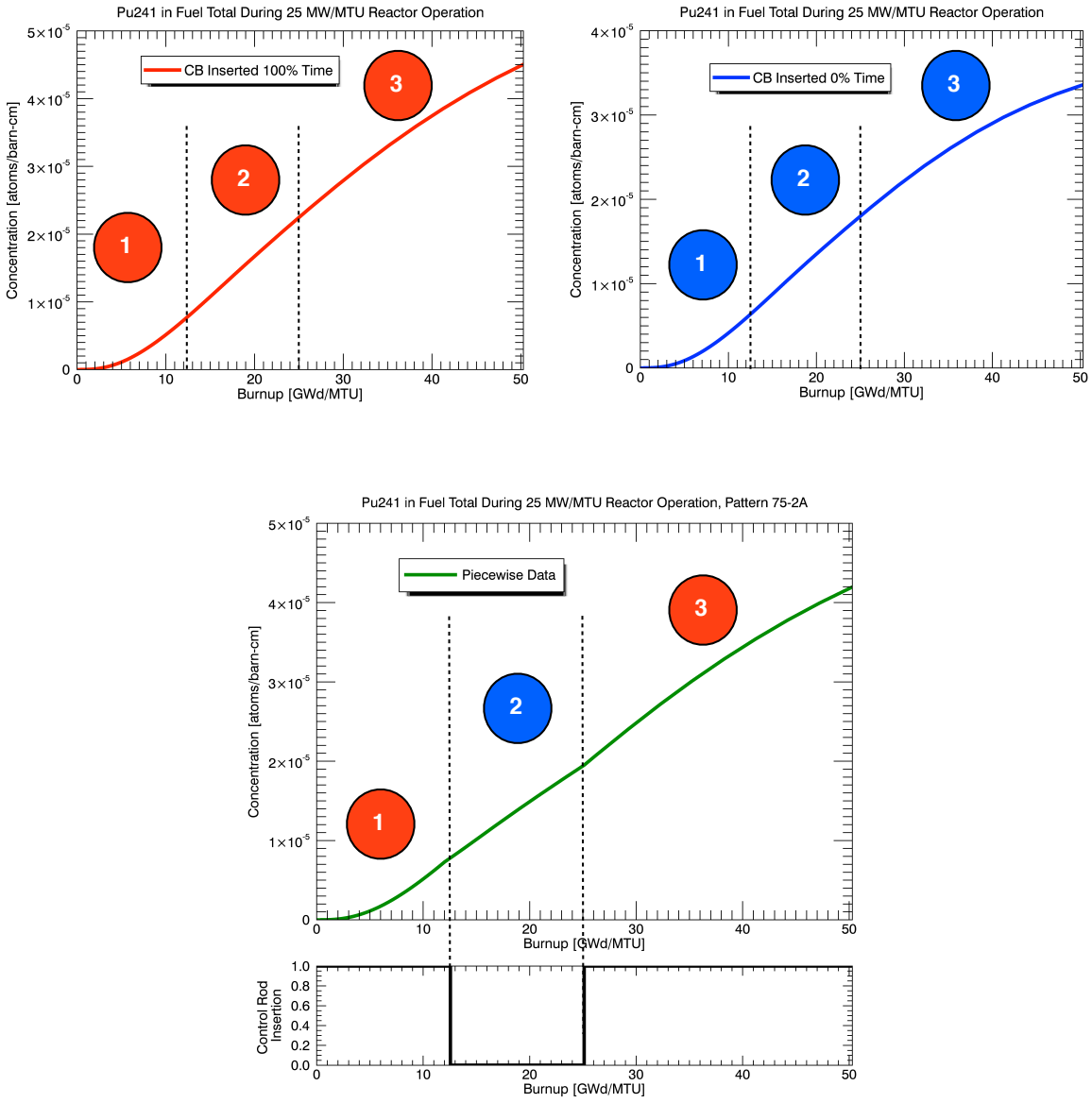

Figure 17. Above is a specific example to demonstrate how the piecewise data is constructed from the reference solutions. The reference solutions for ^{241}Pu over 50 GWd/MTU of in-reactor irradiation are shown at the top of the figure as the rodded and unrodded functions. Based on the control blade history variable, which is plotted at the bottom (75% time rodded, pattern 2A in Table 7), the piecewise data is constructed from the reference solutions.

3.3 Criteria for Success and Hypotheses

There are several criteria for which this approach will be most successful and accurate in prediction of nuclide densities in BWR UNF. The desired criteria include:

1. The sign of the derivative of the present reference solution (rodded or urodded data) being used must match the sign of the derivatives of the time-dependent data obtained from TRITON.
2. The prediction of nuclide densities must be bounded by the rodded and unrodded cases.
3. The prediction of nuclide densities must be conservative with respect to fuel reactivity.

It was anticipated that there are some cases in which the above criteria are not satisfied. As an example, Fig. 18 shows the data for ^{239}Pu in the 50% time rodded case, pattern 50-1A from Table 7. The ^{239}Pu density function has predominately positive derivatives with respect to burnup in the rodded and unrodded cases over the in-reactor fuel assembly lifetime. The actual behavior of the density function, however, shows significant decrease in density during the second half of the in-reactor fuel assembly lifetime (negative derivative with respect to burnup).

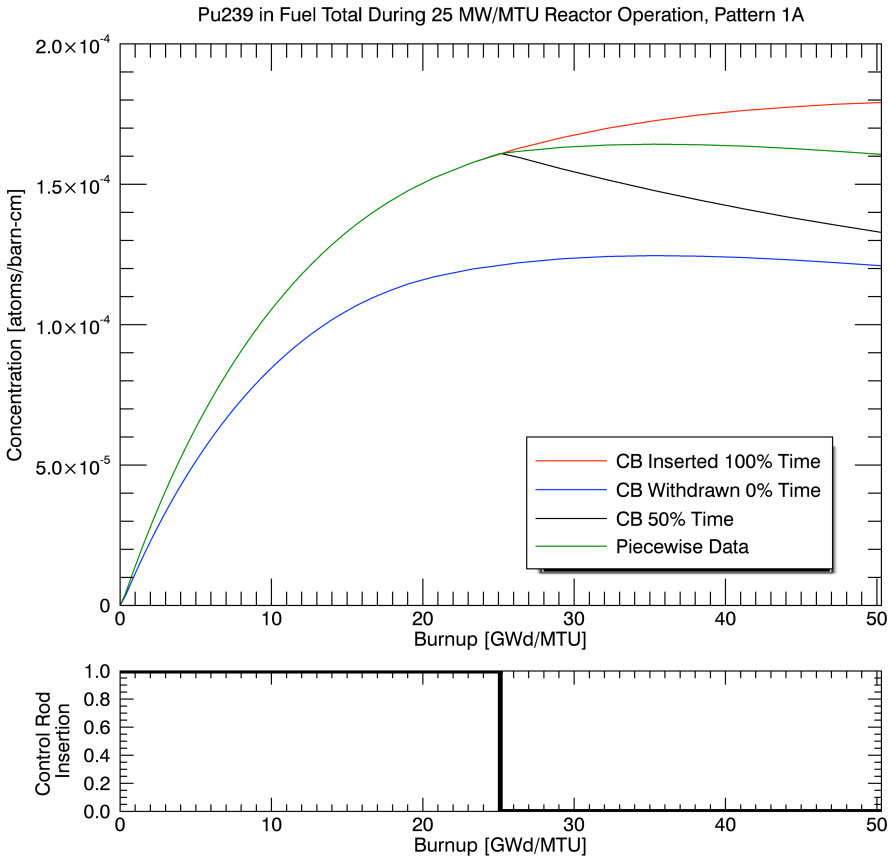

Figure 18. The total ^{239}Pu density in the modeled single GE-14 fuel assembly for the rodded, unrodded, 50-1A control blade pattern (Table 7), and the piecewise data calculation.

3.4 Assessment of Conservative Predictions

For the purposes of calculating criticality of UNF in a storage configuration, it is necessary to know whether the predicted nuclide densities are conservative with respect to reactivity (i.e. k_{eff}) . In this case conservative indicates that the prediction will over-estimate nuclide density in the direction that will increase the k_{eff} of the storage configuration calculations. This is so that the actual k_{eff} of the UNF in the storage configuration will be bounded by the calculations.

In this research, the nuclides that are in consideration for burnup credit are put into

three categories.

1.) Fissile and fissionable nuclides. Increased densities of these nuclides will always increase the reactivity of the fuel. As such, increased density predicted for these nuclides is a conservative prediction.

2.) Neutron poisons. Increased densities of these nuclides will always decrease the reactivity of the fuel. As such, decreased density predicted for these nuclides is a conservative prediction. This group includes the fission products as well as ^{155}Gd and ^{237}Np.

3.) Fertile nuclides. These nuclides must be assessed on a nuclide-to-nuclide and case-to-case basis. Some of them have a greater absorption of neutrons than transmutation and reaction to produce neutrons. Others behave oppositely.

CHAPTER 4

RESULTS

In this chapter, results obtained from the methods described in Chapter 3 are given for the 29 nuclides in consideration for the time-dependent control blade insertion cases that were shown in Figure 10 and Table 7. The results (nuclide densities) obtained with the PDA method are compared with the rodded and unrodded cases and with the time-dependent control blade insertion case results obtained from TRITON. The desired result of the PDA method is to accurately predict nuclide densities in high burnup BWR UNF, therefore this chapter focuses on nuclide densities for a hypothesized discharge burnup for a fuel assembly of 50.3 GWd/MTU (2010 days of 25 MW operation).

4.1 Time-Dependent Control Blade Insertion Effect On Storage Criticality

As was done in Section 2.4.4 in order to demonstrate the difference in criticality of the storage configuration based on the rodded and unrodded operating conditions, this has also been done for the time-dependent control blade insertion patterns. As before, in order to assess the effect of control blade use on UNF that is placed in the dry storage configuration, a sequence of modeling approaches is applied. First the fuel is depleted using the T-DEPL module (described in section 2.6) to simulate in-reactor fuel assembly irradiation. Nuclide densities are tracked through this process. Then fuel cooling is simulated using the ORIGEN-ARP module, which simulates the decay and buildup of actinides and fission products over the time spent in the spent fuel pool. Finally, the isotopic concentrations are taken and placed into the reactor fuel bundle configuration (no control rod present), and a 2-D NEWT transport calculation is performed. This will yield a k_{inf} value that is proportional to what would be expected from the dry storage configuration.

These calculations create an envelope of possible criticality values which are bounded by the rodded and unrodded cases, and enclosed by the 1A/1B control blade insertion patterns as seen in Fig. This demonstrates that the criticality of the UNF in the storage configuration is bounded by the rodded and unrodded cases. For a time-dependent control blade insertion pattern, criticality is bounded by the 1A/1B control blade insertion patterns.

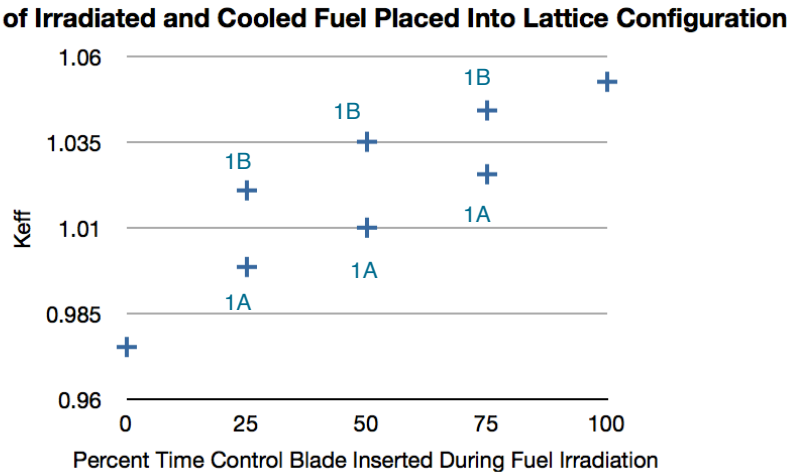

Figure 19. k_{eff} values for irradiated and cooled fuel placed into the lattice configuration for the rodded, unrodded 1A and 1B sequences.

4.2 Nuclide Densities for Rodded and Unrodded Cases

It was anticipated that the rodded and unrodded cases of irradiation for the modeled fuel assembly would be bounding cases in density to the time-dependent cases of control rod history. The density data for the rodded and unrodded cases for the 29 nuclides of importance for BUC are presented in Table 10 and their trends in behavior are analyzed.

Table 10. TRITON simulated density values (atom/barn-cm) at 50 GWd/MTU for the rodded and unrodded cases.

Fissile Nuclides

	U-235	Pu-239	Pu-241
Rodded	2.2780E-04	1.7910E-04	4.5020E-05
Unrodded	1.7100E-04	1.2100E-04	3.3560E-05

Fission Product Nuclides

	Mo-95	Tc-99	Ru-101	Rh-103
Rodded	5.7650E-05	6.2650E-05	6.1680E-05	3.3980E-05
Unrodded	5.9500E-05	6.4120E-05	6.2620E-05	3.2570E-05

	Ag-109	Cs-133	Nd-143	Nd-145
Rodded	5.9750E-06	6.5180E-05	4.3440E-05	3.5470E-05
Unrodded	5.7510E-06	6.6920E-05	3.9950E-05	3.6280E-05

	Sm-147	Sm-149	Sm-150	Sm-151
Rodded	5.3050E-06	1.0550E-07	1.5260E-05	6.3400E-07
Unrodded	5.7660E-06	6.5390E-08	1.5160E-05	4.4650E-07

	Sm-152	Eu-151	Eu-153	Gd-155
Rodded	4.8070E-06	1.2300E-09	6.2890E-06	7.0150E-08
Unrodded	5.2830E-06	6.2790E-10	6.2220E-06	4.7030E-08

Table 10 continued.

Fertile Nuclides

	U-234	U-236	U-238	Pu-238
Rodded	2.9180E-06	1.3950E-04	0.02095	8.6500E-06
Unrodded	3.0000E-06	1.4060E-04	0.02108	6.7260E-06
	Pu-242	**Am-241**	**Am-243**	**Pu-240**
Rodded	1.7270E-05	2.5670E-06	4.8420E-06	7.4300E-05
Unrodded	1.8600E-05	1.7260E-06	4.6350E-06	6.6770E-05

Table 10 shows that time-independent control blade presence decreases thermal fission of ^{235}U while increasing production of ^{239}Pu and ^{241}Pu at the given burnup. This behavior is expected from the time-independent cases of control blade use, which create neutron spectral shifts that are static through the in-reactor fuel assembly lifetime. For the rodded and unrodded cases, which have approximately static neutron spectrums, many of the nuclides in consideration here reach a density saturation at the given burnup.

The density values for the listed fission products show different trends with control blade use. This can be attributed to the terms in Eq. (1) described in Section 2.6.2 (Bateman equation). The final density values have complex dependencies on flux magnitude and energy and nuclide densities. These dependencies make it very difficult to heuristically reason through trends in accumulation and depletion of fission products.

Fertile uranium isotope densities decrease with the use of control blades in the rodded case compared to the unrodded. This indicates that the production of these isotopes has decreased, the transmutation has increased, or both of these have occurred. For the case of ^{234}U, the decay chain in Fig. 5 indicates that a faster spectrum would

decrease ^{234}U production through decreased production of ^{238}Pu and the (n,2n) reaction in ^{234}U would be increased. For ^{236}U, thermal absorption and the (n,γ) reaction of ^{235}U is decreased resulting in lower ^{236}U density values. For ^{238}U, transmutation to ^{237}U through a fast (n,2n) reaction is more predominant in the rodded case compared to the unrodded. There is an increase in ^{238}Pu, ^{240}Pu, ^{241}Am, and ^{243}Am with the rodded case. This results from a decrease in thermal fission and an increase in transmutation (and beta decay). ^{242}Pu experiences a decrease in density in the rodded case.

The trends seen in the rodded case compared to that in the unrodded case for the 28 nuclides are summarized in Table 11. This table indicates the directional change in density of the burnup credit nuclides with the rodded case compared to the rodded case. If the density of a particular nuclide is higher for the rodded case the arrow points upward and if the density of that nuclide is lower for the rodded case, the arrow points downward. Whether these trends hold true for the time-dependent control blade insertion patterns will be investigated. For those nuclides that do not retain the same trend, there may be some dependence on nuclide density.

Table 11. The directional change in nuclide density value based on the rodded case compared to the unrodded case is summarized below.

	Effect of Control Blade In Rodded and Unrodded cases
Ag 109	⇧
Am 241	⇧
Am 243	⇧
Cs 133	⇩
Eu 151	⇧
Eu 153	⇧
Gd 155	⇧
Mo 95	⇩
Nd 143	⇧
Nd 145	⇩
Np 237	⇧
Pu 238	⇧
Pu 239	⇧
Pu 240	⇧
Pu 241	⇧
Pu 242	⇩
Rh 103	⇧
Ru 101	⇩
Sm 147	⇩
Sm 149	⇧
Sm 150	⇧
Sm 151	⇧
Sm 152	⇩
Tc 99	⇩
U 234	⇩
U 235	⇧
U 236	⇩
U 238	⇩

4.3 Nuclide Densities as a Function of Time Percentage Control Blade Insertion

In this section, nuclide densities as a function of control blade insertion time (%) are presented and analyzed. Figures 20-22, respectively, show the results of the three

fissile nuclides. Figures 22-35, respectively, show the results of the fourteen fission-product nuclides. Figures 37-44, respectively, show the results of the eight fertile nuclides. The actual nuclide density values fore each case of the PDA method and the TRITON data are provided in Appendix A.

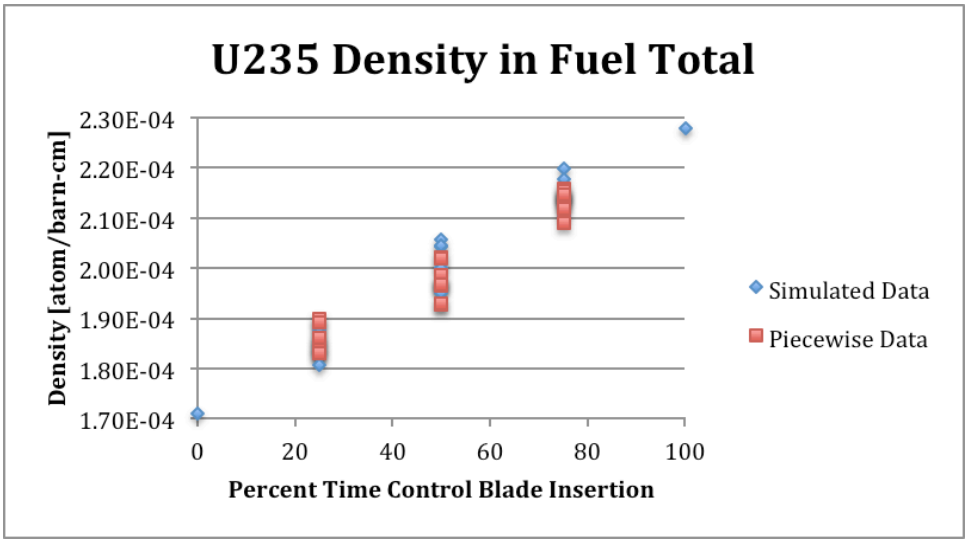

Figure 20. ^{235}U density in the total of the fuel in the assembly based on the rodded and urnrodded TRITON data and the time-dependent PDA method data.

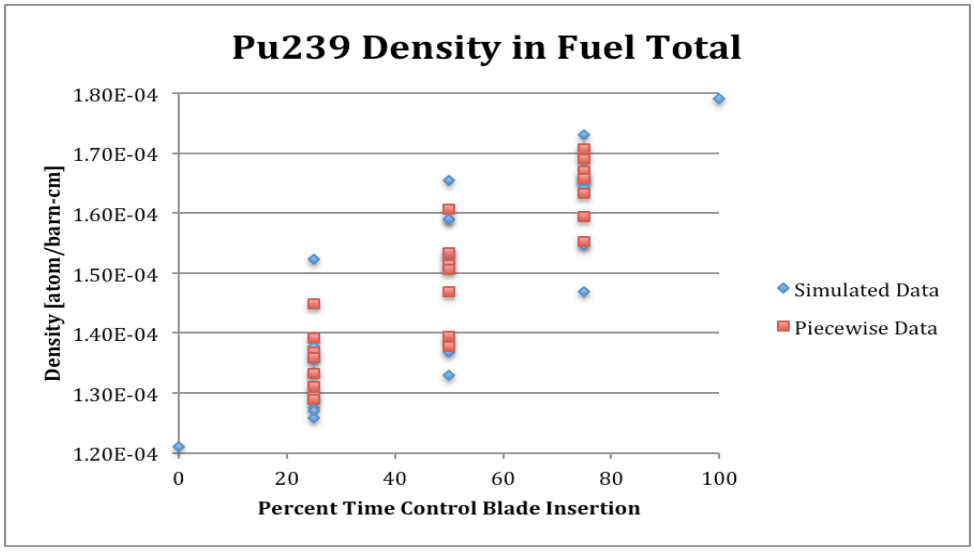

Figure 21. ^{239}Pu density in the total of the fuel in the assembly based on the rodded and urnrodded TRITON data and the time-dependent PDA method data.

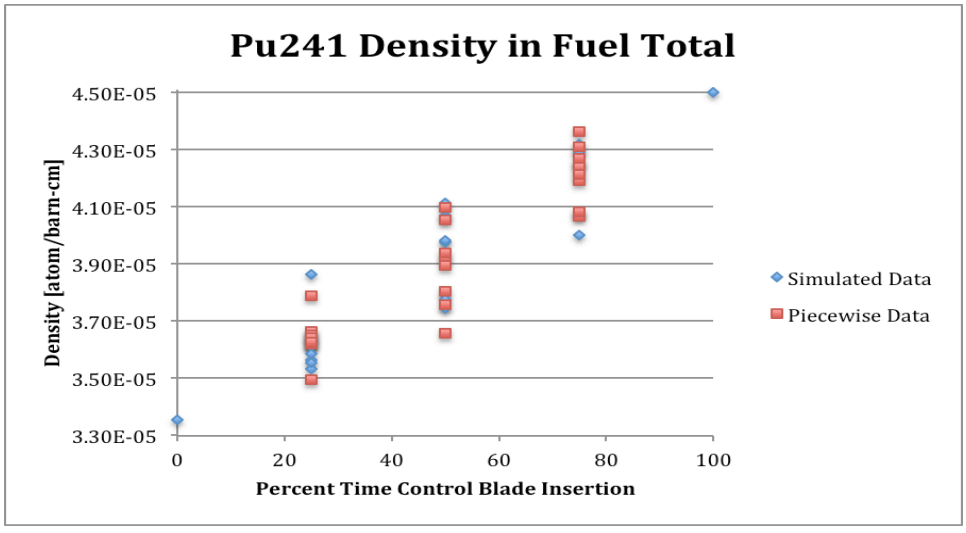

Figure 22. ^{241}Pu density in the total of the fuel in the assembly based on the rodded and urnrodded TRITON data and the time-dependent PDA method data.

Figures 20-22 show that for the fissile nuclides, density values increase in a fairly uniform manner with increasing control blade insertion time. For the fissile nuclides there are no density values predicted (by the PDA method or by TRITON simulation) that are outside the bounds of the rodded and unrodded cases. ^{235}U shows a very small spread of density values for each of the time percent control blade insertion times despite the varying patterns within. The PDA method performs very well in predicting the nuclide density of ^{235}U with a largest disparity from the TRITON data of 5.8% difference. ^{239}Pu shows the largest variance in density values of the fissile nuclides and the largest percent difference between the PDA method and the TRITON data values. The percent differences between the results of TRITON simulation and that of the PDA method are as large as 20.9% (this occurs for the 50-1A pattern). Using the PDA method, there is no apparent tendency for over or under predicting the nuclide densities compared to that obtained from TRITON simulation. The density values for ^{241}Pu are approximately a factor of 1/3 smaller than the density values for ^{235}U and ^{239}Pu, and the PDA method is very accurate in predicting density values of ^{241}Pu, the largest percent error being 3.1%.

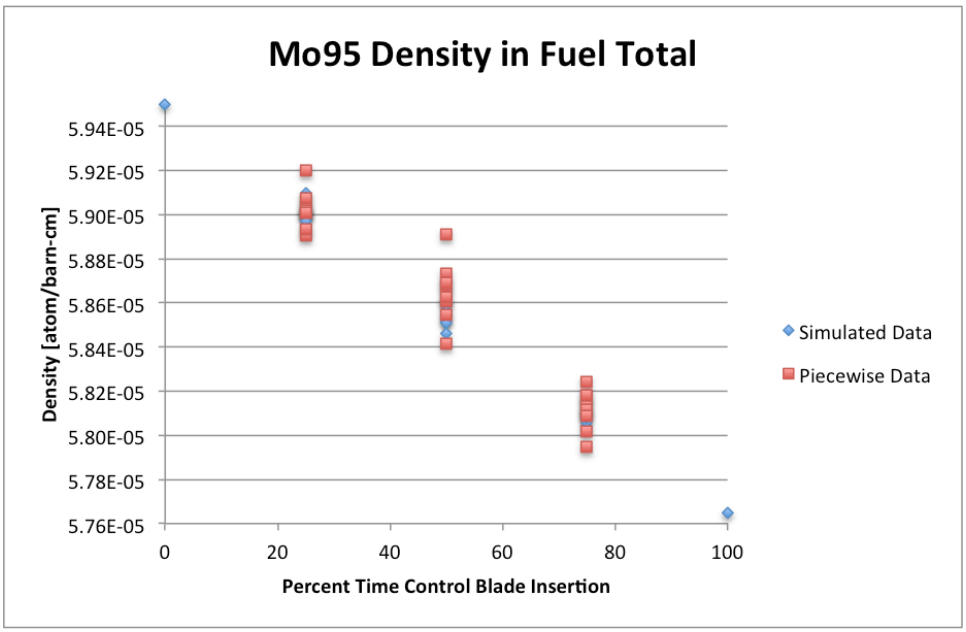

Figure 23. ^{95}Mo density in the total of the fuel in the assembly based on the rodded and urnrodded TRITON data and the time-dependent PDA method

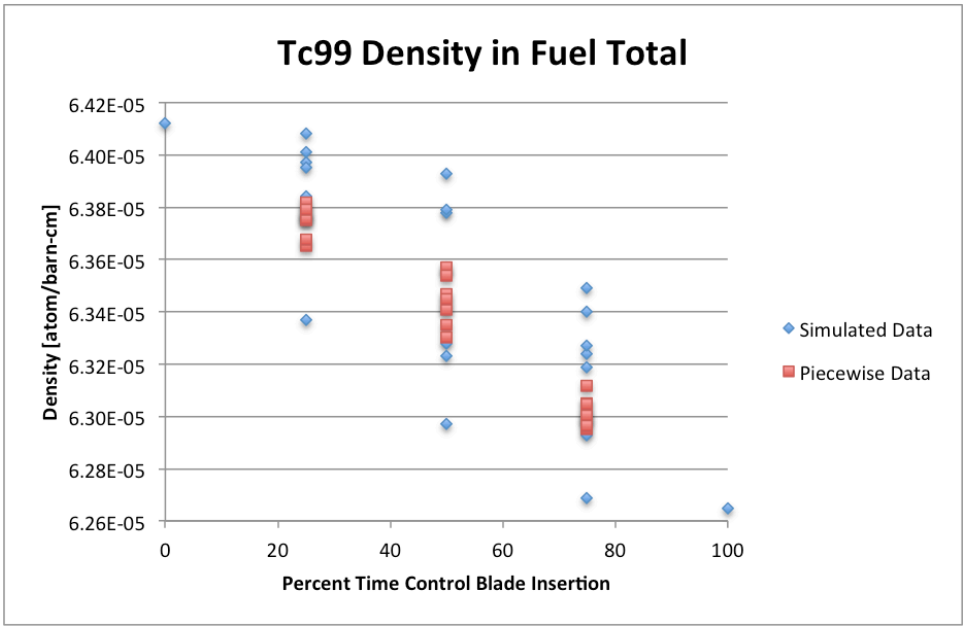

Figure 24. ^{99}Tc density in the total of the fuel in the assembly based on the rodded and urnrodded TRITON data and the time-dependent PDA method

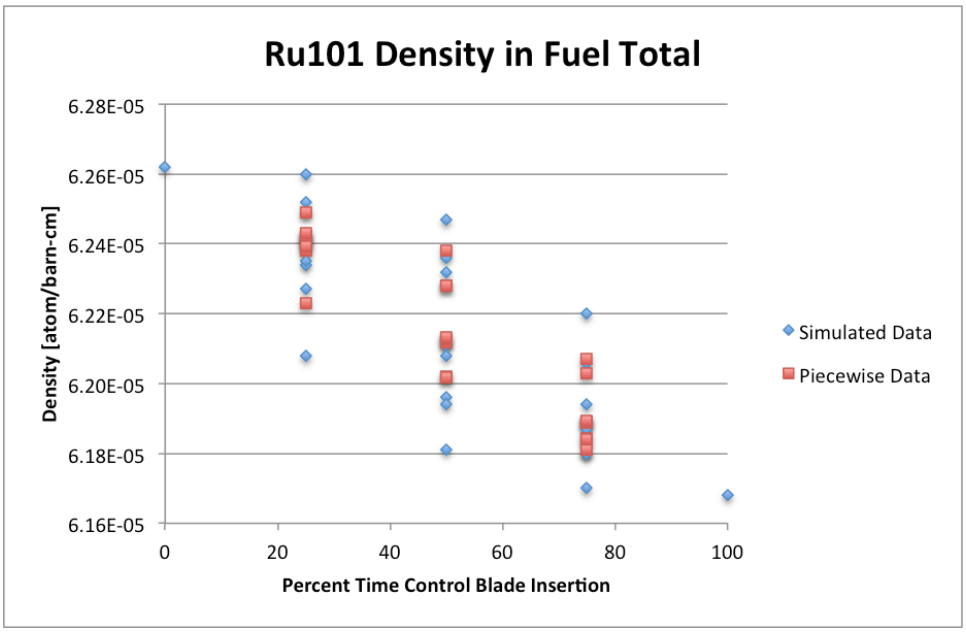
Ru101 Density in Fuel Total
6.28E-05
6.26E-05
6.24E-05
6.22E-05
6.20E-05
6.18E-05
6.16E-05
Density [atom/barn-cm]
0
20
40
60
80
100
Percent Time Control Blade Insertion
Simulated Data
Piecewise Data

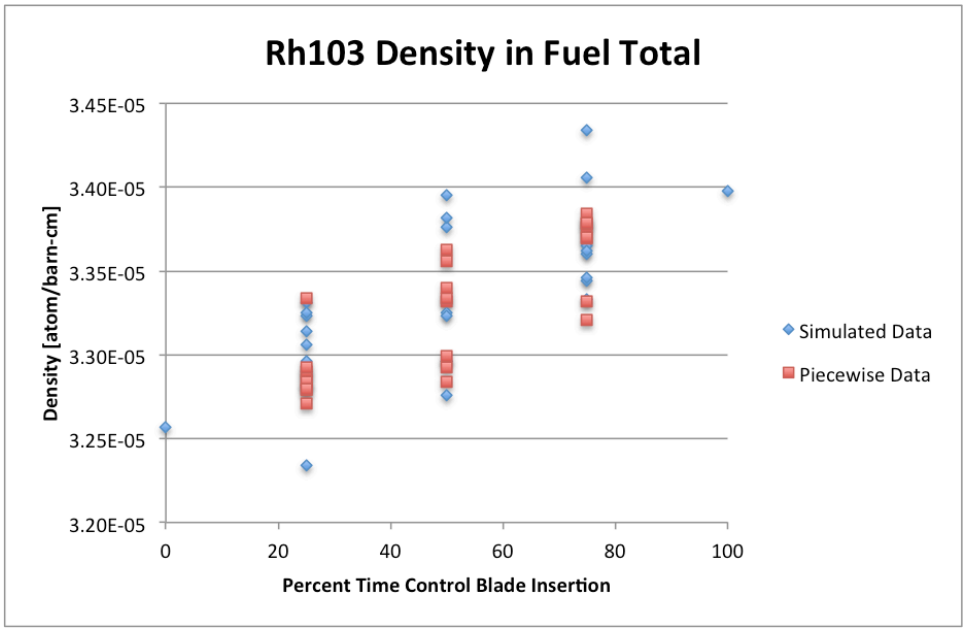
Rh103 Density in Fuel Total
3.45E-05
3.40E-05
3.35E-05
3.30E-05
3.25E-05
3.20E-05
Density [atom/barn-cm]
0
20
40
60
80
100
Percent Time Control Blade Insertion
Simulated Data
Piecewise Data

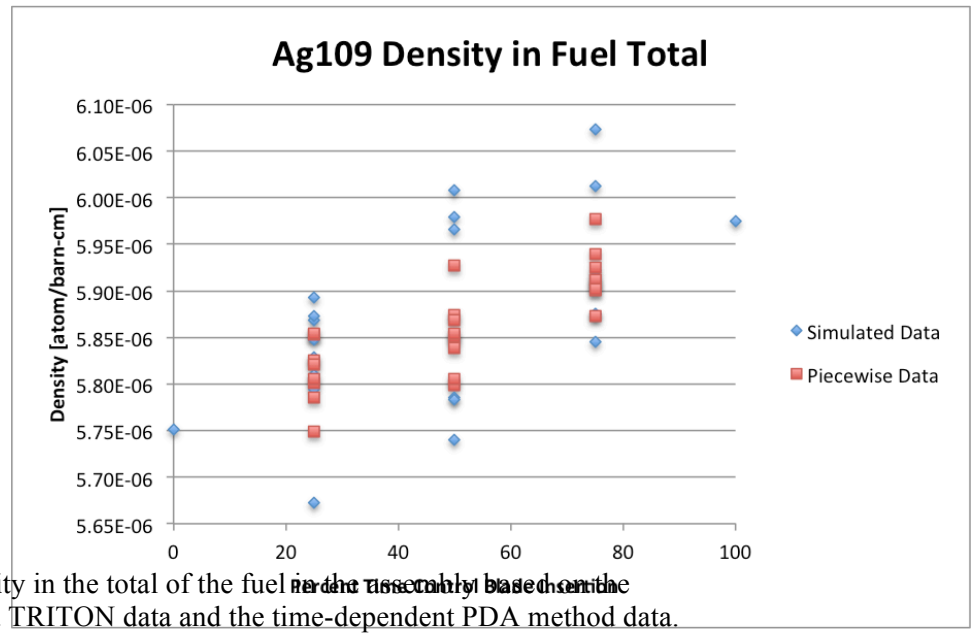

Figure 27. ^{109}Ag density in the total of the fuel in the assembly based on the rodded and urnrodded TRITON data and the time-dependent PDA method data.

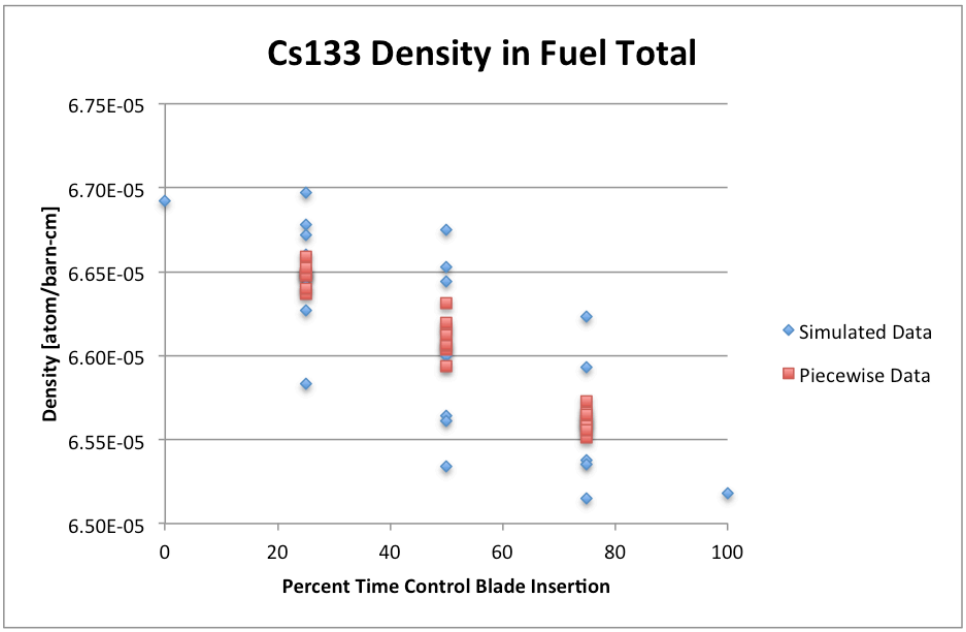

Figure 29. Sm density in the total of the fuel in the assembly used on the rodded and urnrodded TRITON data and the time-dependent PDA method data.

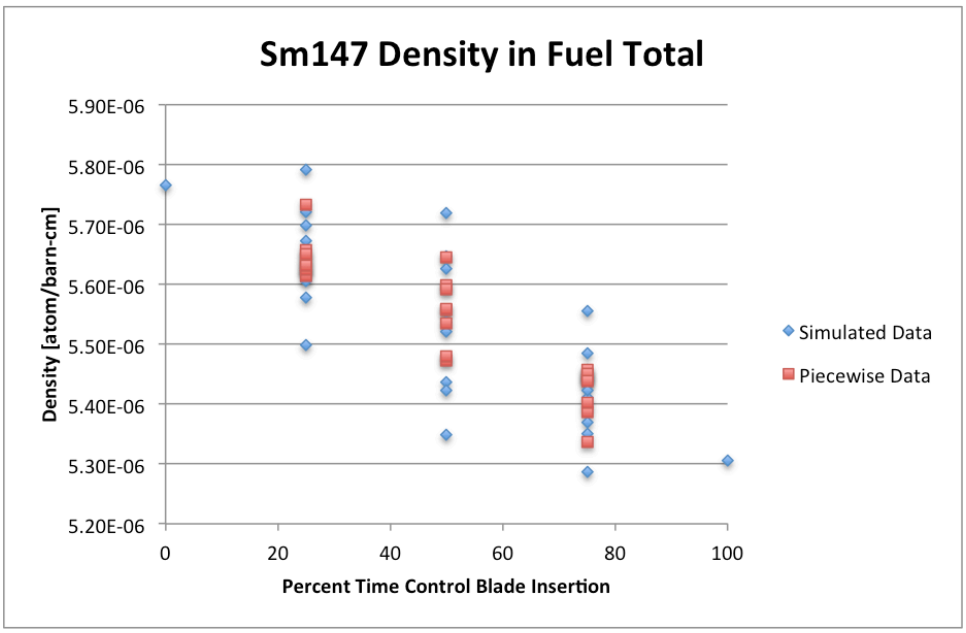

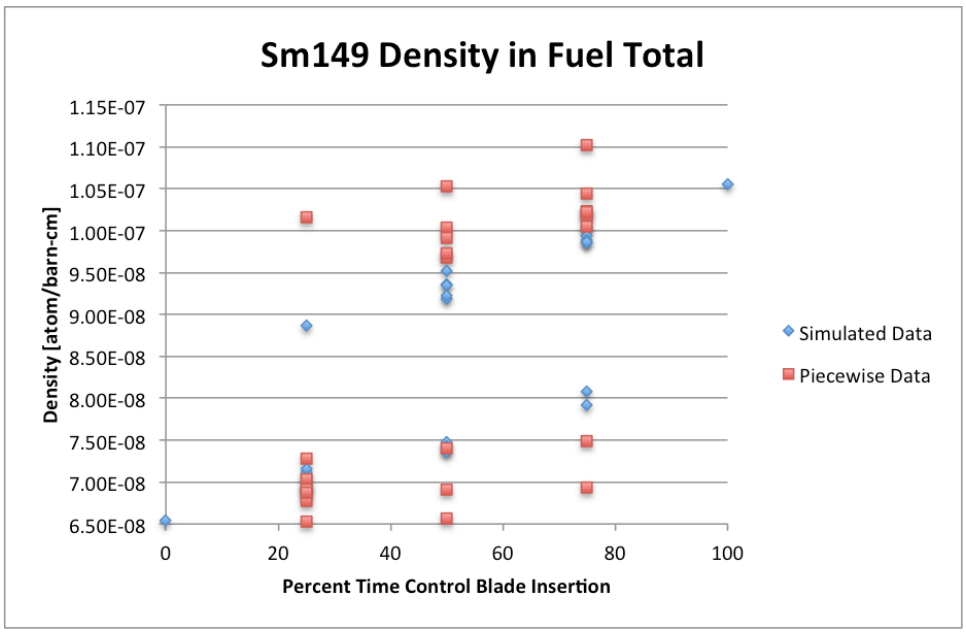

Figure 31: ^{152}Sm density in the total of the fuel in the assembly based on the rodded and unrodded TRITON data and the time-dependent PDA method data.

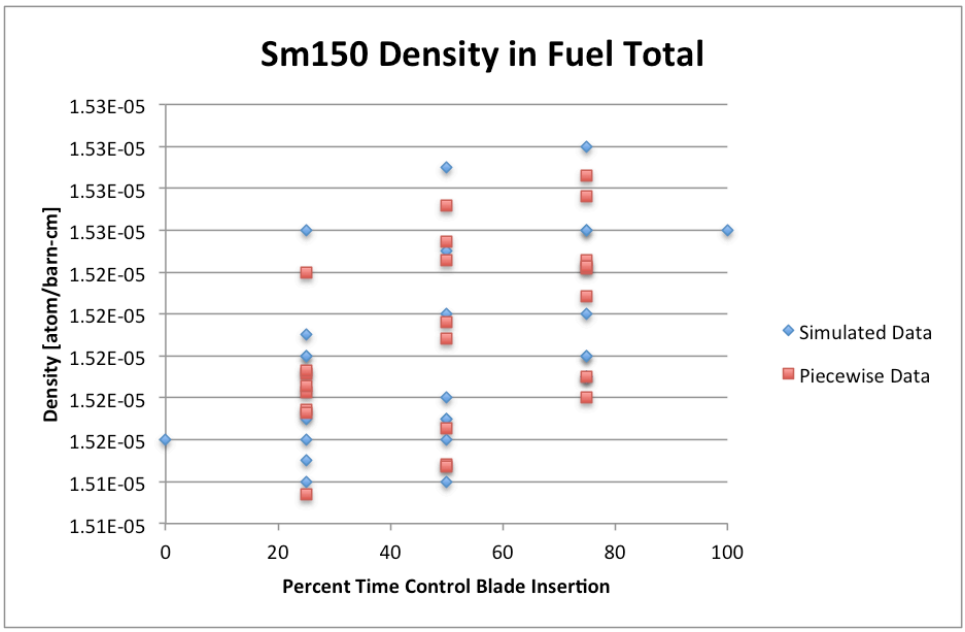

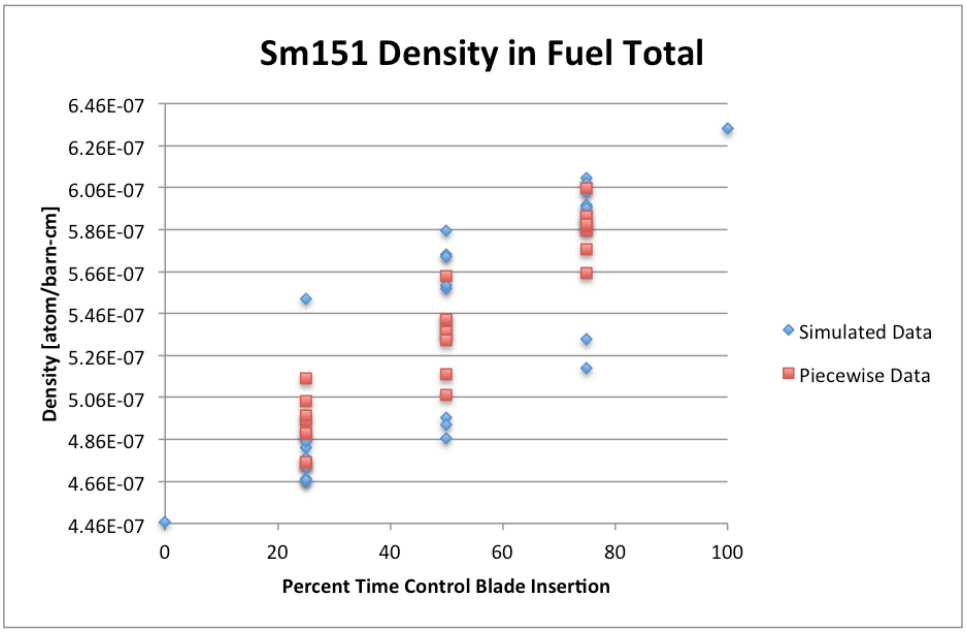

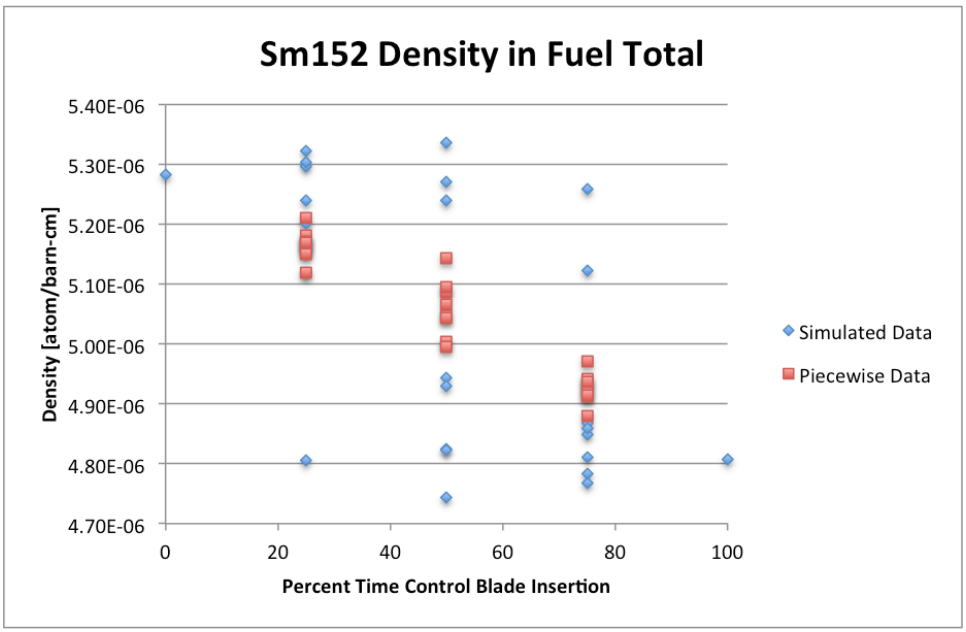
Sm152 Density in Fuel Total
5.40E-06
5.30E-06
5.20E-06
5.10E-06
5.00E-06
4.90E-06
4.80E-06
4.70E-06
Density [atom/barn-cm]
0
20
40
60
80
100
Percent Time Control Blade Insertion
Simulated Data
Piecewise Data

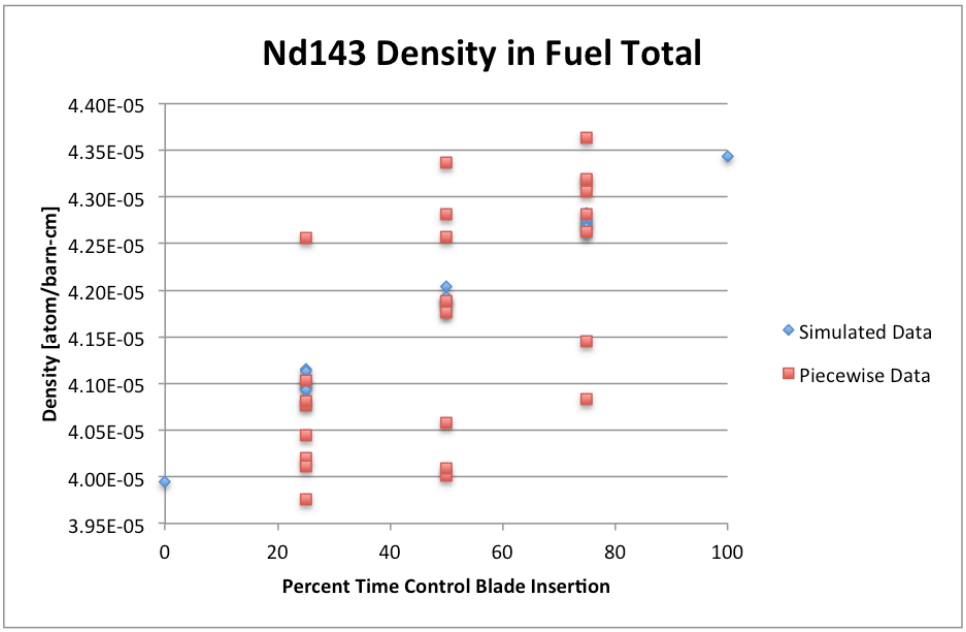
Nd143 Density in Fuel Total
4.40E-05
4.35E-05
4.30E-05
4.25E-05
4.20E-05
4.15E-05
4.10E-05
4.05E-05
4.00E-05
3.95E-05
Density [atom/barn-cm]
0
20
40
60
80
100
Percent Time Control Blade Insertion
Simulated Data
Piecewise Data

rodded and unrodded TRITON data and the time-dependent PDA method data.

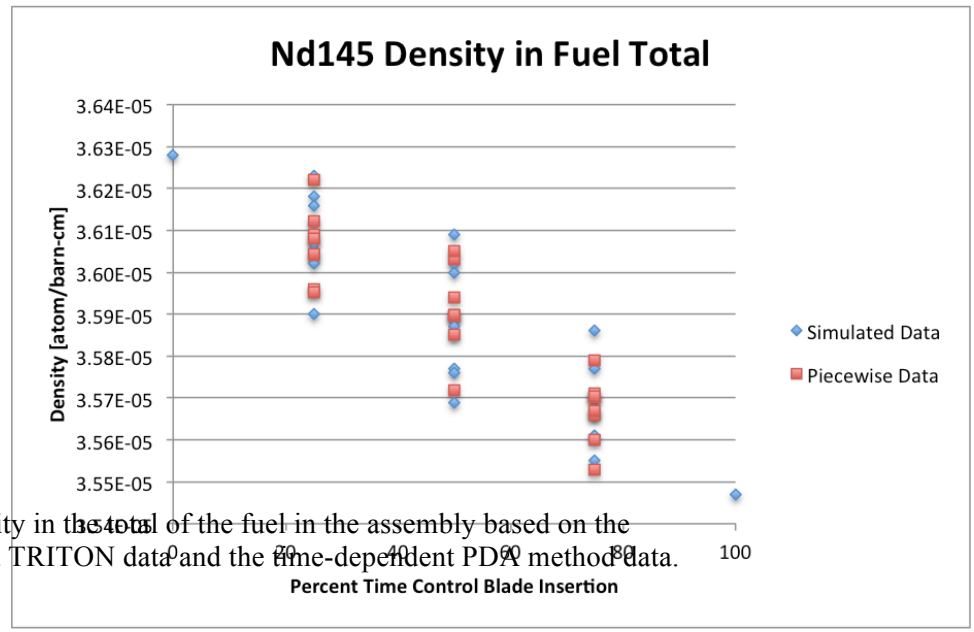

Figure 35. ^{145}Nd density in the total of the fuel in the assembly based on the rodded and urnrodded TRITON data and the time-dependent PDA method data.

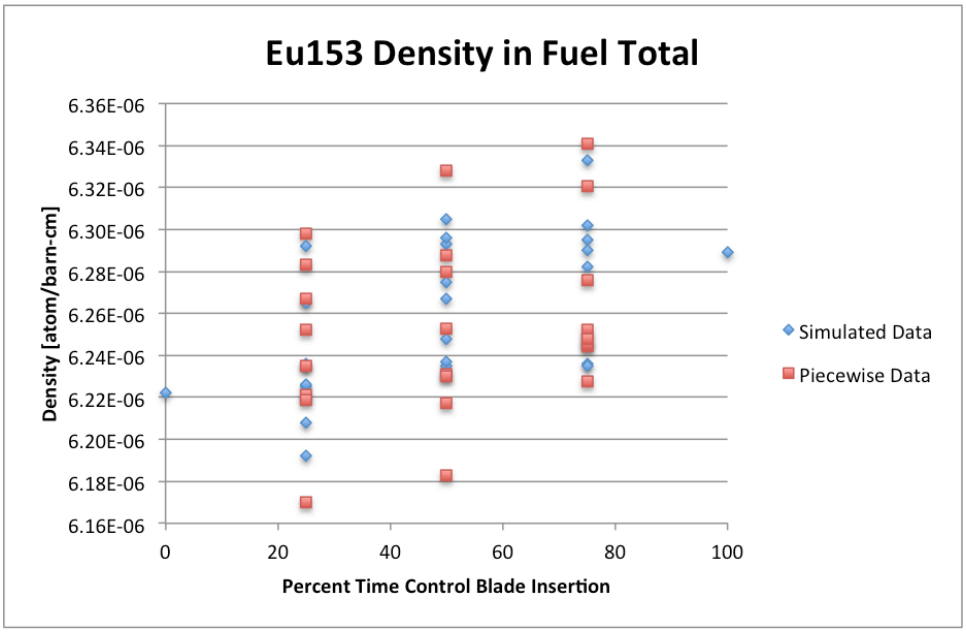

For the majority of the data shown, the fission product nuclides retain the behavior demonstrated in Table 11 from the rodded and unrodded cases. However, of the fission product nuclides, only molybdenum, technecium, rubidium, samarium-151, and neodymium-145 show bounding behavior with respect to the PDA method and TRITON data. This indicates that for a control blade insertion percentage for a lattice, the change in nuclide densities for the remaining fission product nuclides is not always in the same direction as that in Table 11. The fission product isotopes, which are not uni-directional in density change with control blade time insertion percentage include ^{103}Rh, ^{109}Ag, ^{133}Cs, ^{147}Sm, ^{149}Sm, ^{150}Sm, ^{152}Sm, ^{143}Nd, and ^{153}Eu.

Among the fission-product nuclides, Figures 28-32 show that samarium isotopes by far have the largest percent errors between the PDA method and TRITON simulations. There are several samarium isotopes that have nuclide densities that are outside the bounds of the rodded and unrodded cases. Fig. 36 further shows that the production of ^{149}Sm appears to be heavily influenced by hardening of neutron spectrum resulting from control blade insertion. The difference in the density saturation levels between the rodded and urodded cases can clearly be seen in Fig. 37. There is also a spectral shift cause by gadolinium that is partly responsible for the behavior of the samarium density curve. The data for ^{153}Eu contains many density values that are not bounded by rodded and unrodded cases. The percent error in the PDA method for ^{153}Eu compared to the TRITON data is large.

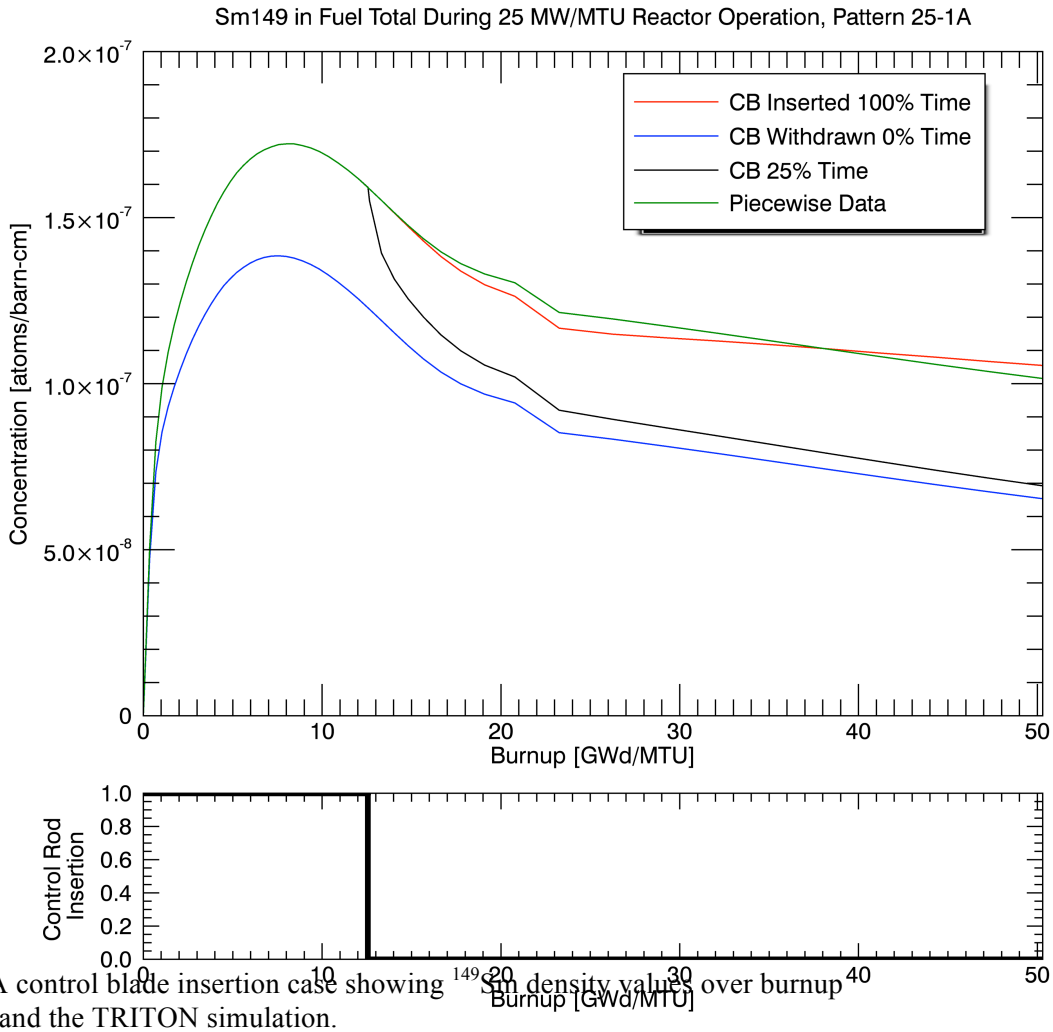

Figure 37. The 25-1A control blade insertion case showing ^{149}Sm density values over burnup for the PDA method and the TRITON simulation.

As an aside to this research, a problem has been encountered with the time steps being used and should be taken into account in the future. Figure 38 shows the rodded and unrodded density curves for gadolinium and ^{149}Sm. After 830 days of fuel assembly irradiation, the change in gadolinium density reaches a large negative value. At this point, a burnup step of approximately 100 days is being used. Judging by the sudden change in

the 149Sm density over this burnup step (seen in Figs. 37 and 38), smaller burnup steps should be used during the depletion of the gadolinium.

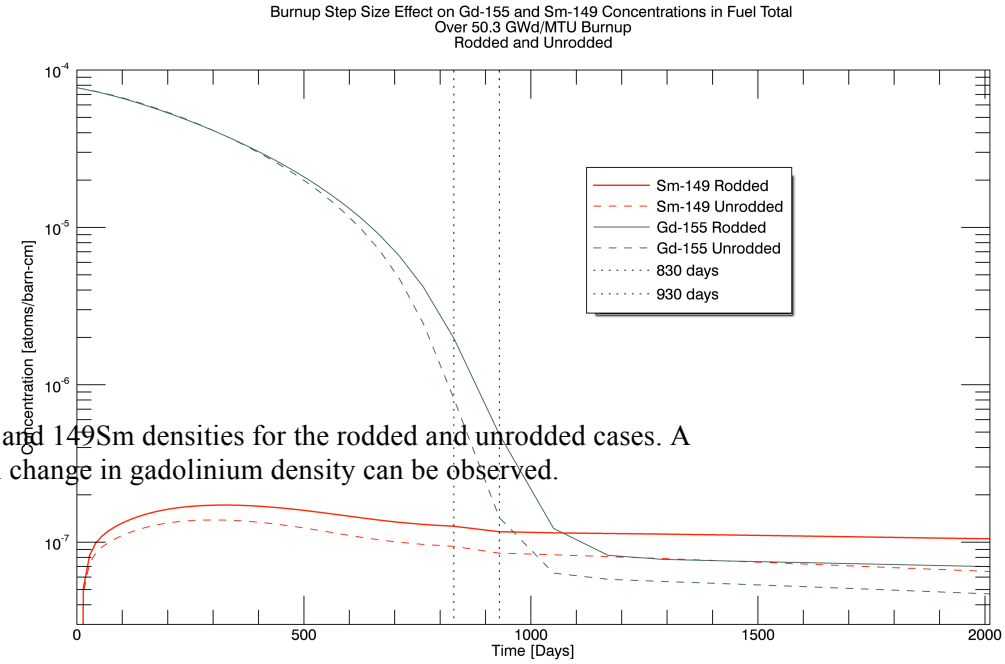

Figure 38. 155Gd and 149Sm densities for the rodded and unrodded cases. A spectral shift from change in gadolinium density can be observed.

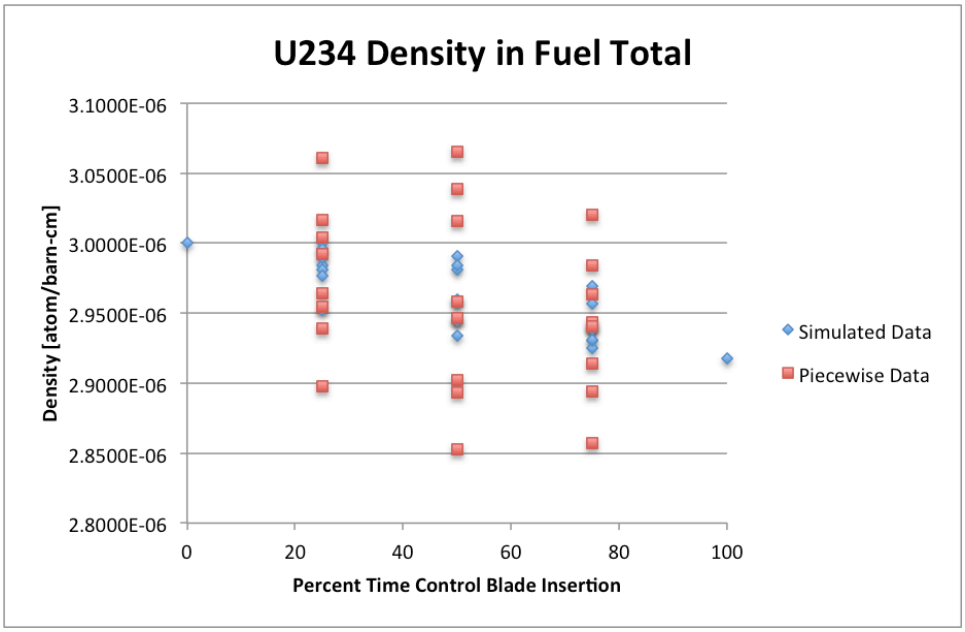
U234 Density in Fuel Total
3.1000E-06
3.0500E-06
3.0000E-06
2.9500E-06
2.9000E-06
2.8500E-06
2.8000E-06
Density [atom/barn-cm]
0
20
40
60
80
100
Percent Time Control Blade Insertion
Simulated Data
Piecewise Data

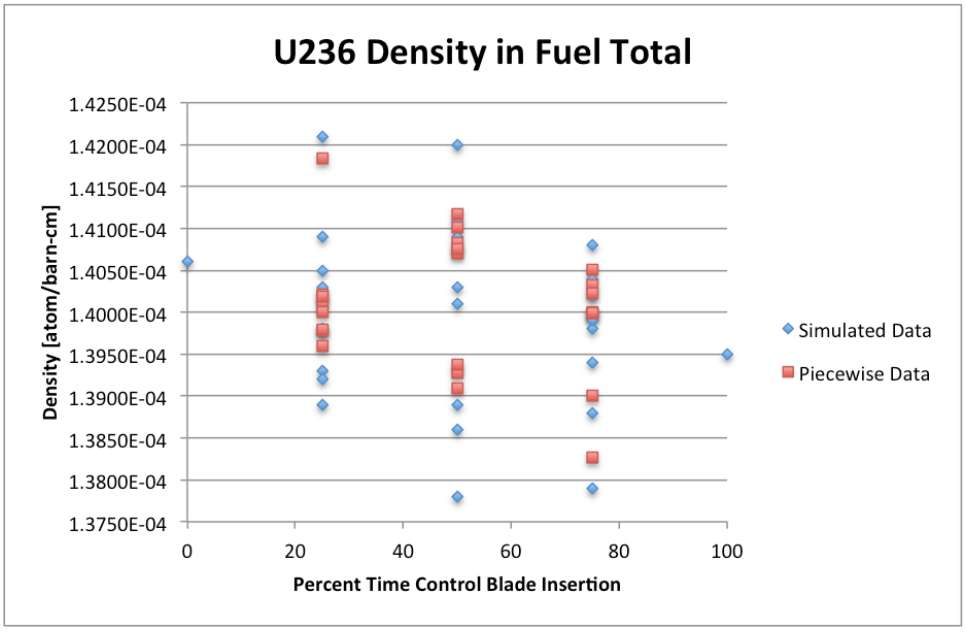
U236 Density in Fuel Total
1.4250E-04
1.4200E-04
1.4150E-04
1.4100E-04
1.4050E-04
1.4000E-04
1.3950E-04
1.3900E-04
1.3850E-04
1.3800E-04
1.3750E-04
Density [atom/barn-cm]
0
20
40
60
80
100
Percent Time Control Blade Insertion
Simulated Data
Piecewise Data

rodded and unrodded TRITON data and the time-dependent PDA method data.

rodded and unrodded TRITON data and the time-dependent PDA method data.

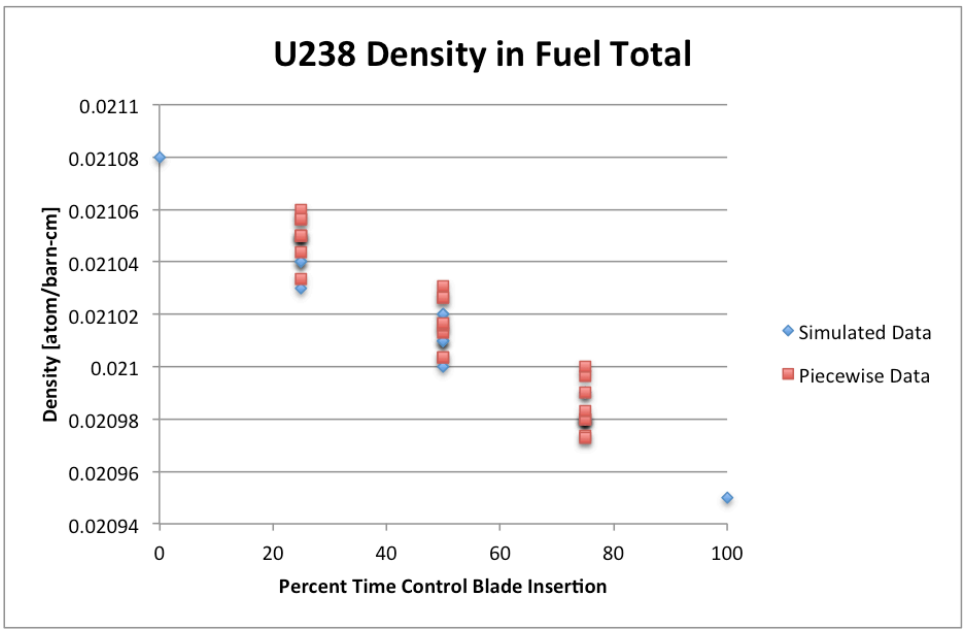

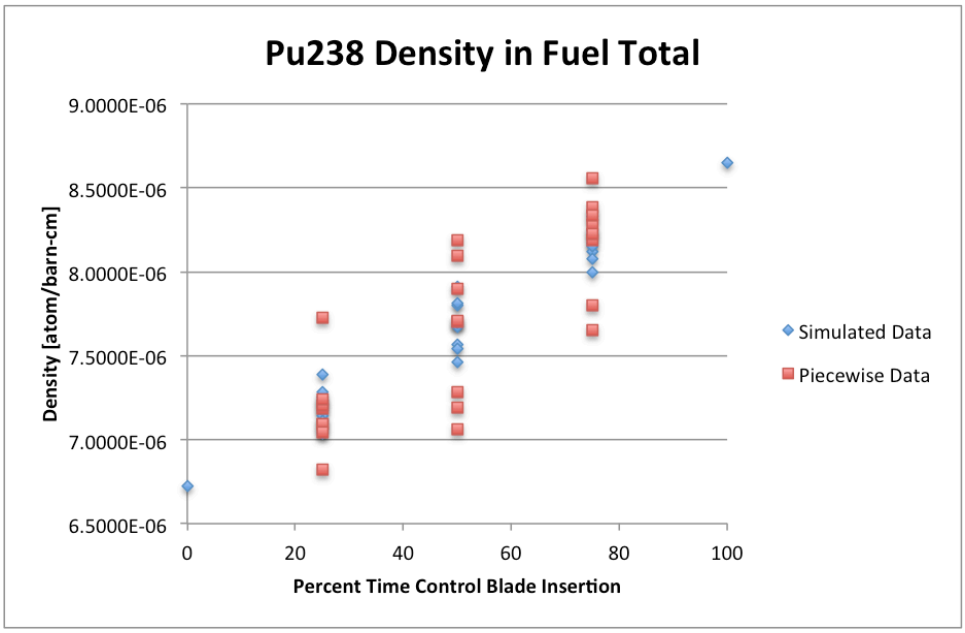

rodded and urnrodded TRITON data and the time-dependent PDA method data.

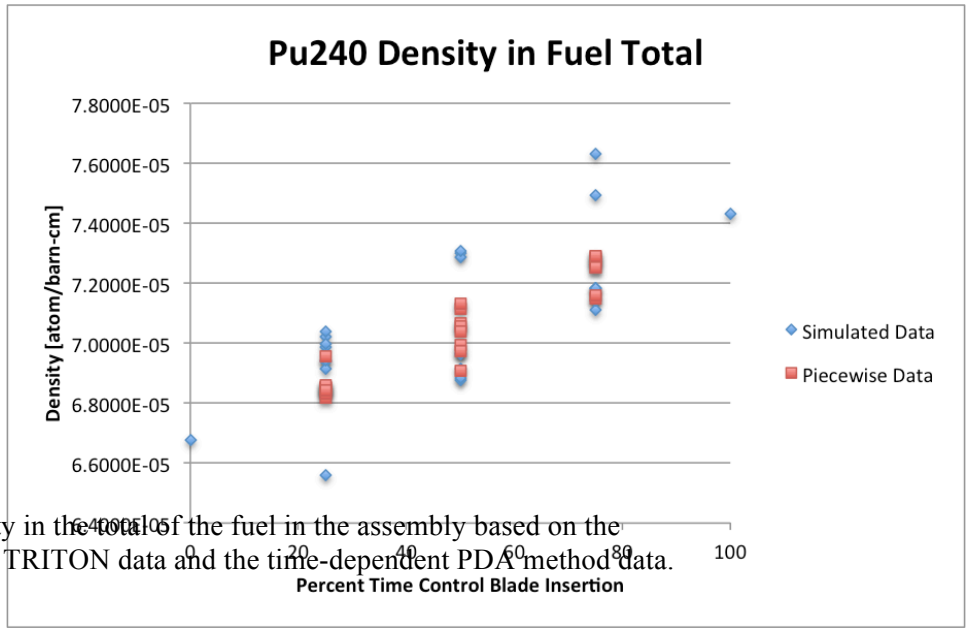

Figure 44. ^{242}Pu density in the total of the fuel in the assembly based on the rodded and urnrodded TRITON data and the time-dependent PDA method data.

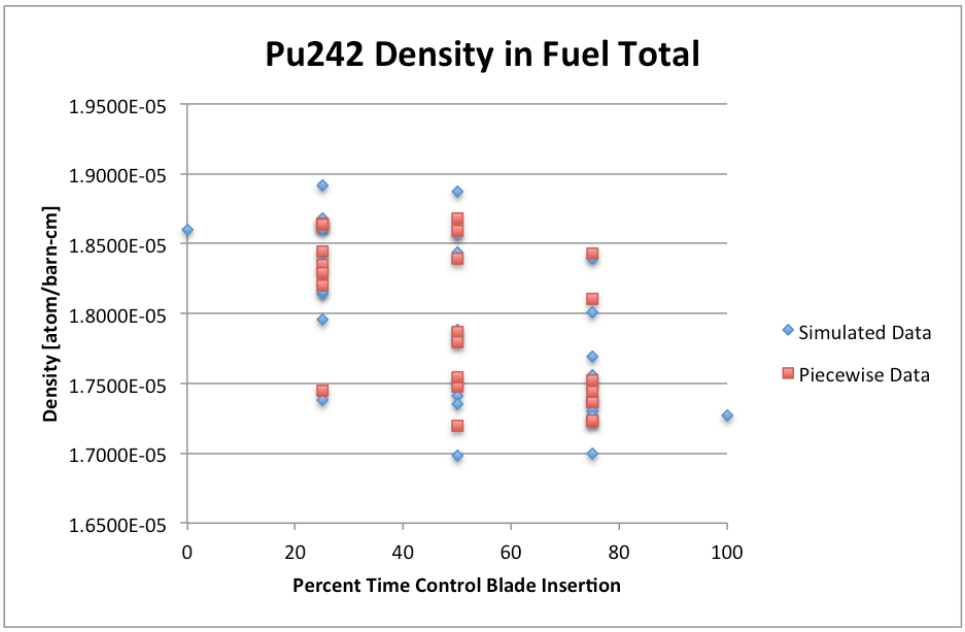

rodded and unrodded TRITON data and the time-dependent PDA method data.

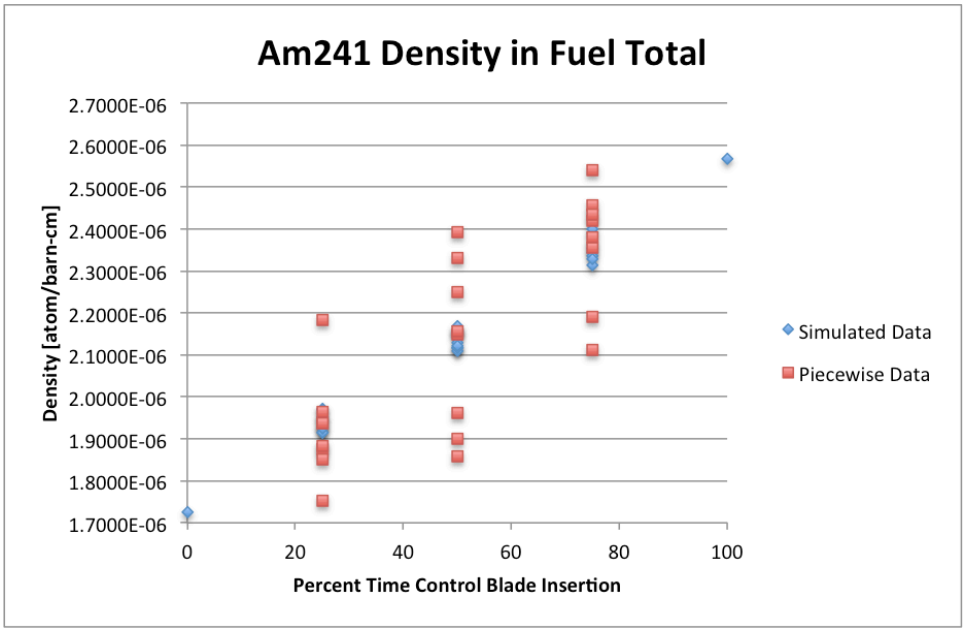

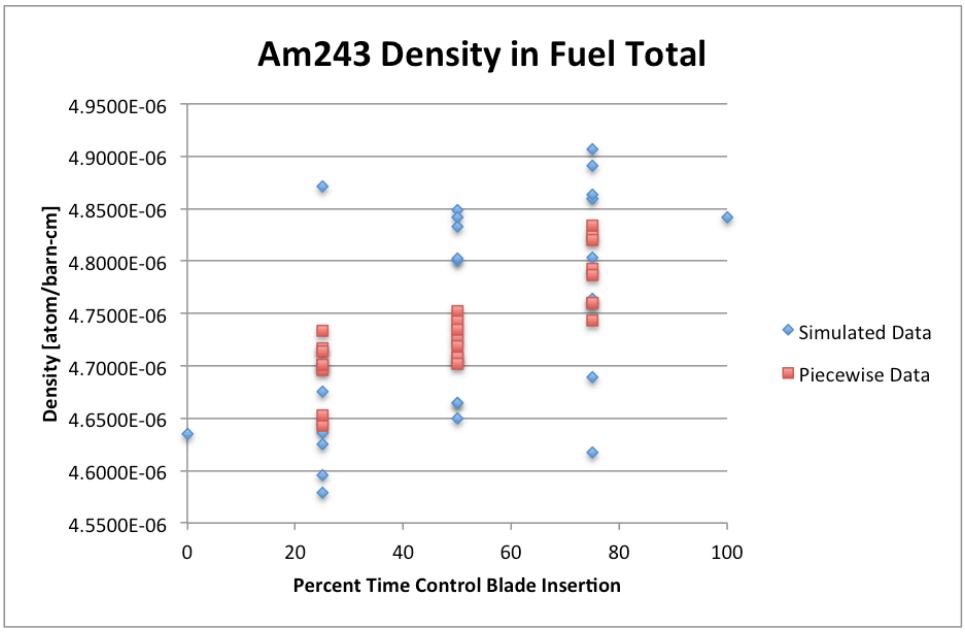

For ^{234}U only the result obtained from the PDA method is outside the bounds. For ^{236}U, data from the PDA method and TRITON simulation is outside the bounds. However, even for the TRITON values that are outside the bounds, the PDA method does a good job of accurately predicting the nuclide density. ^{240}Pu contains TRITON simulations outside the bounding cases. ^{242}Pu contains TRITON and PDA method data outside the bounds. In the case of ^{241}Am, the results are bounded but the errors are relatively high. ^{243}Am contains a significant amount of TRITON simulations outside the set boundaries.

4.4 Nuclide Densities in Temporally Reversed Control Blade Insertion Patterns

The control blade insertion patterns that are given in Fig. 15 and Table 7 of section 2.4.6 have been constructed such that the set of "A" patterns are weighted to have the majority of the control blade insertion time occurring in the first half of the in-reactor fuel lifetime. The "B" patterns are the temporal reverse of their "A" counterparts and therefore have the majority of the control blade insertion occurring during the second half of the in-reactor fuel lifetime. Utilizing this property of the control blade insertion patterns, the burnup dependence of the nuclide densities (behavior based on the A/B patterns) will indicate whether the sequence (1,2,3,4) is of significance.

During analysis of the A/B pattern results, the PDA method results showed no significant patterns or behavior in comparing the A/B patterns of a particular control blade insertion sequence. For some nuclides the PDA method predicted lower A density values, for others lower B density values and for others there were mixed results. This inconsistent behavior comes about because the rodded and unrodded density functions

are different for each nuclide. The PDA method utilizes the difference in the rodded and urodded density curve to accumulate the differences in final density values for the different control blade insertion patterns. Each resulting density value is therefore averaged in a different way.

There also has not been found a consistent behavior between the TRITON data and the PDA method for a given A/B pattern. This indicates that, aside from the dependence of density on time percent control blade insertion, there is no correlation between temporally reversed control blade insertion sequences. The A/B patterns can result in very similar or very different values depending on the control blade insertion pattern. One important result that has been noted from analysis of the data is that for ^{235}U and ^{239}Pu the nuclide densities are bounded by the rodded and unrodded densities. In addition to that, the concentrations of these fissile nuclides for a given control blade insertion time are bounded by the 1A and 1B control blade insertion patterns and these densities are shown in Figure 46.

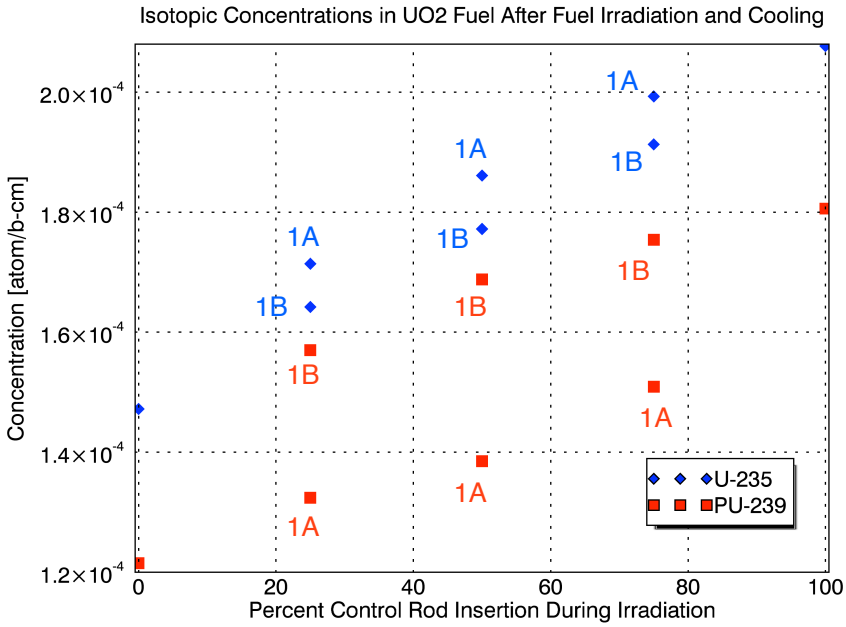

The PDA method can be described as a way of averaging the rodded and unrodded solutions using the control blade insertion pattern. As a result, control blade insertion patterns that are similar when temporally reverse (when 2A is similar to 2B etc.) result in similar values using the PDA method. The balance and skewedness of control blade insertion over the in-reactor fuel assembly lifetime is examined in the next section.

4.5 PDA Method Error Correlation to Control Blade Insertion Patterns

In addition to the control blade time percentage insertion and temporal weighting, the control blade insertion patterns were designed with varying insertion and withdrawal rates. For each time insertion percentage (25,50,75) that is used there are four temporally reversed patterns (A/B) that are increasing in the rate of control blade insertion and withdrawal (1,2,3,4). This is done to research the difference between large continuous

burnup periods with control blades inserted or withdrawn and highly varying control blade insertion conditions. Through analysis of the TRITON data and PDA method data values, it was found that increasing the control blade insertion/withdrawal rate has no effect on the accuracy of the PDA method compared to the TRITON data results.

However, during the analysis of control blade insertion rate it was found that for control blade use that is balanced throughout the in-reactor fuel assembly lifetime, the PDA method data is very accurate (i.e. control blade use that is skewed to one half of the in-reactor fuel lifetime results in poor PDA method performance) compared to the TRITON simulated results. In order to illustrate this finding the control blade insertion patterns have been divided into two groups, which are shown in Table 12. In this grouping, group one corresponds to the control blade insertion patterns where the control blades are inserted approximately equal times in the first and second halves of the in-reactor fuel lifetime. Group two corresponds to control blade insertion patterns that are highly skewed towards the beginning or end of the in-reactor fuel lifetime. Figures 47-49 and 55-60 demonstrate the error in the PDA method compared to the TRITON data for groups one and two of control blade insertion.

CB Insertion Time %	Group 1 (Balanced)	Group 2 (Skewed)
25	2A, 2B, 3A, 3B	1A, 1B, 4A, 4B
50	3A, 3B	1A, 1B, 2A, 2B, 4A, 4B
75	2A, 2B, 4A, 4B	1A, 1B, 3A, 3B

data in group 1 (balanced) and group 2 (skewed) control blade insertion cases.

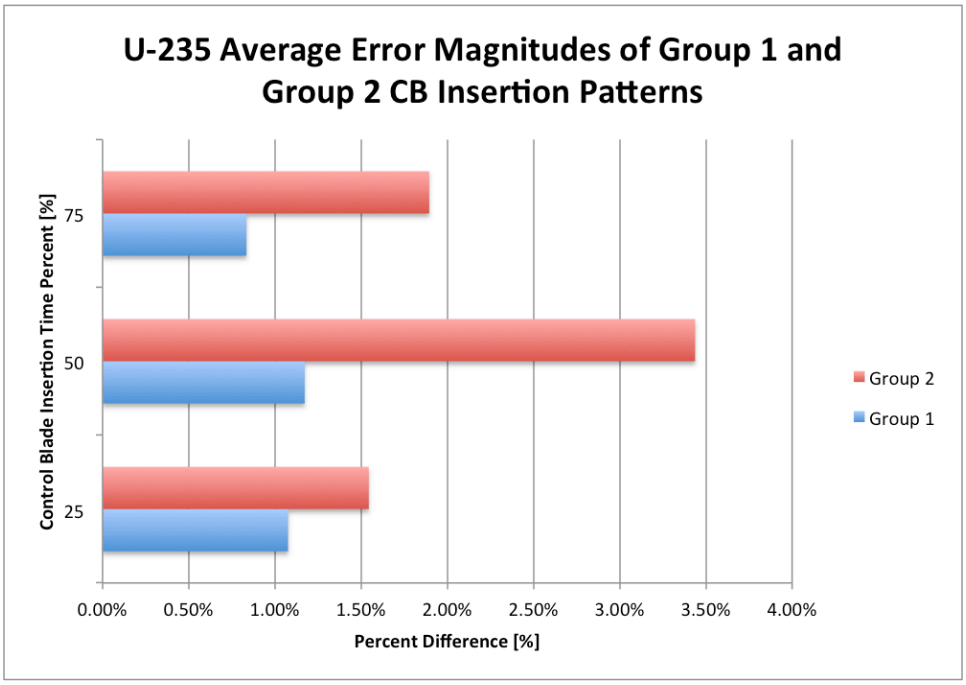

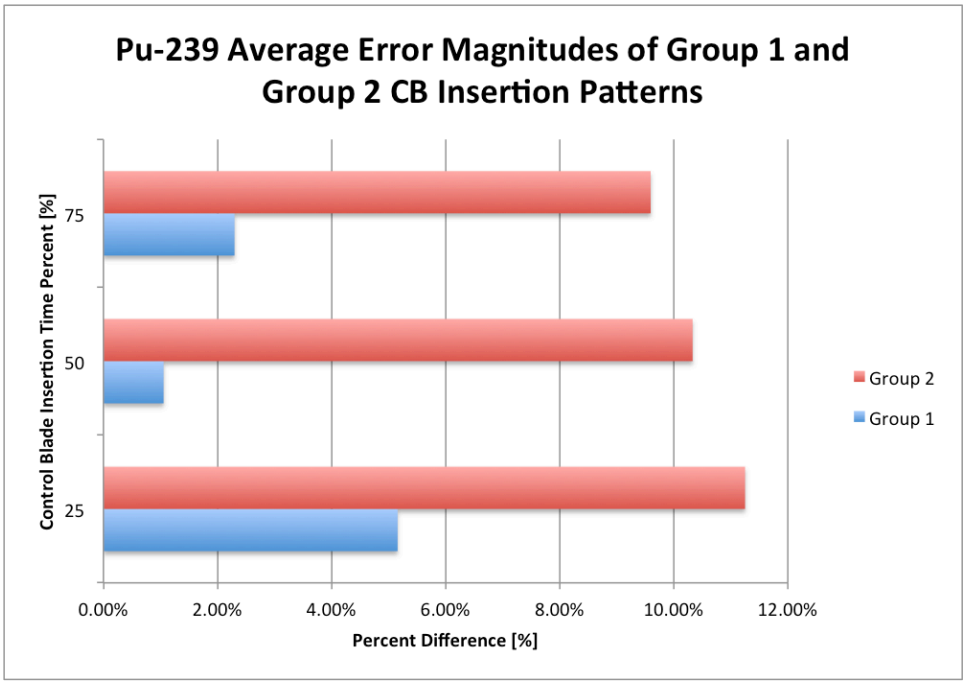

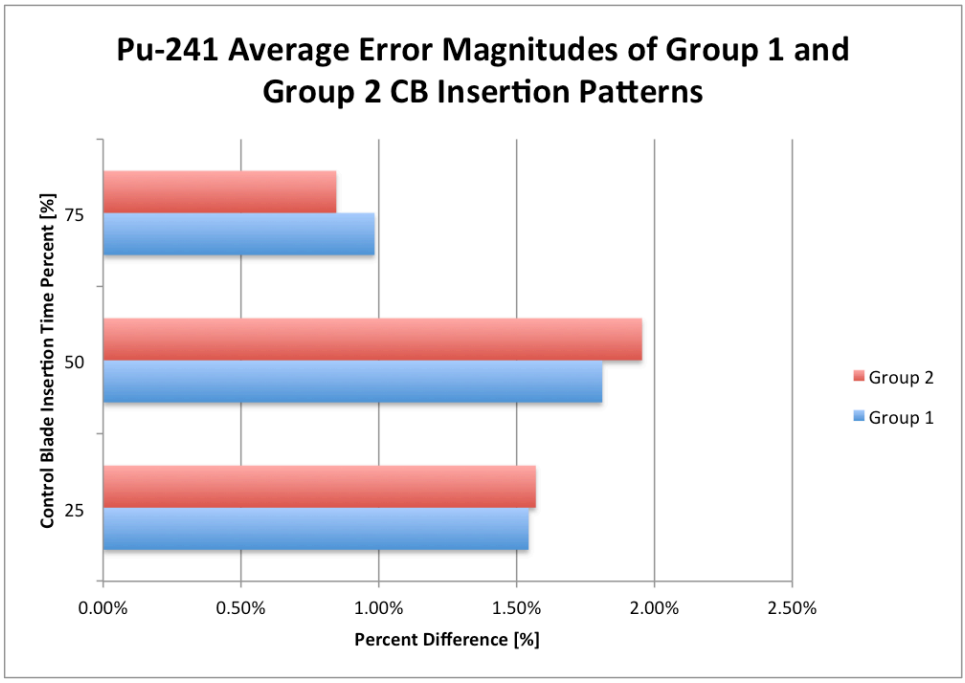

Figures show that for ^{235}U and ^{239}Pu the balanced control blade insertion patterns (Group 1) have much lower error in the PDA method compared to the TRITON results. This leads to one of the major shortcomings of the PDA method, which is its inability to predict density values of saturated (or nearly saturated) nuclides that undergo spectral shifts (control blade insertion). Figures 50 and 51 demonstrate the effect of control blade insertion or withdrawal on ^{239}Pu concentration in the last 25% burnup of the fuel assembly. Since ^{239}Pu is a major contributor to fuel reactivity of UNF in a storage configuration, such a shortcoming in the PDA method is not acceptable.

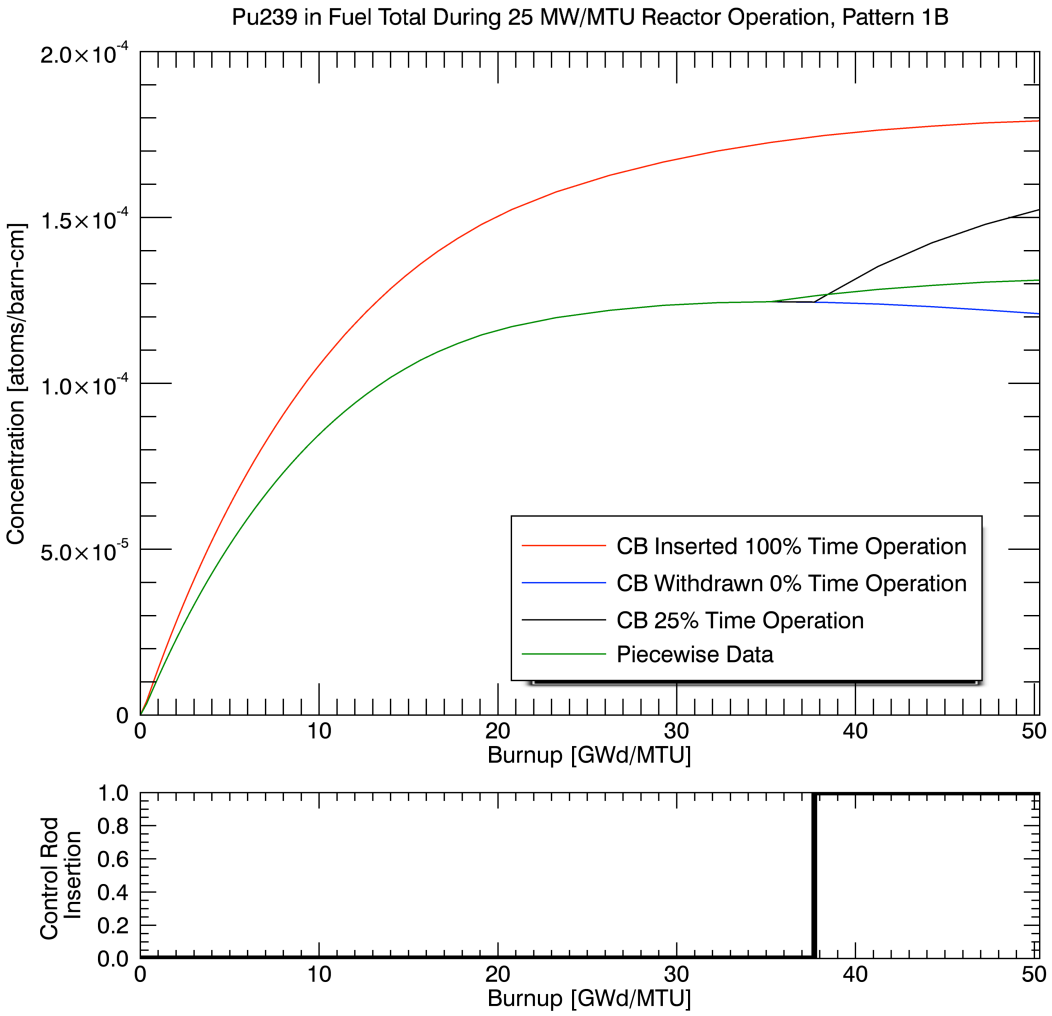
Pu239 in Fuel Total During 25 MW/MTU Reactor Operation, Pattern 1B
Concentration [atoms/barn-cm]
2.0×10-4
1.5×10-4
1.0×10-4
5.0×10-5
0
0
10
20
30
40
50
Burnup [GWd/MTU]
CB Inserted 100% Time Operation
CB Withdrawn 0% Time Operation
CB 25% Time Operation
Piecewise Data
Control Rod Insertion
1.0
0.8
0.6
0.4
0.2
0.0
0
10
20
30
40
50
Burnup [GWd/MTU]

data.

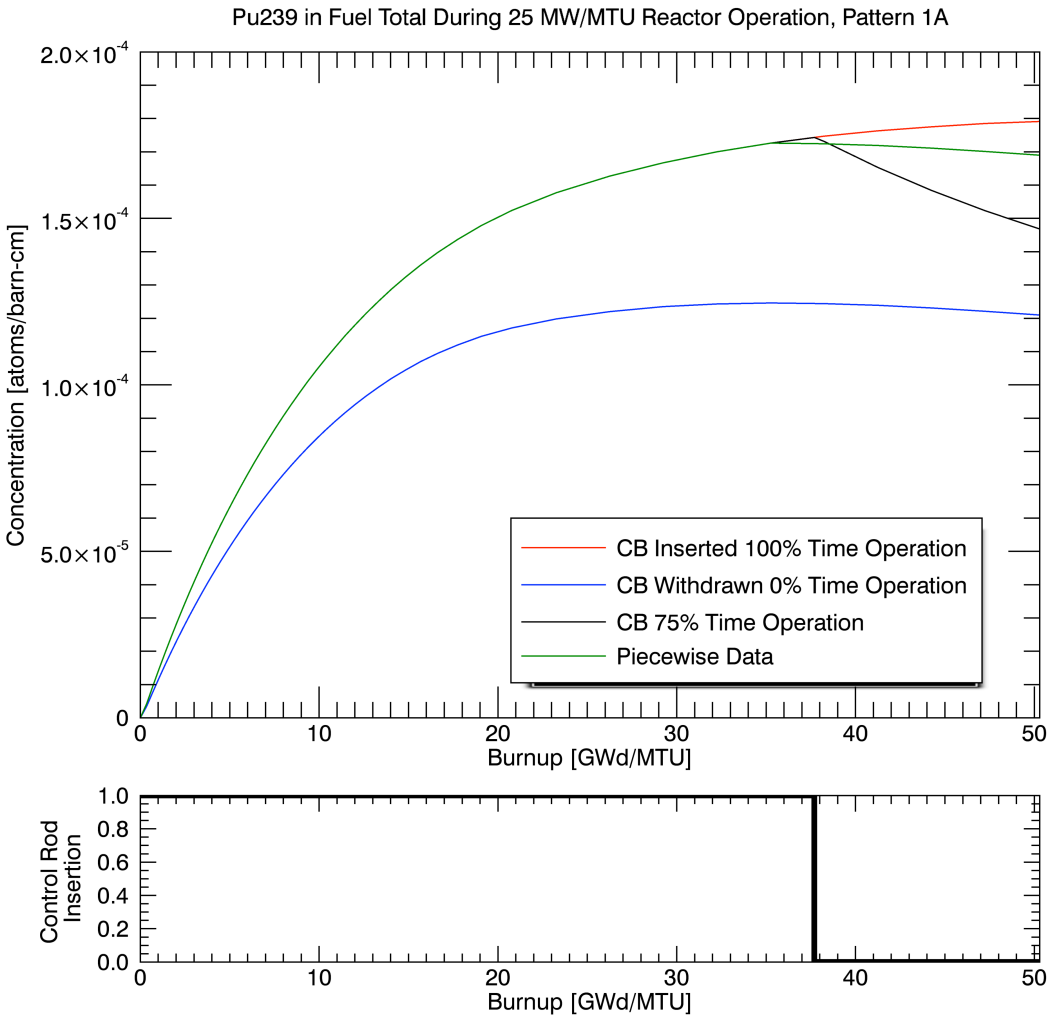

The trend of lower error for group one control blade insertion patterns is not shared by ^{241}Pu, as nearly all control blade insertion patterns are predicted accurately for this nuclide. This leads to a very important result in determining nuclides that can be treated effectively using the PDA method. It can be seen in Fig. 52 that an even (group 1) control blade insertion pattern results in a very accurate prediction of ^{235}U density using the PDA method compared to the density predicted by TRITON. Figure 53 demonstrates

that a more skewed control blade insertion pattern can cause a more significant difference in ^{235}U density at the desired burnup value. Figure 54 shows that the slopes as a function of burnup of ^{241}Pu for the rodded and unrodded cases are subtly different and control blade insertion/withdrawal does not cause dramatic changes in the slope. This makes ^{241}Pu and any nuclide with similar properties a very good candidate to use with the PDA method. This can be true for nuclides that are building up or depleting during the in-reactor fuel assembly lifetime.

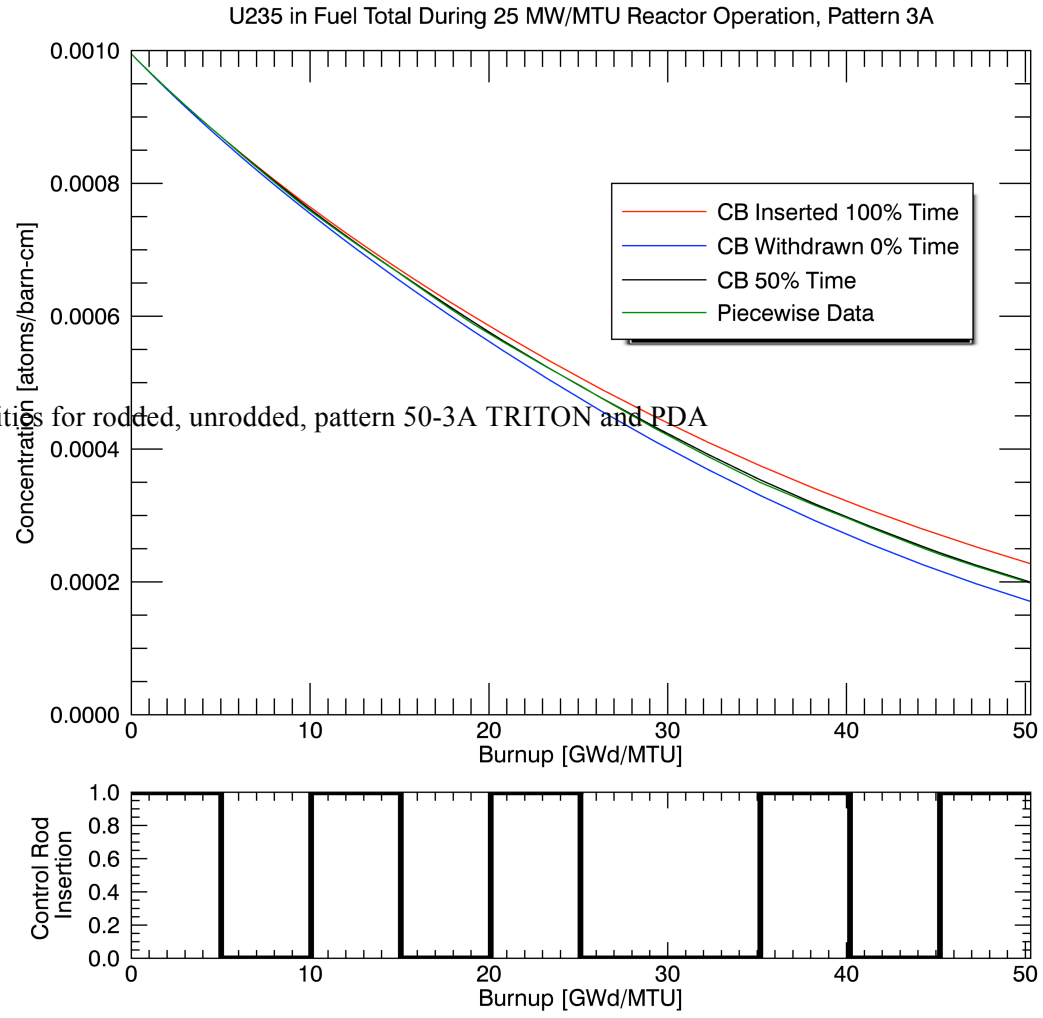

Figure 52. ^{235}U densities for rodded, unrodded, pattern 50-3A TRITON and PDA method data.

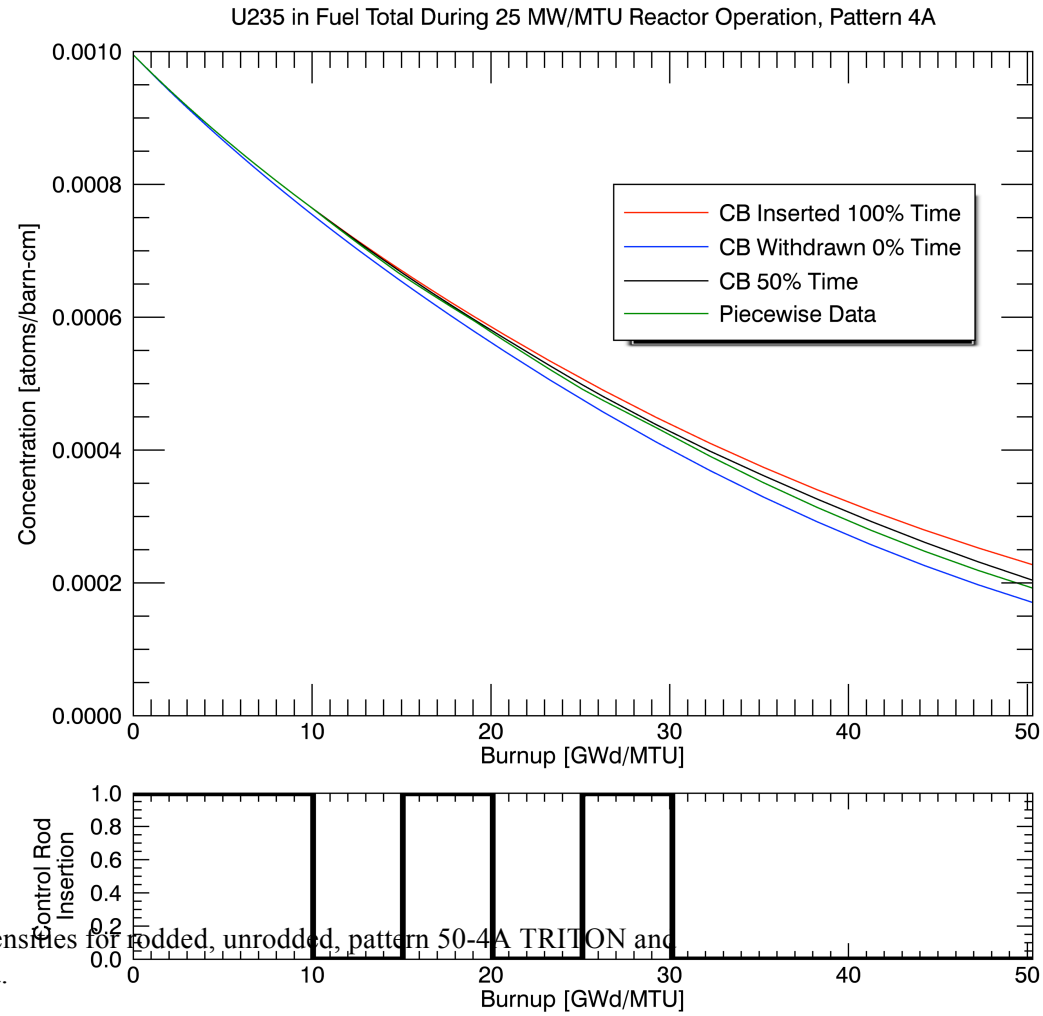

Figure 53. ^{235}U densities for rodded, unrodded, pattern 50-4A TRITON and PDA method data.

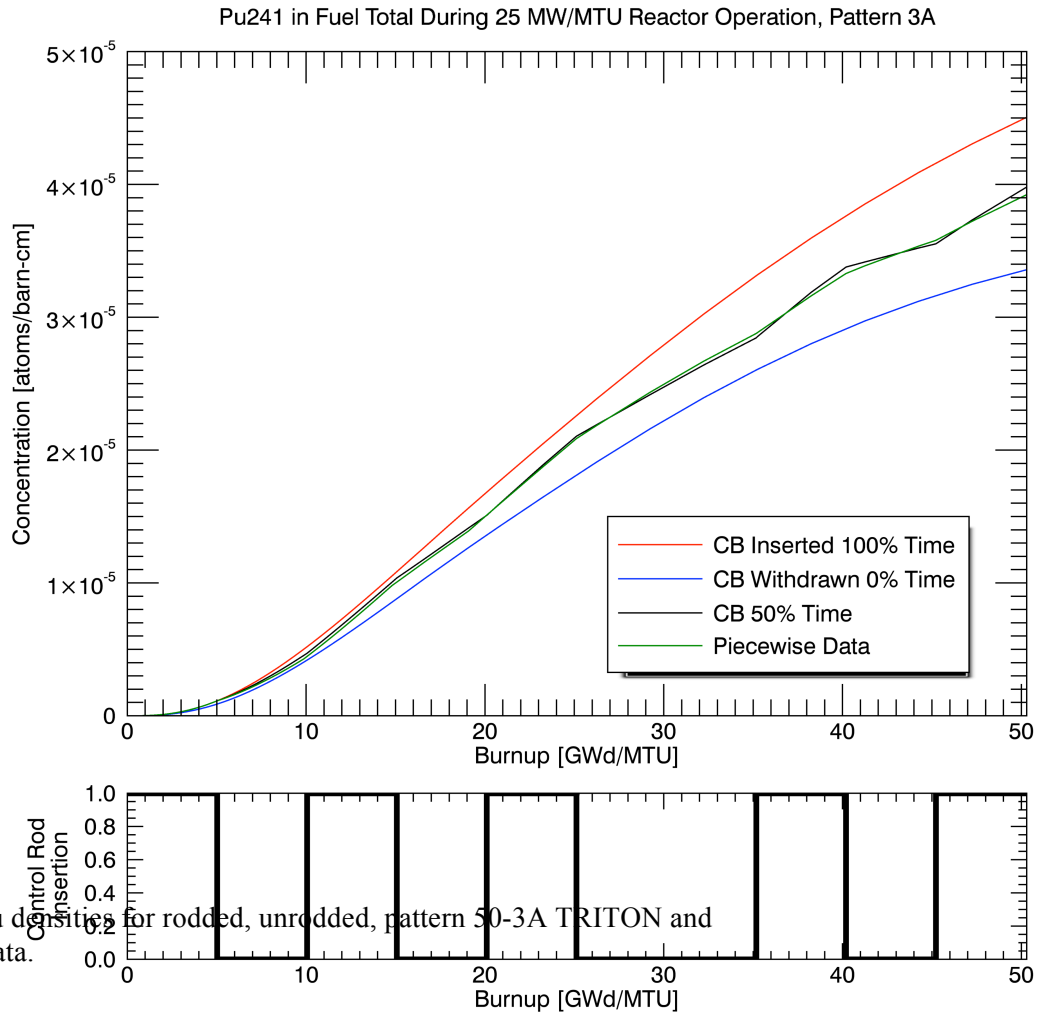

Figure 54. ^{241}Pu densities for rodded, unrodded, pattern 50-3A TRITON and PDA method data.

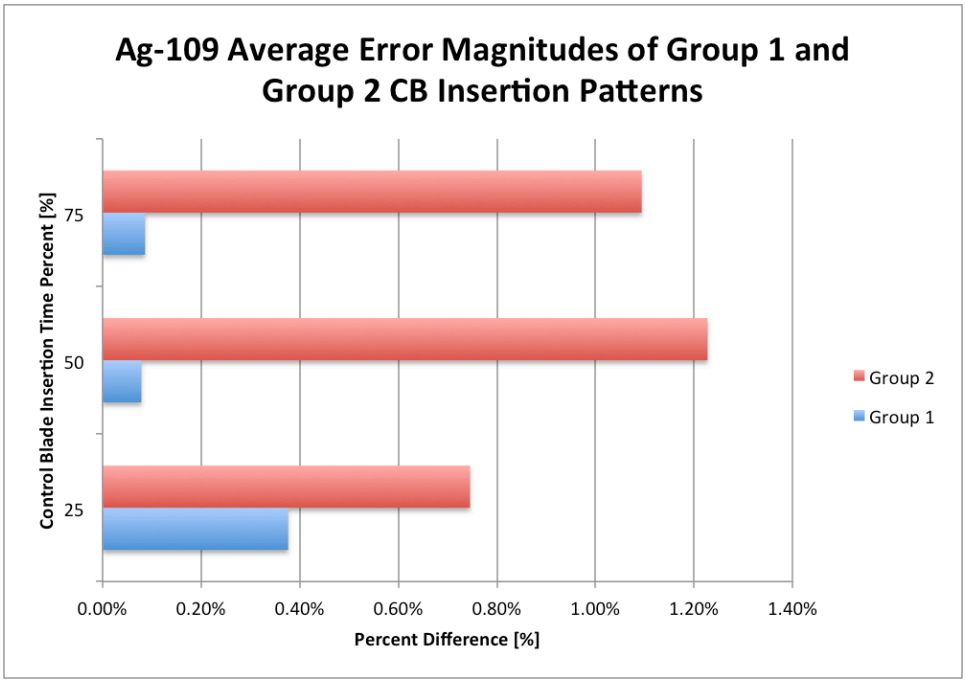

The plot for ^{109}Ag is representative of the fission products ^{95}Mo, ^{99}Tc, ^{101}Ru, ^{103}Rh, ^{133}Cs, ^{143}Nd, and ^{145}Nd as all of these listed nuclides share similar patterns in PDA method error. This group of fission products has subtly changing density curves similar to that of the fissile nuclides seen previously. This gives these fission products similar behavior with respect to control blade insertion and prediction of nuclide densities using the PDA method. These nuclides do not reach saturation in the 50.3 GWd/MTU of fuel assembly exposure, but gradually build up in a similar fashion to which the fissile nuclides deplete.

group 1 (balanced) and group 2 (skewed) control blade insertion cases.

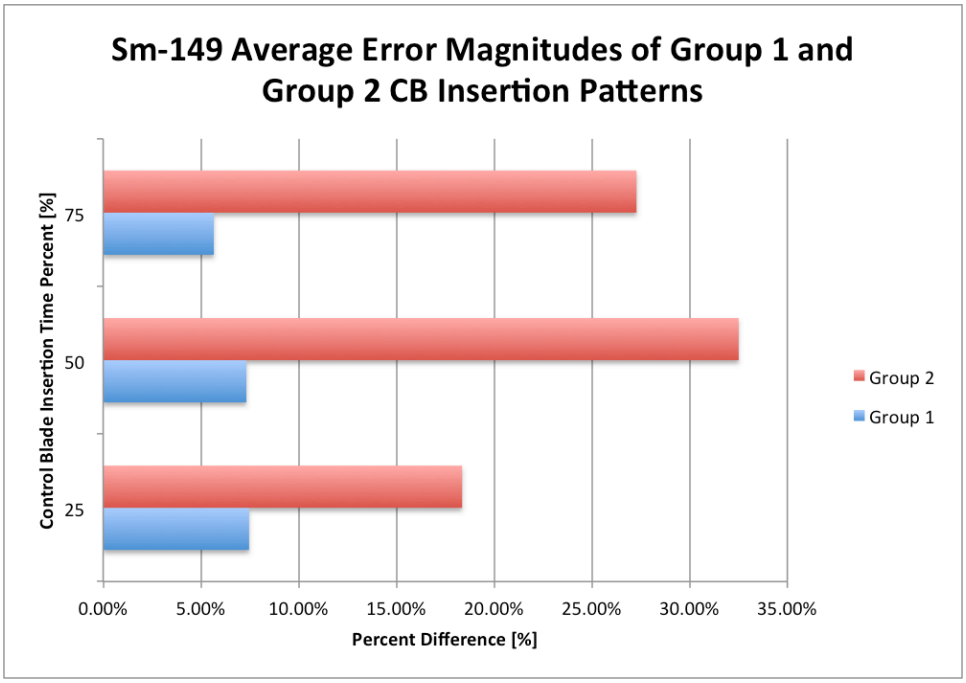

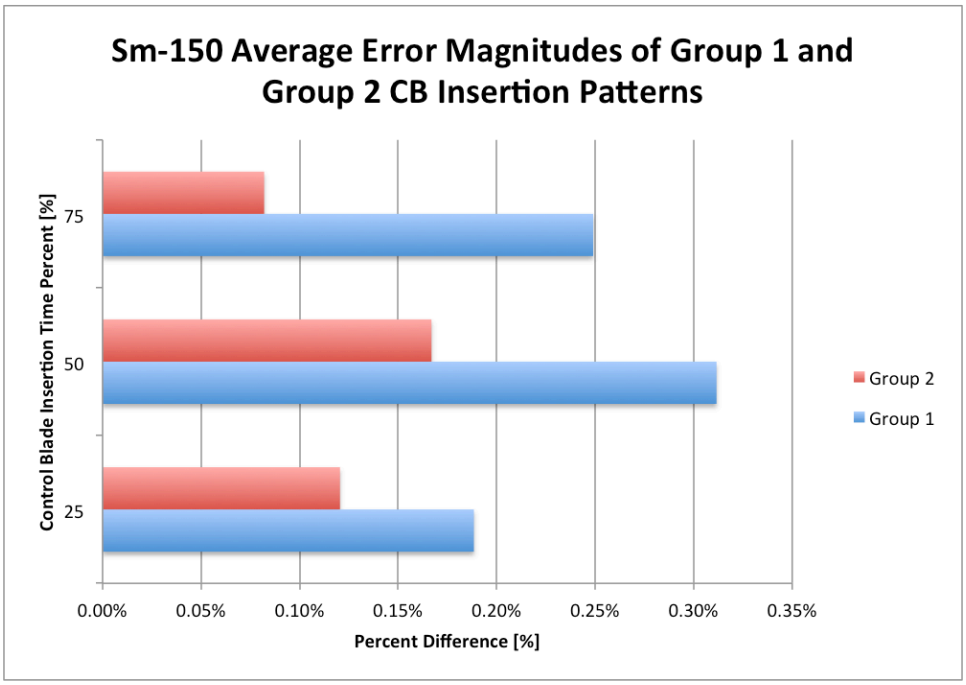

The trend of increased accuracy for group one holds true for Sm isotopes of mass number 147,149, 151, and 152 while ^{150}Sm is the standout, going against the trend. ^{149}Sm and ^{151}Sm are of special consideration as they reach saturation during the 50.3 GWd/MTU fuel assembly irradiation. They reach saturation because of their very large neutron capture cross-sections causes their accumulation and transmutation to reach an equilibrium state. Behavior in the density curves can be compared to that of ^{239}Pu where a change in control rod state near the end of the in-reactor fuel assembly lifetime can have a dramatic effect on the density value. This is a change that cannot be accurately predicted by the PDA method.

Figure 58. ^{234}U error magnitudes in the PDA method compared to TRITON data in group 1 (balanced) and group 2 (skewed) control blade insertion cases.

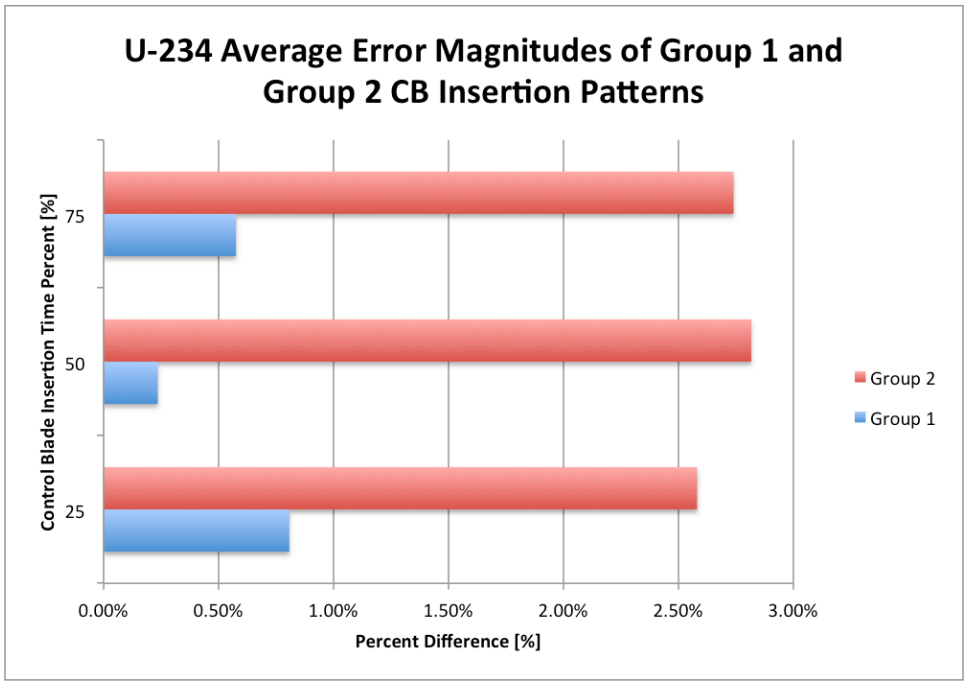

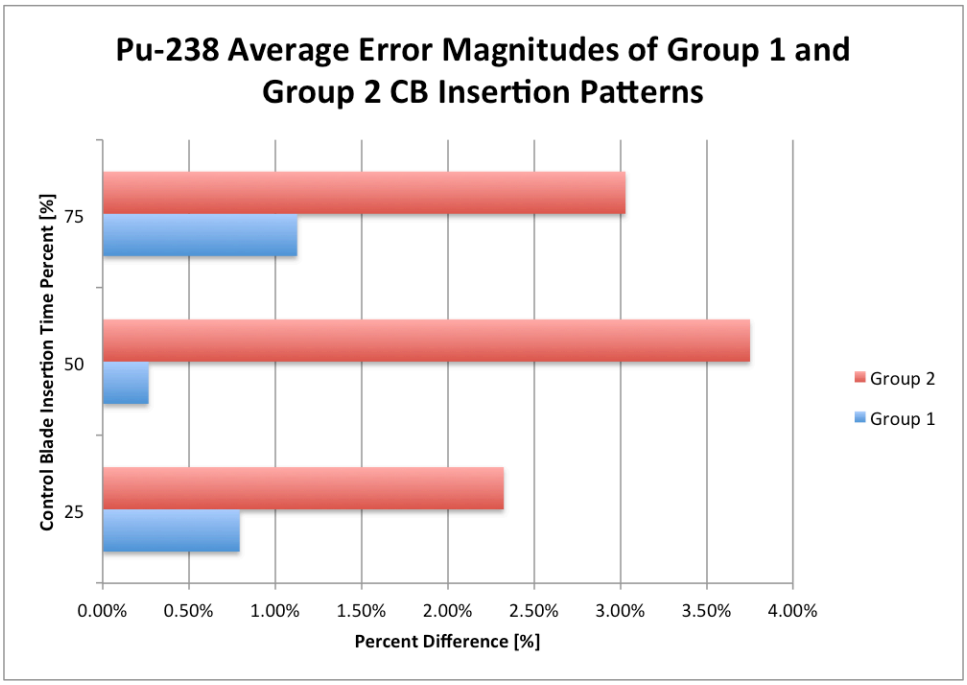

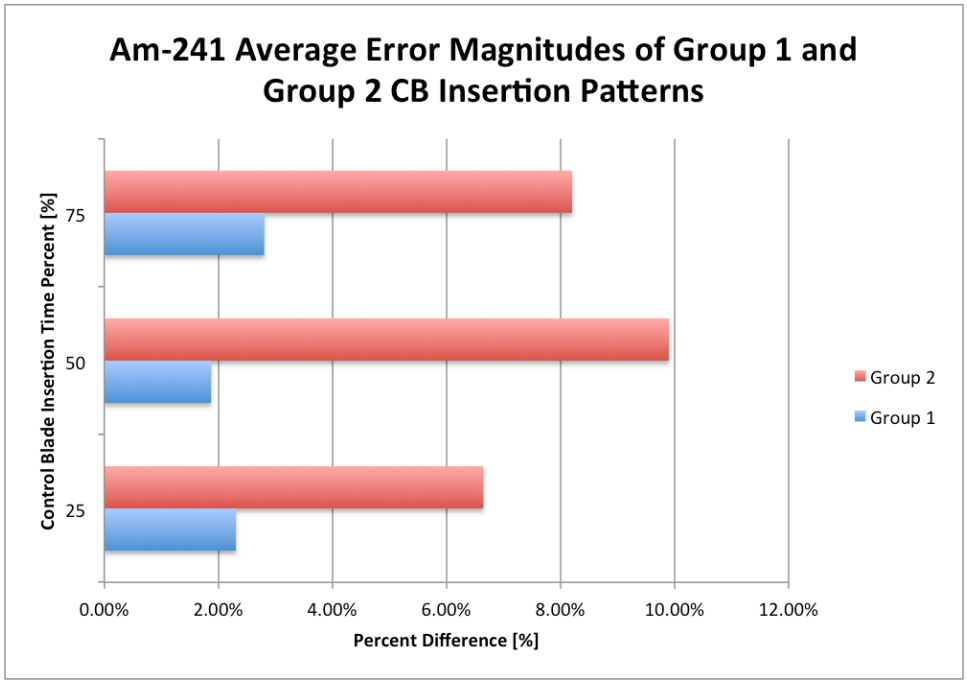

Trend true for ^{234}U, not ^{236}U or ^{238}U. True for ^{238}Pu, may be less true for ^{240}Pu and ^{242}Pu. Holds

Group two control blade insertion patterns show greatly improved PDA method data compared to TRITON for the fertile nuclides of ^{234}U, ^{238}Pu, ^{240}Pu, and ^{241}Am. ^{236}U, ^{238}U, ^{242}Pu, and ^{243}Am do not have these improvements in accuracy with group one compared to group two insertion patterns. ^{236}U, ^{242}Pu, and ^{243}Am have many TRITON and PDA method density values outside of the bounds of the rodded and unrodded cases, so it is expected to result in inaccurate predictions.

CHAPTER 5

CONCLUSIONS AND REMARKS

5.1 PDA Method Conclusions

For some nuclides and control blade insertion patterns, the PDA method is capable of accurately predicting nuclide densities that are found in BWR UNF at high burnup values. Most specifically this includes the fissile nuclides of ^{235}U and ^{241}Pu. Several of the nuclides studied have shown to have their densities bounded by the rodded and unrodded control blade insertion cases while a significant number of the nuclides are not bounded. Nuclides from the fissile, fission product and fertile groupings that are bounded are the best candidates to be used in the PDA method. Control blade insertion patterns which are not skewed towards the beginning or end of the in-reactor fuel assembly lifetime also show very accurate results in the PDA method. However, even for the bounded nuclides with the favorable CB insertion patterns, the PDA method shows no ability to err with conservatism with respect to fuel reactivity. Since the PDA method is most effective for certain nuclides and particular CB insertion patterns and is not effective for all nuclides and it is not conservative in nature, the PDA method can be characterized as unreliable as an approach to determine nuclide densities for BUC applications.

5.2 PDA Method Shortcomings

A problem with the PDA method that was not anticipated in the original conception of the methodology was that many nuclide densities that were obtained in the

time-dependent control blade insertion cases with either TRITON simulation or with the PDA method fall outside of the bounds of the rodded and unrodded cases. Because of this feature, the density value library used (based on the rodded and unrodded case densities) does not contain bounding information for all nuclides. As a result, it is difficult to accurately calculate the time-dependent nuclide densities. While the rodded and unrodded cases yield maximum and minimum fuel reactivity values, the rodded and unrodded cases do not yield bounding values in nuclide densities and they are therefore not always conservative from the viewpoint of nuclear criticality safety.

The other significant problem with the PDA method is that it does not take into account the state of the system (density values of nuclides (and saturation) and neutron flux spectrum). As has been mentioned previously, the PDA method is effectively a way of averaging nuclide density values based on the rodded and unrodded cases using a time-dependent control blade insertion pattern. Neutron energy spectrum is the largest piece of physics that is not being utilized effectively in the PDA method. For many of the nuclides that have been studied, neutron spectrum has a large effect on the saturation concentration of nuclides in the reactor fuel. A change in spectrum that is skewed toward the beginning or the end of the in-reactor fuel assembly lifetime has a large effect on the nuclide density and creates a large difference from the averaging done in the PDA method.

5.3 Future Work/Alternate Approaches

Future work should include two routes to improve upon the prediction capabilities of the PDA method and TRITON simulation while attempting to minimize computational time and resources. One method is to create a library of flux (with energy spectrum) and

cross section values based on the rodded and urodded cases. It should be determined how this flux spectrum and cross-sections change with burnup in order to determine how the library should be built. This information can be used to indicate whether the initial rodded and urodded spectrums and cross-sections are sufficient to be used throughout the burnup of the fuel or if higher burnup spectrums and cross sections need to also be used. After the library of flux spectrum and cross sections is established, it can be used in ORIGEN depletion sequence to rapidly deplete the fuel with appropriate conditions. The second approach is to create a library of branch calculations with the control blade state being changed at each step. Based on this information, the change in density with introduction or withdrawal of control blade state can be determined and the change in density can be scaled with burnup and magnitude (this approach is discussed in GENPMAXS for homogenized cross sections [24]). In conclusion, while the PDA method can be reliable in specific cases, a new method needs to be developed so that no nuclide densities fall outside of that of the rodded and unrodded cases and spectral effects are taken into account.

APPENDIX A

END OF IN-REACTOR FUEL ASSEMBLY LIFETIME DENSITY VALUES FOR BUC NUCLIDES

The following tables show the end of in-reactor fuel assembly lifetime nuclide densities. The results obtained from both the piecewise approach and PARCS simulation are presented. The rodded and unrodded values are also given at the bottom of each table for reference. Values for the predicted and simulated data that are outside of the bounds of the rodded and unrodded case density values are highlighted in red. Percent differences have been calculated for each piecewise-PARCS pair that corresponds to a time-dependent control rod pattern. Negative percent difference indicates that the piecewise data approach underestimates the nuclide density compared to that obtained from PARCS.

25% Time Control Blade Insertion

Fissile and Fissionable Isotopes

	U235 Density [atom/barn-cm]	Percent Difference Between Simulated and Piecewise	Pu239 Density [atom/barn-cm]	Percent Difference Between Simulated and Piecewise	Pu241 Density [atom/barn-cm]	Percent Difference Between Simulated and Piecewise
1A Simulated	1.8920E-04		1.2580E-04		3.5340E-05	
1A Piecewise	1.8340E-04	-3.1%	1.4493E-04	15.2%	3.4949E-05	-1.1%
1B Simulated	1.8070E-04		1.5230E-04		3.8630E-05	

1B Piecewise	1.8300E-04	1.3%	1.3110E-04	-13.9%	3.7900E-05	-1.9%
2A Simulated	1.8760E-04		1.2750E-04		3.5630E-05	
2A Piecewise	1.8986E-04	1.2%	1.3675E-04	7.3%	3.6653E-05	2.9%
2B Simulated	1.8630E-04		1.3340E-04		3.6120E-05	
2B Piecewise	1.8454E-04	-0.9%	1.2932E-04	-3.1%	3.6198E-05	0.2%
3A Simulated	1.8580E-04		1.3550E-04		3.6410E-05	
3A Piecewise	1.8520E-04	-0.3%	1.3317E-04	-1.7%	3.6511E-05	0.3%
3B Simulated	1.8740E-04		1.3080E-04		3.5860E-05	
3B Piecewise	1.8600E-04	-0.7%	1.3588E-04	3.9%	3.6202E-05	1.0%
4A Simulated	1.8790E-04		1.2700E-04		3.5550E-05	
4A Piecewise	1.8926E-04	0.7%	1.3906E-04	9.5%	3.6414E-05	2.4%
4B Simulated	1.8520E-04		1.3770E-04		3.6580E-05	
4B Piecewise	1.8314E-04	-1.1%	1.2892E-04	-6.4%	3.6268E-05	-0.9%
Rodded	2.2780E-04		1.7910E-04		4.5020E-05	
Unrodded	1.7100E-04		1.2100E-04		3.3560E-05	

Fission Products

	Mo95 Density [atom/barn-cm]	Percent Difference Between Simulated and Piecewise	Tc99 Density [atom/barn-cm]	Percent Difference Between Simulated and Piecewise
1A Simulated	5.9100E-05		6.4080E-05	
1A Piecewise	5.9200E-05	0.2%	6.3820E-05	-0.4%
1B Simulated	5.8950E-05		6.3370E-05	
1B Piecewise	5.9010E-05	0.1%	6.3770E-05	0.6%
2A Simulated	5.9060E-05		6.3970E-05	
2A	5.8906E-05	-0.3%	6.3651E-05	-0.5%

Piecewise				
2B Simulated	5.8990E-05		6.3820E-05	
2B Piecewise	5.9034E-05	0.1%	6.3769E-05	-0.1%
3A Simulated	5.9000E-05		6.3800E-05	
3A Piecewise	5.9020E-05	0.0%	6.3750E-05	-0.1%
3B Simulated	5.9030E-05		6.3950E-05	
3B Piecewise	5.9007E-05	0.0%	6.3754E-05	-0.3%
4A Simulated	5.9080E-05		6.4010E-05	
4A Piecewise	5.8933E-05	-0.2%	6.3675E-05	-0.5%
4B Simulated	5.8970E-05		6.3840E-05	
4B Piecewise	5.9074E-05	0.2%	6.3789E-05	-0.1%
Rodded	5.7650E-05		6.2650E-05	
Unrodded	5.9500E-05		6.4120E-05	
	Ru101 Density [atom/barn-cm]	**Percent Difference Between Simulated and Piecewise**	**Rh103 Density [atom/barn-cm]**	**Percent Difference Between Simulated and Piecewise**
1A Simulated	6.2600E-05		3.3310E-05	
1A Piecewise	6.2490E-05	-0.2%	3.2709E-05	-1.8%
1B Simulated	6.2080E-05		3.2340E-05	
1B Piecewise	6.2230E-05	0.2%	3.3340E-05	3.1%
2A Simulated	6.2490E-05		3.3230E-05	
2A Piecewise	6.2409E-05	-0.1%	3.2788E-05	-1.3%
2B Simulated	6.2340E-05		3.3060E-05	
2B Piecewise	6.2411E-05	0.1%	3.2854E-05	-0.6%
3A Simulated	6.2350E-05		3.2960E-05	

3A Piecewise	6.2380E-05	0.0%	3.2901E-05	-0.2%
3B Simulated	6.2430E-05		3.3140E-05	
3B Piecewise	6.2423E-05	0.0%	3.2840E-05	-0.9%
4A Simulated	6.2520E-05		3.3250E-05	
4A Piecewise	6.2432E-05	-0.1%	3.2797E-05	-1.4%
4B Simulated	6.2270E-05		3.2900E-05	
4B Piecewise	6.2391E-05	0.2%	3.2924E-05	0.1%
Rodded	6.1680E-05		3.3980E-05	
Unrodded	6.2620E-05		3.2570E-05	
	Ag109 Density [atom/barn-cm]	**Percent Difference Between Simulated and Piecewise**	**Cs133 Density [atom/barn-cm]**	**Percent Difference Between Simulated and Piecewise**
1A Simulated	5.8930E-06		6.6970E-05	
1A Piecewise	5.8250E-06	-1.2%	6.6590E-05	-0.6%
1B Simulated	5.6720E-06		6.5830E-05	
1B Piecewise	5.7490E-06	1.4%	6.6490E-05	1.0%
2A Simulated	5.8690E-06		6.6720E-05	
2A Piecewise	5.8534E-06	-0.3%	6.6369E-05	-0.5%
2B Simulated	5.8290E-06		6.6410E-05	
2B Piecewise	5.8006E-06	-0.5%	6.6491E-05	0.1%
3A Simulated	5.8100E-06		6.6410E-05	
3A Piecewise	5.8050E-06	-0.1%	6.6480E-05	0.1%
3B Simulated	5.8480E-06		6.6600E-05	
3B Piecewise	5.8205E-06	-0.5%	6.6480E-05	-0.2%
4A	5.8730E-06		6.6780E-05	

Simulated				
4A Piecewise	5.8539E-06	-0.3%	6.6399E-05	-0.6%
4B Simulated	5.7940E-06		6.6270E-05	
4B Piecewise	5.7856E-06	-0.1%	6.6521E-05	0.4%
Rodded	5.9750E-06		6.5180E-05	
Unrodded	5.7510E-06		6.6920E-05	
	Nd143 Density [atom/barn-cm]	**Percent Difference Between Simulated and Piecewise**	**Nd145 Density [atom/barn-cm]**	**Percent Difference Between Simulated and Piecewise**
1A Simulated	4.0840E-05		3.6230E-05	
1A Piecewise	3.9760E-05	-2.6%	3.6040E-05	-0.5%
1B Simulated	4.0990E-05		3.5900E-05	
1B Piecewise	4.2560E-05	3.8%	3.6220E-05	0.9%
2A Simulated	4.0960E-05		3.6160E-05	
2A Piecewise	4.0206E-05	-1.8%	3.5959E-05	-0.6%
2B Simulated	4.1150E-05		3.6070E-05	
2B Piecewise	4.0764E-05	-0.9%	3.6091E-05	0.1%
3A Simulated	4.1050E-05		3.6070E-05	
3A Piecewise	4.0810E-05	-0.6%	3.6080E-05	0.0%
3B Simulated	4.1030E-05		3.6120E-05	
3B Piecewise	4.0442E-05	-1.4%	3.6042E-05	-0.2%
4A Simulated	4.0930E-05		3.6180E-05	
4A Piecewise	4.0108E-05	-2.0%	3.5951E-05	-0.6%
4B Simulated	4.1130E-05		3.6020E-05	
4B Piecewise	4.1034E-05	-0.2%	3.6121E-05	0.3%

Rodded	4.3440E-05		3.5470E-05	
Unrodded	3.9950E-05		3.6280E-05	
	Sm147 Density [atom/barn-cm]	**Percent Difference Between Simulated and Piecewise**	**Sm149 Density [atom/barn-cm]**	**Percent Difference Between Simulated and Piecewise**
1A Simulated	5.7910E-06		6.9280E-08	
1A Piecewise	5.7335E-06	-1.0%	1.0159E-07	46.6%
1B Simulated	5.4990E-06		8.8640E-08	
1B Piecewise	5.6140E-06	2.1%	7.0370E-08	-20.6%
2A Simulated	5.6980E-06		6.9410E-08	
2A Piecewise	5.6309E-06	-1.2%	6.0639E-08	-12.6%
2B Simulated	5.6050E-06		7.0690E-08	
2B Piecewise	5.6246E-06	0.3%	6.9071E-08	-2.3%
3A Simulated	5.6220E-06		7.1160E-08	
3A Piecewise	5.6425E-06	0.4%	6.5300E-08	-8.2%
3B Simulated	5.6720E-06		7.0160E-08	
3B Piecewise	5.6564E-06	-0.3%	7.2740E-08	3.7%
4A Simulated	5.7210E-06		6.9320E-08	
4A Piecewise	5.6508E-06	-1.2%	6.7779E-08	-2.2%
4B Simulated	5.5780E-06		7.1620E-08	
4B Piecewise	5.6306E-06	0.9%	6.8771E-08	-4.0%
Rodded	5.3050E-06		1.0550E-07	
Unrodded	5.7660E-06		6.5390E-08	

	Sm150 Density [atom/barn-cm]	Percent Difference Between Simulated and Piecewise	Sm151 Density [atom/barn-cm]	Percent Difference Between Simulated and Piecewise
1A Simulated	1.5140E-05		4.6570E-07	
1A Piecewise	1.5134E-05	0.0%	5.1500E-07	10.6%
1B Simulated	1.5260E-05		5.5280E-07	
1B Piecewise	1.5240E-05	-0.1%	4.8860E-07	-11.6%
2A Simulated	1.5160E-05		4.6750E-07	
2A Piecewise	1.5192E-05	0.2%	4.9512E-07	5.9%
2B Simulated	1.5200E-05		4.7730E-07	
2B Piecewise	1.5174E-05	-0.2%	4.7478E-07	-0.5%
3A Simulated	1.5210E-05		4.8200E-07	
3A Piecewise	1.5193E-05	-0.1%	4.8880E-07	1.4%
3B Simulated	1.5170E-05		4.7300E-07	
3B Piecewise	1.5173E-05	0.0%	4.9740E-07	5.2%
4A Simulated	1.5150E-05		4.6680E-07	
4A Piecewise	1.5183E-05	0.2%	5.0422E-07	8.0%
4B Simulated	1.5200E-05		4.8520E-07	
4B Piecewise	1.5185E-05	-0.1%	4.7528E-07	-2.0%
Rodded	1.5260E-05		6.3400E-07	
Unrodded	1.5160E-05		4.4650E-07	

	Sm152 Density [atom/barn-cm]	Percent Difference Between Simulated and Piecewise	Eu153 Density [atom/barn-cm]	Percent Difference Between Simulated and Piecewise
1A Simulated	5.3230E-06		6.2650E-06	
1A Piecewise	5.2110E-06	-2.1%	6.2668E-06	0.0%
1B Simulated	4.8060E-06		6.2920E-06	
1B Piecewise	5.1190E-06	6.5%	6.1700E-06	-1.9%
2A Simulated	5.2970E-06		6.2250E-06	
2A Piecewise	5.1585E-06	-2.6%	6.2833E-06	0.9%
2B Simulated	5.2020E-06		6.1920E-06	
2B Piecewise	5.1675E-06	-0.7%	6.2349E-06	0.7%
3A Simulated	5.1540E-06		6.2350E-06	
3A Piecewise	5.1810E-06	0.5%	6.2212E-06	-0.2%
3B Simulated	5.2400E-06		6.2260E-06	
3B Piecewise	5.1717E-06	-1.3%	6.2520E-06	0.4%
4A Simulated	5.3030E-06		6.2360E-06	
4A Piecewise	5.1502E-06	-2.9%	6.2981E-06	1.0%
4B Simulated	5.1190E-06		6.2080E-06	
4B Piecewise	5.1685E-06	1.0%	6.2189E-06	0.2%
Rodded	4.8070E-06		6.2890E-06	
Unrodded	5.2830E-06		6.2220E-06	

Fertile Isotopes

	U234 Density [atom/barn-cm]	Percent Difference Between Simulated and Piecewise	U236 Density [atom/barn-cm]	Percent Difference Between Simulated and Piecewise
1A Simulated	3.0000E-06		1.4210E-04	
1A Piecewise	2.8980E-06	-3.4%	1.4183E-04	-0.2%
1B Simulated	2.9520E-06		1.3890E-04	
1B Piecewise	3.0610E-06	3.7%	1.4010E-04	0.9%
2A Simulated	2.9950E-06		1.4050E-04	
2A Piecewise	2.9547E-06	-1.3%	1.3978E-04	-0.5%
2B Simulated	2.9840E-06		1.3930E-04	
2B Piecewise	3.0043E-06	0.7%	1.3959E-04	0.2%
3A Simulated	2.9810E-06		1.3980E-04	
3A Piecewise	2.9920E-06	0.4%	1.4000E-04	0.1%
3B Simulated	2.9890E-06		1.4030E-04	
3B Piecewise	2.9640E-06	-0.8%	1.4021E-04	-0.1%
4A Simulated	2.9960E-06		1.4090E-04	
4A Piecewise	2.9387E-06	-1.9%	1.4019E-04	-0.5%
4B Simulated	2.9770E-06		1.3920E-04	
4B Piecewise	3.0163E-06	1.3%	1.3979E-04	0.4%
Rodded	2.9180E-06		1.3950E-04	
Unrodded	3.0000E-06		1.4060E-04	

	U238 Density [atom/barn-cm]	Percent Difference Between Simulated and Piecewise	Pu238 Density [atom/barn-cm]	Percent Difference Between Simulated and Piecewise
1A Simulated	0.02105		7.0390E-06	
1A Piecewise	0.02105	0.0%	6.8204E-06	-3.1%
1B Simulated	0.02103		7.3860E-06	
1B Piecewise	0.02105	0.1%	7.7260E-06	4.6%
2A Simulated	0.02105		7.1420E-06	
2A Piecewise	0.0210336	-0.1%	7.0954E-06	-0.7%
2B Simulated	0.02104		7.2540E-06	
2B Piecewise	0.0210564	0.1%	7.1862E-06	-0.9%
3A Simulated	0.02104		7.2330E-06	
3A Piecewise	0.02105	0.0%	7.2013E-06	-0.4%
3B Simulated	0.02105		7.1730E-06	
3B Piecewise	0.02106	0.0%	7.0936E-06	-1.1%
4A Simulated	0.02105		7.1140E-06	
4A Piecewise	0.0210436	0.0%	7.0437E-06	-1.0%
4B Simulated	0.02104		7.2860E-06	
4B Piecewise	0.0210564	0.1%	7.2422E-06	-0.6%
Rodded	0.02095		8.6500E-06	
Unrodded	0.02108		6.7260E-06	

	Pu240 Density [atom/barn-cm]	Percent Difference Between Simulated and Piecewise	Pu242 Density [atom/barn-cm]	Percent Difference Between Simulated and Piecewise
1A Simulated	6.9390E-05		1.8920E-05	
1A Piecewise	6.8180E-05	-1.7%	1.8643E-05	-1.5%
1B Simulated	6.5610E-05		1.7380E-05	
1B Piecewise	6.9570E-05	6.0%	1.7444E-05	0.4%
2A Simulated	7.0220E-05		1.8600E-05	
2A Piecewise	6.8533E-05	-2.4%	1.8634E-05	0.2%
2B Simulated	7.0370E-05		1.8140E-05	
2B Piecewise	6.8327E-05	-2.9%	1.8349E-05	1.2%
3A Simulated	6.9150E-05		1.8160E-05	
3A Piecewise	6.8530E-05	-0.9%	1.8289E-05	0.7%
3B Simulated	6.9880E-05		1.8420E-05	
3B Piecewise	6.8494E-05	-2.0%	1.8442E-05	0.1%
4A Simulated	6.9970E-05		1.8680E-05	
4A Piecewise	6.8587E-05	-2.0%	1.8635E-05	-0.2%
4B Simulated	6.9420E-05		1.7960E-05	
4B Piecewise	6.8417E-05	-1.4%	1.8197E-05	1.3%
Rodded	7.4300E-05		1.7270E-05	
Unrodded	6.6770E-05		1.8600E-05	

	Am241 Density [atom/barn-cm]	Percent Difference Between Simulated and Piecewise	Am243 Density [atom/barn-cm]	Percent Difference Between Simulated and Piecewise
1A Simulated	1.9140E-06		4.7150E-06	
1A Piecewise	1.7518E-06	-8.5%	4.6432E-06	-1.5%
1B Simulated	1.9150E-06		4.8710E-06	
1B Piecewise	2.1820E-06	13.9%	4.6530E-06	-4.5%
2A Simulated	1.9290E-06		4.5960E-06	
2A Piecewise	1.8745E-06	-2.8%	4.7169E-06	2.6%
2B Simulated	1.9720E-06		4.5790E-06	
2B Piecewise	1.9367E-06	-1.8%	4.7339E-06	3.4%
3A Simulated	1.9530E-06		4.6750E-06	
3A Piecewise	1.9363E-06	-0.9%	4.6962E-06	0.5%
3B Simulated	1.9510E-06		4.6360E-06	
3B Piecewise	1.8837E-06	-3.5%	4.7011E-06	1.4%
4A Simulated	1.9250E-06		4.6250E-06	
4A Piecewise	1.8499E-06	-3.9%	4.7014E-06	1.7%
4B Simulated	1.9700E-06		4.6440E-06	
4B Piecewise	1.9647E-06	-0.3%	4.7135E-06	1.5%
Rodded	2.5670E-06		4.8420E-06	
Unrodded	1.7260E-06		4.6350E-06	

50% Time Control Blade Insertion

Fissile and Fissionable Isotopes

	U235 Density [atom/barn-cm]	Percent Difference Between Simulated and Piecewise	Pu239 Density [atom/barn-cm]	Percent Difference Between Simulated and Piecewise	Pu241 Density [atom/barn-cm]	Percent Difference Between Simulated and Piecewise
1A Simulated	2.0560E-04		1.3290E-04		3.7460E-05	
1A Piecewise	2.0226E-04	-1.6%	1.6068E-04	20.9%	3.8042E-05	1.6%
1B Simulated	1.9500E-04		1.6540E-04		4.1140E-05	
1B Piecewise	1.9654E-04	0.8%	1.3942E-04	-15.7%	4.0538E-05	-1.5%
2A Simulated	2.0430E-04		1.3880E-04		3.7910E-05	
2A Piecewise	1.9694E-04	-3.6%	1.5325E-04	10.4%	3.7587E-05	-0.9%
2B Simulated	1.9690E-04		1.5890E-04		4.0700E-05	
2B Piecewise	2.0186E-04	2.5%	1.4685E-04	-7.6%	4.0993E-05	0.7%
3A Simulated	2.0000E-04		1.5160E-04		3.9760E-05	
3A Piecewise	1.9861E-04	-0.7%	1.5341E-04	1.2%	3.9195E-05	-1.4%
3B Simulated	2.0000E-04		1.5270E-04		3.9830E-05	
3B Piecewise	1.9670E-04	-1.6%	1.5130E-04	-0.9%	3.8954E-05	-2.2%
4A Simulated	2.0450E-04		1.3680E-04		3.7750E-05	
4A Piecewise	1.9264E-04	-5.8%	1.5054E-04	10.0%	3.6562E-05	-3.1%
4B Simulated	1.9660E-04		1.5890E-04		4.0640E-05	
4B Piecewise	1.9301E-04	-1.8%	1.3779E-04	-13.3%	3.9379E-05	-3.1%
Rodded	2.2780E-04		1.7910E-04		4.5020E-05	
Unrodded	1.7100E-04		1.2100E-04		3.3560E-05	

Fission Products

	Mo95 Density [atom/barn-cm]	Percent Difference Between Simulated and Piecewise	Tc99 Density [atom/barn-cm]	Percent Difference Between Simulated and Piecewise
1A	5.8660E-05		6.3930E-05	

Simulated				
1A Piecewise	5.8606E-05	-0.1%	6.3351E-05	-0.9%
1B Simulated	5.8460E-05		6.2970E-05	
1B Piecewise	5.8544E-05	0.1%	6.3419E-05	0.7%
2A Simulated	5.8590E-05		6.3780E-05	
2A Piecewise	5.8734E-05	0.2%	6.3469E-05	-0.5%
2B Simulated	5.8520E-05		6.3230E-05	
2B Piecewise	5.8416E-05	-0.2%	6.3301E-05	0.1%
3A Simulated	5.8560E-05		6.3560E-05	
3A Piecewise	5.8625E-05	0.1%	6.3411E-05	-0.2%
3B Simulated	5.8540E-05		6.3570E-05	
3B Piecewise	5.8679E-05	0.2%	6.3447E-05	-0.2%
4A Simulated	5.8610E-05		6.3790E-05	
4A Piecewise	5.8909E-05	0.5%	6.3569E-05	-0.3%
4B Simulated	5.8510E-05		6.3280E-05	
4B Piecewise	5.8692E-05	0.3%	6.3538E-05	0.4%
Rodded	5.7650E-05		6.2650E-05	
Unrodded	5.9500E-05		6.4120E-05	
	Ru101 Density [atom/barn-cm]	**Percent Difference Between Simulated and Piecewise**	**Rh103 Density [atom/barn-cm]**	**Percent Difference Between Simulated and Piecewise**
1A Simulated	6.2470E-05		3.3950E-05	
1A Piecewise	6.2279E-05	-0.3%	3.2927E-05	-3.0%
1B Simulated	6.1810E-05		3.2760E-05	
1B Piecewise	6.2021E-05	0.3%	3.3624E-05	2.6%
2A Simulated	6.2320E-05		3.3760E-05	

2A Piecewise	6.2281E-05	-0.1%	3.2993E-05	-2.3%
2B Simulated	6.1960E-05		3.2960E-05	
2B Piecewise	6.2019E-05	0.1%	3.3558E-05	1.8%
3A Simulated	6.2110E-05		3.3250E-05	
3A Piecewise	6.2116E-05	0.0%	3.3318E-05	0.2%
3B Simulated	6.2080E-05		3.3230E-05	
3B Piecewise	6.2128E-05	0.1%	3.3339E-05	0.3%
4A Simulated	6.2360E-05		3.3820E-05	
4A Piecewise	6.2381E-05	0.0%	3.2840E-05	-2.9%
4B Simulated	6.1940E-05		3.2960E-05	
4B Piecewise	6.2134E-05	0.3%	3.3401E-05	1.3%
Rodded	6.1680E-05		3.3980E-05	
Unrodded	6.2620E-05		3.2570E-05	
	Ag109 Density [atom/barn-cm]	**Percent Difference Between Simulated and Piecewise**	**Cs133 Density [atom/barn-cm]**	**Percent Difference Between Simulated and Piecewise**
1A Simulated	6.0080E-06		6.6750E-05	
1A Piecewise	5.9274E-06	-1.3%	6.6039E-05	-1.1%
1B Simulated	5.7400E-06		6.5340E-05	
1B Piecewise	5.7986E-06	1.0%	6.6061E-05	1.1%
2A Simulated	5.9660E-06		6.6440E-05	
2A Piecewise	5.8746E-06	-1.5%	6.6161E-05	-0.4%
2B Simulated	5.7850E-06		6.5640E-05	
2B Piecewise	5.8514E-06	1.1%	6.5939E-05	0.5%
3A Simulated	5.8520E-06		6.6000E-05	
3A	5.8540E-06	0.0%	6.6067E-05	0.1%

Piecewise				
3B Simulated	5.8460E-06		6.5950E-05	
3B Piecewise	5.8388E-06	-0.1%	6.6120E-05	0.3%
4A Simulated	5.9790E-06		6.6530E-05	
4A Piecewise	5.8689E-06	-1.8%	6.6311E-05	-0.3%
4B Simulated	5.7830E-06		6.5610E-05	
4B Piecewise	5.8054E-06	0.4%	6.6195E-05	0.9%
Rodded	5.9750E-06		6.5180E-05	
Unrodded	5.7510E-06		6.6920E-05	
	Nd143 Density [atom/barn-cm]	**Percent Difference Between Simulated and Piecewise**	**Nd145 Density [atom/barn-cm]**	**Percent Difference Between Simulated and Piecewise**
1A Simulated	4.1760E-05		3.6090E-05	
1A Piecewise	4.0016E-05	-4.2%	3.5719E-05	-1.0%
1B Simulated	4.2040E-05		3.5690E-05	
1B Piecewise	4.3374E-05	3.2%	3.6031E-05	1.0%
2A Simulated	4.1920E-05		3.6000E-05	
2A Piecewise	4.0574E-05	-3.2%	3.5851E-05	-0.4%
2B Simulated	4.1900E-05		3.5770E-05	
2B Piecewise	4.2816E-05	2.2%	3.5899E-05	0.4%
3A Simulated	4.1830E-05		3.5870E-05	
3A Piecewise	4.1762E-05	-0.2%	3.5894E-05	0.1%
3B Simulated	4.1870E-05		3.5850E-05	
3B Piecewise	4.1890E-05	0.0%	3.5941E-05	0.3%
4A Simulated	4.1890E-05		3.6020E-05	
4A Piecewise	4.0094E-05	-4.3%	3.5897E-05	-0.3%

4B Simulated	4.1930E-05		3.5760E-05	
4B Piecewise	4.2573E-05	1.5%	3.6050E-05	0.8%
Rodded	4.3440E-05		3.5470E-05	
Unrodded	3.9950E-05		3.6280E-05	
	Sm147 Density [atom/barn-cm]	**Percent Difference Between Simulated and Piecewise**	**Sm149 Density [atom/barn-cm]**	**Percent Difference Between Simulated and Piecewise**
1A Simulated	5.7190E-06		7.3490E-08	
1A Piecewise	5.5984E-06	-2.1%	9.6839E-08	31.8%
1B Simulated	5.3480E-06		9.5140E-08	
1B Piecewise	5.4726E-06	2.3%	7.4051E-08	-22.2%
2A Simulated	5.6260E-06		7.4770E-08	
2A Piecewise	5.5921E-06	-0.6%	1.0527E-07	40.8%
2B Simulated	5.4360E-06		9.3540E-08	
2B Piecewise	5.4789E-06	0.8%	6.5619E-08	-29.8%
3A Simulated	5.5370E-06		9.1920E-08	
3A Piecewise	5.5573E-06	0.4%	9.7253E-08	5.8%
3B Simulated	5.5210E-06		9.2210E-08	
3B Piecewise	5.5598E-06	0.7%	1.0037E-07	8.8%
4A Simulated	5.6470E-06		7.4320E-08	
4A Piecewise	5.6455E-06	0.0%	9.9081E-08	33.3%
4B Simulated	5.4220E-06		9.3500E-08	
4B Piecewise	5.5356E-06	2.1%	6.9114E-08	-26.1%
Rodded	5.3050E-06		1.0550E-07	
Unrodded	5.7660E-06		6.5390E-08	

	Sm150 Density [atom/barn-cm]	Percent Difference Between Simulated and Piecewise	Sm151 Density [atom/barn-cm]	Percent Difference Between Simulated and Piecewise
1A Simulated	1.5140E-05		4.8640E-07	
1A Piecewise	1.5166E-05	0.2%	5.6362E-07	15.9%
1B Simulated	1.5290E-05		5.8560E-07	
1B Piecewise	1.5254E-05	-0.2%	5.1688E-07	-11.7%
2A Simulated	1.5180E-05		4.9620E-07	
2A Piecewise	1.5148E-05	-0.2%	5.4328E-07	9.5%
2B Simulated	1.5250E-05		5.7430E-07	
2B Piecewise	1.5272E-05	0.1%	5.3722E-07	-6.5%
3A Simulated	1.5170E-05		5.5800E-07	
3A Piecewise	1.5216E-05	0.3%	5.4318E-07	-2.7%
3B Simulated	1.5160E-05		5.5960E-07	
3B Piecewise	1.5208E-05	0.3%	5.3703E-07	-4.0%
4A Simulated	1.5170E-05		4.9290E-07	
4A Piecewise	1.5147E-05	-0.1%	5.3348E-07	8.2%
4B Simulated	1.5220E-05		5.7340E-07	
4B Piecewise	1.5246E-05	0.2%	5.0741E-07	-11.5%
Rodded	1.5260E-05		6.3400E-07	
Unrodded	1.5160E-05		4.4650E-07	
	Sm152 Density [atom/barn-cm]	**Percent Difference Between Simulated and Piecewise**	**Eu153 Density [atom/barn-cm]**	**Percent Difference Between Simulated and Piecewise**
1A Simulated	5.3370E-06		6.2670E-06	
1A	5.0865E-06	-4.7%	6.3281E-06	1.0%

Piecewise				
1B Simulated	4.7440E-06		6.2480E-06	
1B Piecewise	5.0035E-06	5.5%	6.1829E-06	-1.0%
2A Simulated	5.2390E-06		6.2350E-06	
2A Piecewise	5.0955E-06	-2.7%	6.2797E-06	0.7%
2B Simulated	4.8240E-06		6.2930E-06	
2B Piecewise	4.9945E-06	3.5%	6.2313E-06	-1.0%
3A Simulated	4.9430E-06		6.3050E-06	
3A Piecewise	5.0474E-06	2.1%	6.2527E-06	-0.8%
3B Simulated	4.9290E-06		6.2960E-06	
3B Piecewise	5.0651E-06	2.8%	6.2299E-06	-1.1%
4A Simulated	5.2700E-06		6.2370E-06	
4A Piecewise	5.1425E-06	-2.4%	6.2874E-06	0.8%
4B Simulated	4.8230E-06		6.2750E-06	
4B Piecewise	5.0435E-06	4.6%	6.2171E-06	-0.9%
Rodded	4.8070E-06		6.2890E-06	
Unrodded	5.2830E-06		6.2220E-06	

Fertile Isotopes

	U234 Density [atom/barn-cm]	Percent Difference Between Simulated and Piecewise	U236 Density [atom/barn-cm]	Percent Difference Between Simulated and Piecewise
1A Simulated	2.99E-06		0.000142	
1A Piecewise	2.85E-06	-4.6%	0.000141008	-0.7%
1B Simulated	2.93E-06		0.0001378	
1B	3.07E-06	4.5%	0.000139092	0.9%

Piecewise				
2A Simulated	2.98E-06		0.0001409	
2A Piecewise	2.90E-06	-2.6%	0.000140822	-0.1%
2B Simulated	2.95E-06		0.0001389	
2B Piecewise	3.02E-06	2.4%	0.000139278	0.3%
3A Simulated	2.96E-06		0.0001403	
3A Piecewise	2.95E-06	-0.5%	0.000140703	0.3%
3B Simulated	2.96E-06		0.0001401	
3B Piecewise	2.96E-06	0.0%	0.000140749	0.5%
4A Simulated	2.98E-06		0.0001411	
4A Piecewise	2.89E-06	-3.0%	0.000141172	0.1%
4B Simulated	2.95E-06		0.0001386	
4B Piecewise	3.04E-06	3.2%	0.000139379	0.6%
Rodded	2.92E-06		0.0001395	
Unrodded	3.00E-06		0.0001406	
	U238 Density [atom/barn-cm]	**Percent Difference Between Simulated and Piecewise**	**Pu238 Density [atom/barn-cm]**	**Percent Difference Between Simulated and Piecewise**
1A Simulated	0.02102		7.46E-06	
1A Piecewise	0.0210036	-0.1%	7.19E-06	-3.7%
1B Simulated	0.021		7.91E-06	
1B Piecewise	0.0210264	0.1%	8.19E-06	3.4%
2A Simulated	0.02102		7.57E-06	
2A Piecewise	0.0210264	0.0%	7.28E-06	-3.8%
2B Simulated	0.02101		7.80E-06	
2B Piecewise	0.0210036	0.0%	8.10E-06	3.8%

3A Simulated	0.02101		7.67E-06	
3A Piecewise	0.021013	0.0%	7.70E-06	0.4%
3B Simulated	0.02101		7.70E-06	
3B Piecewise	0.0210156	0.0%	7.71E-06	0.1%
4A Simulated	0.02102		7.55E-06	
4A Piecewise	0.0210164	0.0%	7.06E-06	-6.4%
4B Simulated	0.02101		7.81E-06	
4B Piecewise	0.0210308	0.1%	7.90E-06	1.1%
Rodded	0.02095		8.65E-06	
Unrodded	0.02108		6.73E-06	
	Pu240 Density [atom/barn-cm]	**Percent Difference Between Simulated and Piecewise**	**Pu242 Density [atom/barn-cm]**	**Percent Difference Between Simulated and Piecewise**
1A Simulated	7.30E-05		1.8870E-05	
1A Piecewise	6.99E-05	-4.2%	1.8677E-05	-1.0%
1B Simulated	6.88E-05		1.6980E-05	
1B Piecewise	7.11E-05	3.5%	1.7193E-05	1.3%
2A Simulated	7.29E-05		1.8440E-05	
2A Piecewise	6.97E-05	-4.3%	1.8392E-05	-0.3%
2B Simulated	6.88E-05		1.7410E-05	
2B Piecewise	7.13E-05	3.7%	1.7478E-05	0.4%
3A Simulated	6.96E-05		1.7880E-05	
3A Piecewise	7.07E-05	1.5%	1.7868E-05	-0.1%
3B Simulated	6.97E-05		1.7810E-05	
3B Piecewise	7.06E-05	1.3%	1.7797E-05	-0.1%

4A Simulated	7.31E-05		1.8560E-05	
4A Piecewise	6.91E-05	-5.5%	1.8593E-05	0.2%
4B Simulated	6.92E-05		1.7350E-05	
4B Piecewise	7.04E-05	1.8%	1.7542E-05	1.1%
Rodded	7.43E-05		1.7270E-05	
Unrodded	6.68E-05		1.8600E-05	
	Am241 Density [atom/barn-cm]	**Percent Difference Between Simulated and Piecewise**	**Am243 Density [atom/barn-cm]**	**Percent Difference Between Simulated and Piecewise**
1A Simulated	2.1280E-06		4.6650E-06	
1A Piecewise	1.9003E-06	-10.7%	4.7251E-06	1.3%
1B Simulated	2.1560E-06		4.8000E-06	
1B Piecewise	2.3927E-06	11.0%	4.7519E-06	-1.0%
2A Simulated	2.1690E-06		4.6650E-06	
2A Piecewise	1.9625E-06	-9.5%	4.7421E-06	1.7%
2B Simulated	2.1160E-06		4.8330E-06	
2B Piecewise	2.3305E-06	10.1%	4.7349E-06	-2.0%
3A Simulated	2.1090E-06		4.8490E-06	
3A Piecewise	2.1492E-06	1.9%	4.7082E-06	-2.9%
3B Simulated	2.1180E-06		4.8420E-06	
3B Piecewise	2.1569E-06	1.8%	4.7074E-06	-2.8%
4A Simulated	2.1570E-06		4.6500E-06	
4A Piecewise	1.8585E-06	-13.8%	4.7020E-06	1.1%
4B Simulated	2.1210E-06		4.8020E-06	
4B Piecewise	2.2505E-06	6.1%	4.7187E-06	-1.7%

Rodded	2.5670E-06		4.8420E-06	
Unrodded	1.7260E-06		4.6350E-06	

75 % Time Control Blade insertion

Fissile and Fissionable Isotopes

	U235 Density [atom/barn-cm]	Percent Difference Between Simulated and Piecewise	Pu239 Density [atom/barn-cm]	Percent Difference Between Simulated and Piecewise	Pu241 Density [atom/barn-cm]	Percent Difference Between Simulated and Piecewise
1A Simulated	2.1980E-04		1.4690E-04		4.0010E-05	
1A Piecewise	2.1580E-04	-1.8%	1.6900E-04	15.0%	4.0680E-05	1.7%
1B Simulated	2.1040E-04		1.7300E-04		4.3180E-05	
1B Piecewise	2.1540E-04	2.4%	1.5517E-04	-10.3%	4.3631E-05	1.0%
2A Simulated	2.1270E-04		1.7090E-04		4.2940E-05	
2A Piecewise	2.0894E-04	-1.8%	1.6335E-04	-4.4%	4.1927E-05	-2.4%
2B Simulated	2.1460E-04		1.6440E-04		4.2540E-05	
2B Piecewise	2.1426E-04	-0.2%	1.7078E-04	3.9%	4.2382E-05	-0.4%
3A Simulated	2.1780E-04		1.5460E-04		4.0750E-05	
3A Piecewise	2.1300E-04	-2.2%	1.6583E-04	7.3%	4.0828E-05	0.2%
3B Simulated	2.1200E-04		1.6910E-04		4.2900E-05	
3B Piecewise	2.1450E-04	1.2%	1.5935E-04	-5.8%	4.3103E-05	0.5%
4A Simulated	2.1390E-04		1.6610E-04		4.2490E-05	
4A Piecewise	2.1466E-04	0.4%	1.6707E-04	0.6%	4.2693E-05	0.5%
4B Simulated	2.1400E-04		1.6530E-04		4.2440E-05	
4B Piecewise	2.1174E-04	-1.1%	1.6581E-04	0.3%	4.2130E-05	-0.7%
Rodded	2.2780E-04		1.7910E-04		4.5020E-05	

Unrodded	1.7100E-04		1.2100E-04		3.3560E-05	

Fission Products

	Mo95 Density [atom/barn-cm]	Percent Difference Between Simulated and Piecewise	Tc99 Density [atom/barn-cm]	Percent Difference Between Simulated and Piecewise
1A Simulated	5.8160E-05		6.3490E-05	
1A Piecewise	5.8140E-05	0.0%	6.3000E-05	-0.8%
1B Simulated	5.8040E-05		6.2690E-05	
1B Piecewise	5.7950E-05	-0.2%	6.2950E-05	0.4%
2A Simulated	5.8060E-05		6.2930E-05	
2A Piecewise	5.8244E-05	0.3%	6.3119E-05	0.3%
2B Simulated	5.8130E-05		6.3190E-05	
2B Piecewise	5.8116E-05	0.0%	6.3001E-05	-0.3%
3A Simulated	5.8110E-05		6.3400E-05	
3A Piecewise	5.8180E-05	0.1%	6.3050E-05	-0.6%
3B Simulated	5.8080E-05		6.2980E-05	
3B Piecewise	5.8017E-05	-0.1%	6.3004E-05	0.0%
4A Simulated	5.8090E-05		6.3240E-05	
4A Piecewise	5.8089E-05	0.0%	6.2966E-05	-0.4%
4B Simulated	5.8100E-05		6.3270E-05	
4B Piecewise	5.8183E-05	0.1%	6.3046E-05	-0.4%
Rodded	5.7650E-05		6.2650E-05	
Unrodded	5.9500E-05		6.4120E-05	

	Ru101 Density [atom/barn-cm]	Percent Difference Between Simulated and Piecewise	Rh103 Density [atom/barn-cm]	Percent Difference Between Simulated and Piecewise
1A Simulated	6.2200E-05		3.4340E-05	
1A Piecewise	6.2070E-05	-0.2%	3.3210E-05	-3.3%
1B Simulated	6.1700E-05		3.3330E-05	
1B Piecewise	6.1810E-05	0.2%	3.3841E-05	1.5%
2A Simulated	6.1800E-05		3.3440E-05	
2A Piecewise	6.1891E-05	0.1%	3.3763E-05	1.0%
2B Simulated	6.1940E-05		3.3650E-05	
2B Piecewise	6.1889E-05	-0.1%	3.3697E-05	0.1%
3A Simulated	6.2060E-05		3.4060E-05	
3A Piecewise	6.2030E-05	0.0%	3.3319E-05	-2.2%
3B Simulated	6.1800E-05		3.3460E-05	
3B Piecewise	6.1843E-05	0.1%	3.3781E-05	1.0%
4A Simulated	6.1870E-05		3.3600E-05	
4A Piecewise	6.1842E-05	0.0%	3.3784E-05	0.5%
4B Simulated	6.1890E-05		3.3620E-05	
4B Piecewise	6.1893E-05	0.0%	3.3700E-05	0.2%
Rodded	6.1680E-05		3.3980E-05	
Unrodded	6.2620E-05		3.2570E-05	
	Ag109 Density [atom/barn-cm]	Percent Difference Between Simulated and Piecewise	Cs133 Density [atom/barn-cm]	Percent Difference Between Simulated and Piecewise
1A Simulated	6.0730E-06		6.6230E-05	
1A	5.9770E-06	-1.6%	6.5610E-05	-0.9%

Piecewise				
1B Simulated	5.8450E-06		6.5150E-05	
1B Piecewise	5.9010E-06	1.0%	6.5510E-05	0.6%
2A Simulated	5.8750E-06		6.5380E-05	
2A Piecewise	5.8726E-06	0.0%	6.5731E-05	0.5%
2B Simulated	5.9220E-06		6.5680E-05	
2B Piecewise	5.9254E-06	0.1%	6.5609E-05	-0.1%
3A Simulated	6.0120E-06		6.5930E-05	
3A Piecewise	5.9390E-06	-1.2%	6.5660E-05	-0.4%
3B Simulated	5.8750E-06		6.5350E-05	
3B Piecewise	5.9115E-06	0.6%	6.5580E-05	0.4%
4A Simulated	5.9080E-06		6.5550E-05	
4A Piecewise	5.9117E-06	0.1%	6.5557E-05	0.0%
4B Simulated	5.9130E-06		6.5590E-05	
4B Piecewise	5.9021E-06	-0.2%	6.5646E-05	0.1%
Rodded	5.9750E-06		6.5180E-05	
Unrodded	5.7510E-06		6.6920E-05	
	Nd143 Density [atom/barn-cm]	**Percent Difference Between Simulated and Piecewise**	**Nd145 Density [atom/barn-cm]**	**Percent Difference Between Simulated and Piecewise**
1A Simulated	4.2720E-05		3.5860E-05	
1A Piecewise	4.0830E-05	-4.4%	3.5530E-05	-0.9%
1B Simulated	4.2830E-05		3.5550E-05	
1B Piecewise	4.3630E-05	1.9%	3.5710E-05	0.5%
2A Simulated	4.2730E-05		3.5610E-05	
2A Piecewise	4.3184E-05	1.1%	3.5791E-05	0.5%

2B Simulated	4.2600E-05		3.5700E-05	
2B Piecewise	4.2626E-05	0.1%	3.5659E-05	-0.1%
3A Simulated	4.2760E-05		3.5770E-05	
3A Piecewise	4.1450E-05	-3.1%	3.5600E-05	-0.5%
3B Simulated	4.2750E-05		3.5610E-05	
3B Piecewise	4.3192E-05	1.0%	3.5702E-05	0.3%
4A Simulated	4.2690E-05		3.5660E-05	
4A Piecewise	4.3053E-05	0.9%	3.5669E-05	0.0%
4B Simulated	4.2670E-05		3.5670E-05	
4B Piecewise	4.2813E-05	0.3%	3.5704E-05	0.1%
Rodded	4.3440E-05		3.5470E-05	
Unrodded	3.9950E-05		3.6280E-05	
	Sm147 Density [atom/barn-cm]	**Percent Difference Between Simulated and Piecewise**	**Sm149 Density [atom/barn-cm]**	**Percent Difference Between Simulated and Piecewise**
1A Simulated	5.5550E-06		7.9180E-08	
1A Piecewise	5.4570E-06	-1.8%	1.0052E-07	27.0%
1B Simulated	5.2860E-06		1.0030E-07	
1B Piecewise	5.3375E-06	1.0%	6.9300E-08	-30.9%
2A Simulated	5.3700E-06		1.0010E-07	
2A Piecewise	5.4401E-06	1.3%	1.1025E-07	10.1%
2B Simulated	5.4570E-06		9.8550E-08	
2B Piecewise	5.4464E-06	-0.2%	1.0182E-07	3.3%
3A Simulated	5.4840E-06		8.0810E-08	
3A Piecewise	5.4505E-06	-0.6%	1.0230E-07	26.6%
3B	5.3500E-06		9.9350E-08	

Simulated				
3B Piecewise	5.3859E-06	0.7%	7.4830E-08	-24.7%
4A Simulated	5.4110E-06		9.8890E-08	
4A Piecewise	5.4017E-06	-0.2%	1.0446E-07	5.6%
4B Simulated	5.4230E-06		9.8670E-08	
4B Piecewise	5.4384E-06	0.3%	1.0218E-07	3.6%
Rodded	5.3050E-06		1.0550E-07	
Unrodded	5.7660E-06		6.5390E-08	
	Sm150 Density [atom/barn-cm]	**Percent Difference Between Simulated and Piecewise**	**Sm151 Density [atom/barn-cm]**	**Percent Difference Between Simulated and Piecewise**
1A Simulated	1.5190E-05		5.1980E-07	
1A Piecewise	1.5180E-05	-0.1%	5.9190E-07	13.9%
1B Simulated	1.5300E-05		6.1050E-07	
1B Piecewise	1.5286E-05	-0.1%	5.6550E-07	-7.4%
2A Simulated	1.5260E-05		6.0810E-07	
2A Piecewise	1.5228E-05	-0.2%	5.8538E-07	-3.7%
2B Simulated	1.5220E-05		5.9680E-07	
2B Piecewise	1.5246E-05	0.2%	6.0572E-07	1.5%
3A Simulated	1.5200E-05		5.3390E-07	
3A Piecewise	1.5190E-05	-0.1%	5.8730E-07	10.0%
3B Simulated	1.5260E-05		6.0360E-07	
3B Piecewise	1.5276E-05	0.1%	5.7660E-07	-4.5%
4A Simulated	1.5190E-05		5.9760E-07	
4A Piecewise	1.5242E-05	0.3%	5.9227E-07	-0.9%
4B Simulated	1.5200E-05		5.9630E-07	

4B Piecewise	1.5243E-05	0.3%	5.8858E-07	-1.3%
Rodded	1.5260E-05		6.3400E-07	
Unrodded	1.5160E-05		4.4650E-07	
	Sm152 Density [atom/barn-cm]	**Percent Difference Between Simulated and Piecewise**	**Eu153 Density [atom/barn-cm]**	**Percent Difference Between Simulated and Piecewise**
1A Simulated	5.2590E-06		6.2360E-06	
1A Piecewise	4.9710E-06	-5.5%	6.3410E-06	1.7%
1B Simulated	4.7670E-06		6.2500E-06	
1B Piecewise	4.8790E-06	2.3%	6.2442E-06	-0.1%
2A Simulated	4.7830E-06		6.2900E-06	
2A Piecewise	4.9315E-06	3.1%	6.2277E-06	-1.0%
2B Simulated	4.8670E-06		6.3330E-06	
2B Piecewise	4.9225E-06	1.1%	6.2761E-06	-0.9%
3A Simulated	5.1220E-06		6.2350E-06	
3A Piecewise	4.9420E-06	-3.5%	6.3208E-06	1.4%
3B Simulated	4.8110E-06		6.2820E-06	
3B Piecewise	4.9117E-06	2.1%	6.2522E-06	-0.5%
4A Simulated	4.8490E-06		6.2950E-06	
4A Piecewise	4.9141E-06	1.3%	6.2454E-06	-0.8%
4B Simulated	4.8590E-06		6.3020E-06	
4B Piecewise	4.9364E-06	1.6%	6.2480E-06	-0.9%
Rodded	4.8070E-06		6.2890E-06	
Unrodded	5.2830E-06		6.2220E-06	

Fertile Isotopes

	U234 Density [atom/barn-cm]	Percent Difference Between Simulated and Piecewise	U236 Density [atom/barn-cm]	Percent Difference Between Simulated and Piecewise
1A Simulated	2.9690E-06		1.4080E-04	
1A Piecewise	2.8570E-06	-3.8%	1.4000E-04	-0.6%
1B Simulated	2.9250E-06		1.3790E-04	
1B Piecewise	3.0200E-06	3.2%	1.3827E-04	0.3%
2A Simulated	2.9300E-06		1.3940E-04	
2A Piecewise	2.9633E-06	1.1%	1.4032E-04	0.7%
2B Simulated	2.9410E-06		1.4040E-04	
2B Piecewise	2.9137E-06	-0.9%	1.4051E-04	0.1%
3A Simulated	2.9570E-06		1.4020E-04	
3A Piecewise	2.8940E-06	-2.1%	1.3999E-04	-0.1%
3B Simulated	2.9310E-06		1.3880E-04	
3B Piecewise	2.9840E-06	1.8%	1.3901E-04	0.2%
4A Simulated	2.9380E-06		1.3980E-04	
4A Piecewise	2.9437E-06	0.2%	1.3999E-04	0.1%
4B Simulated	2.9390E-06		1.3990E-04	
4B Piecewise	2.9403E-06	0.0%	1.4023E-04	0.2%
Rodded	2.9180E-06		1.3950E-04	
Unrodded	3.0000E-06		1.4060E-04	
	U238 Density [atom/barn-cm]	Percent Difference Between Simulated and Piecewise	Pu238 Density [atom/barn-cm]	Percent Difference Between Simulated and Piecewise

1A Simulated	0.02099		7.9950E-06	
1A Piecewise	0.02098	0.0%	7.6500E-06	-4.3%
1B Simulated	0.02098		8.3310E-06	
1B Piecewise	0.02098	0.0%	8.5556E-06	2.7%
2A Simulated	0.02098		8.2240E-06	
2A Piecewise	0.0209964	0.1%	8.2806E-06	0.7%
2B Simulated	0.02098		8.1200E-06	
2B Piecewise	0.0209736	0.0%	8.1898E-06	0.9%
3A Simulated	0.02099		8.0760E-06	
3A Piecewise	0.021	0.0%	7.8010E-06	-3.4%
3B Simulated	0.02098		8.2460E-06	
3B Piecewise	0.02099	0.0%	8.3864E-06	1.7%
4A Simulated	0.02098		8.1670E-06	
4A Piecewise	0.020973	0.0%	8.3362E-06	2.1%
4B Simulated	0.02098		8.1520E-06	
4B Piecewise	0.0209832	0.0%	8.2243E-06	0.9%
Rodded	0.02095		8.6500E-06	
Unrodded	0.02108		6.7260E-06	
	Pu240 Density [atom/barn-cm]	**Percent Difference Between Simulated and Piecewise**	**Pu242 Density [atom/barn-cm]**	**Percent Difference Between Simulated and Piecewise**
1A Simulated	7.6300E-05		1.8390E-05	
1A Piecewise	7.1500E-05	-6.3%	1.8426E-05	0.2%
1B Simulated	7.1820E-05		1.7000E-05	
1B Piecewise	7.2890E-05	1.5%	1.7227E-05	1.3%

2A Simulated	7.1100E-05		1.7300E-05	
2A Piecewise	7.2537E-05	2.0%	1.7236E-05	-0.4%
2B Simulated	7.1430E-05		1.7690E-05	
2B Piecewise	7.2743E-05	1.8%	1.7521E-05	-1.0%
3A Simulated	7.4950E-05		1.8010E-05	
3A Piecewise	7.1590E-05	-4.5%	1.8102E-05	0.5%
3B Simulated	7.1800E-05		1.7270E-05	
3B Piecewise	7.2824E-05	1.4%	1.7367E-05	0.6%
4A Simulated	7.1850E-05		1.7510E-05	
4A Piecewise	7.2906E-05	1.5%	1.7369E-05	-0.8%
4B Simulated	7.1850E-05		1.7560E-05	
4B Piecewise	7.2538E-05	1.0%	1.7441E-05	-0.7%
Rodded	7.4300E-05		1.7270E-05	
Unrodded	6.6770E-05		1.8600E-05	
	Am241 Density [atom/barn-cm]	**Percent Difference Between Simulated and Piecewise**	**Am243 Density [atom/barn-cm]**	**Percent Difference Between Simulated and Piecewise**
1A Simulated	2.3900E-06		4.6170E-06	
1A Piecewise	2.1110E-06	-11.7%	4.8240E-06	4.5%
1B Simulated	2.3630E-06		4.7640E-06	
1B Piecewise	2.5412E-06	7.5%	4.8338E-06	1.5%
2A Simulated	2.3520E-06		4.8910E-06	
2A Piecewise	2.4185E-06	2.8%	4.7601E-06	-2.7%
2B Simulated	2.3140E-06		4.9070E-06	
2B Piecewise	2.3563E-06	1.8%	4.7431E-06	-3.3%

3A Simulated	2.4000E-06		4.6890E-06	
3A Piecewise	2.1905E-06	-8.7%	4.8197E-06	2.8%
3B Simulated	2.3430E-06		4.8030E-06	
3B Piecewise	2.4571E-06	4.9%	4.7928E-06	-0.2%
4A Simulated	2.3350E-06		4.8590E-06	
4A Piecewise	2.4350E-06	4.3%	4.7866E-06	-1.5%
4B Simulated	2.3280E-06		4.8630E-06	
4B Piecewise	2.3812E-06	2.3%	4.7600E-06	-2.1%
Rodded	2.5670E-06		4.8420E-06	
Unrodded	1.7260E-06		4.6350E-06	

REFERENCES

[1] Einziger, R., and Dunn, D., "Identification and Prioritization of the Technical Information Needs Affecting Potential Regulation of Extended Storage and Transportation of Spent Nuclear Fuel," Washington, DC: U.S. Nuclear Regulatory Commission. May 2012..

[2] Anon., "Spent Fuel Storage in Pools and Dry Casks Key Points and Questions and Answers", http://www.nrc.gov/waste/spent-fuel-storage/faqs.html (Accessed October 19, 2014).

[3] Anon., "U.S. Independent Spent Fuel Storage Installations," http://pbadupws.nrc.gov/docs/ML1319/ML13197A187.pdf (Accessed October 19, 2014).

[4] Blue Ribbon Commission on America's Nuclear Future, "Strategy for the Management and Disposal of Used Nuclear Fuel and High Level Radioactive Waste," Washington, DC: U.S. Department of Energy January 2013.

[5] Anon., "Safely Managing Used Nuclear Fuel," http://www.nei.org/Master-Document-Folder/Backgrounders/Fact-Sheets/Safely-Managing-Used-Nuclear-Fuel (Accessed October 19, 2014).

[6] S. M. Bowman, "SCALE 6: Comprehensive Nuclear Safety Analysis Code System," *Nucl. Technol*. **174**(2), 126-148, May 2011.

[7] Anon., "Boiling Water Reactor Sytems", http://www.nrc.gov/reading-rm/basic-ref/teachers/03.pdf (Accessed October 19, 2014).

[8] Technical Training Division in the Office for Analysis and Evaluation of Operational Data, "GE Technology Manual (R-304B)" Washington, DC: U.S. Department of Energy.

[9] Fensin, Michael Lorne, "Optimum Boiling Water Reactor Fuel Design Strategies to Enhance Reactor Shutdown by the Standby Liquid Control System," M.S. Thesis, University of Florida, 2004.

[10] Anon., “Spent Fuel Storage in Pools and Dry Casks”, http://www.nrc.gov/waste/spent-fuel-storage/faqs.html (Accessed October 19, 2014).

[11] U.S. Nuclear Regulatory Commission “NRC Regulations Title 10, Code of Federal Regulations”, http://www.nrc.gov/reading-rm/doc-collections/cfr/ Washington, DC: U.S. Department of Energy July 2012.

[12] Mueller, D.E, Scaglione, J.M., Wagner, J.C., Bowman S.M., "Computational Benchmark for Estimated Reactivity Margin from Fission Products and Minor Actinides in BWR Burnup Credit," *NUREG/CR-7157*, September 2012.

[13] National Nuclear Data Center, “Chart of Nuclides,” http://www.nndc.bnl.gov/chart/ (Accessed November 9, 2014).

[14] Japan Atomic Energy Agency Nuclear Data Center, “Neutron Reaction Sublibrary,” http://wwwndc.jaea.go.jp/jendl/j40/j40.html (Accessed November 9, 2014).

[15] Firestone, R.B., “Fission Product Yields,” http://ie.lbl.gov/fission.html (Accessed October 26, 2014).

[16] Marshall, B.J. and Ade, Brian J. , “Peak Reactivity Burnup Credit for BWR Fuel in Casks Using the Standard Cold Core Geometry Method,” ORNL Letter Report, January 2014.

[17] Division of Spent Fuel Storage and Transportation, “Interim Staff Guidance 8 – Revision 3, Issue: Burnup Credit in the Criticality Analyses of PWR Spent Fuel in Transportation and Storage Casks,” Washington, DC: U.S. Department of Energy September 2012.

[18] Larsen, N.H, “Core Design and Operating Data for Cycles 1 and 2 of Peach Bottom 2,” General Electric Company: Nuclear Energy Engineering Division, June 1978.

[19] Holloway, G.L., J.E. Fawks, and B.W. Crawford, “Core Design and Operating Data for Cycles 2 and 3 of Hatch 1,” N. p., 1984.

[20] SCALE 6.1 – User’s Manual, June 2011.

[21] Dehart, Mark D., Bowman, Stephen M., “Reactor Physics Methods and Analysis Capabilities in SCALE,” Nuclear Technology Volume 174 Number 2 p.196-213, May 2011.

[22] Gauld, Ian C. et al. “Isotopic Depletion and Decay Methods and Analysis Capabilities in SCALE,” Nuclear Technology Volume 174 Number 2 p.169-195, May 2011.

[23] Grummer, R., “CASMO-4/MICROBURN-B2 Methodology,” pbadupws.nrc.gov/docs/ML0522/ML052280107.pdf (Accessed November 26, 2014).

[24] Xu, Y., Downar, T., “GenPMAXS Code for Generating the PARCS Cross Section Interface File PMAXS,” https://engineering.purdue.edu/PARCS/Code/Manual/GENPMAXS/PDF/GenPMAXS_nov28_06.pdf (Accessed October 26, 2014).